MARCH 2019

PhD in Engineering Physics

ESME IŞIK

REPUCLIC OF TURKEY

UNIVERSITY OF GAZİANTEP

GRADUATE SCHOOL OF

NATURAL & APPLIED SCIENCES

THE INVESTIGATION OF THERMOLUMINESCENCE PROPERTIES OF DENTAL CERAMICS

PhD THESIS

IN

ENGINEERING PHYSICS

BY

ESME IŞIK

MARCH 2019

The Investigation of Thermoluminescence Properties of Dental Ceramics

PhD Thesis

in

Engineering Physics

University of Gaziantep

Supervisor

Assoc. Prof. Dr. Hüseyin TOKTAMIŞ

by

Esme IŞIK

March 2019

T.C.
UNIVERSITY OF GAZIANTEP
GRADUATE SCHOOL OF NATURAL & APPLIED SCIENCES
PHYSICS ENGINEERING DEPARTMENT

Name of the thesis: The Investigation of Thermoluminescence Properties of Dental Ceramics
Name of the student: Esme IŞIK
Exam date: 15.03.2019

Approval of the Graduate School of Natural and Applied Sciences

Prof. Dr. A. Necmeddin YAZICI
Director

I certify that this thesis satisfies all the requirements as a thesis for the degree of Doctor of Philosophy.

Prof. Dr. Ramazan KOÇ
Head of Department

This is to certify that we have read this thesis and that in our opinion it is fully adequate, in scope and quality, as a thesis for the degree of Doctor of Philosophy.

Assoc. Prof. Dr. Hüseyin TOKTAMIŞ
Supervisor

Examining Committee Members:	signature
Prof. Dr. A. Necmeddin YAZICI	……..
Prof. Dr. Mustafa TOPAKSU	
Assoc. Prof. Dr. Vural Emir KAFADAR	
Assoc. Prof. Dr. Hüseyin TOKTAMIŞ	
Assist. Prof. Dr. Yusuf Ziya HALEFOĞLU	

I hereby declare that all information in this document has been obtained and presented in accordance with academic rules and ethical conduct. I also declare that, as required by these rules and conduct, I have fully cited and referenced all material and results that are not original to this work.

Esme IŞIK

ABSTRACT

THE INVESTIGATION OF THERMOLUMINESCENCE PROPERTIES OF DENTAL CERAMICS

IŞIK, Esme

PhD in Engineering Physics

Supervisor: Assoc. Prof. Dr. Hüseyin TOKTAMIŞ

March 2019

97 pages

Dental ceramics taken from humans who are potentially exposed to radiation, are commonly used as retrospective dosimetry for quick and reliable dose estimations due to nuclear power plants that are close to settlement of people. Nowadays most people have a dental restoration for the compulsory health problem and aesthetic beauty. Moreover dental restorations are usually applied to the front teeth, it can be considered that the radiation directly interact with the material. Therefore, dental ceramics could be potentially used for retrospective dosimetry purposes since allows a quick and reliable dose assessment in case of nuclear accident or bad use of a nuclear attack. Therefore, dental ceramics that used in restoration of human teeth as an accident dosimetry by thermally stimulated luminescence method have been investigated in this study. Glass ceramic, lithium disilicate glass ceramic and feldspathic dental ceramic which used in this study were obtained from Vivadent ivoclar, Sweden and Turkey, respectively. The aim of the study is to investigate the thermoluminescence dose response, the effects of heating rates on the thermoluminescence characteristics, the stability of the dental ceramics with respect to the cycle of measurement and also fading properties of dental ceramics. Finally we compared the samples with respect to their TL characteristic properties to choose the most suitable dosimetric ceramic.

Key words: dental ceramic, retrospective dosimetry, thermoluminescence, dose response.

ÖZET

DİŞ SERAMİKLERİNİN TERMOLÜMİNESANS ÖZELLİKLERİNİN ARAŞTIRILMASI

IŞIK, Esme
Doktora Tezi, Fizik Mühendisliği Bölümü
Danışman: Doç. Dr. Hüseyin TOKTAMIŞ
Mart 2019
97 sayfa

Nükleer santrallerin yerleşim yerlerine yakınlığından dolayı olası kazalarda doğru ve çabuk doz ölçümü için radyasyona mağruz kalan insanlardan alınan diş seramikleri yaygın olarak kaza dozimetresi olarak kullanılmaktadır. Son zamanlarda birçok insan estetik güzellik veya sağlık için diş kaplaması yaptırmaktadır. Kaplamalar özellikle ön dişlere yapıldığından olası kaza anında radyasyonun direk dişle temas ettiği varsayılabilir. Bundan dolayı bu çalışmada insan dişlerinin restarasyonunda kullanılan diş seramiklerinin termal uyarmalı lüminesans yöntemi kullanılarak kaza dozimetresi olarak kullanılabilirliği incelenmiştir. Termolüminesans özellikleri incelenen cam seramiği, lityum disilikat diş seramiği ve feldspatik diş seramiği Vivadent ivoclar'ın Türkiye ve İsveç şubelerinden temin edilmiştir. Diş seramiklerinin ölçüm döngüsüne göre kararlılıklarını gözlemlemek, termolüminesans doz eğilimini incelemek, ısıtma hızının termoluminesans karakteristiğine etkisini gözlemlemek ve sönümleme özelliklerini etkisini incelemek amaçlanmıştır. Sonuç olarak da termoluminesans karakteristik özellikleri kıyaslanıp iyi bir dozimetre için en uygun numune belirlenmiştir.

Anahtar Kelimeler: diş seramiği, retrospektif dozimetre, termolüminesans, doz cevabı.

To my childirien Mehmet Akif and Kadir Tuna

ACKNOWLEDGEMENT

First of all I would like to thank my supervisor Assoc. Prof. Dr. Hüseyin TOKTAMIŞ for his support and advices during my thesis. I would also thank to Prof. Dr. Necmeddin YAZICI and Mustafa ÖZTAŞ for their support during my thesis. Secondly, I wish to thank my husband, İbrahim IŞIK for his support during all my B.Sc., M.Sc. and P.hD. education and thank my sons M. Akif IŞIK and K. Tuna IŞIK to give me joy of life.

Finally, I would like to thank the University of Gaziantep, Scientific and Research Center for their support with project number of MF.DT.18.18 and Vivadent Ivoclar Company.

CONTENTS

LIST OF FIGURES

LIST OF TABLES

CHAPTER 1:

INTRODUCTION

When a solid heats to a certain temperature, the emission of light produced and this happen is known as thermoluminescence (TL). It is displayed by crystals which have exposed to radiation source such as X-rays, β or γ rays such as alkali halides. The high-energy radiation produce an electron-hole pair, some of these carriers are captured by lattice imperfections, and then removed by the accompanying light emission when the temperature is raised to provide the required amount of kinetic energy [1]. To produce TL light in an insulator or a semiconductor one of the essential condition is that the material must be heated to certain temperature. When the solid is reheated without absorbing radiation sources, the solid does not exhibits TL light. Although TL is based on the same basic principles like other luminescence processes, heat radiation is only a stimulant and is traditionally misleading because it is not an exciting agent [2].

Urbach [3] is generally considered to be credited as offering TL as a potentially useful research tool for trap level analysis. Randall and Wilkins and Garlick and Gibson gave firstly the basic mathematical treatment of TL [4-6], then they began to gain favor in analyzing radiation such as geology, archaeology, medical sciences, health physics, clinical dosimetry, and practices in personnel and environmental monitoring, as well as in defect structures in solids. Farrington Daniels et al. firstly proposed the use of TL for the radiation dosimetry technique by investigations on Lithium fluoride (LiF) like a TL material [1]. Soon after, the idea of using TL for dosimetric applications was captured and many authors started to work in the field of thermoluminescent dosimetry (TLD). In LiF, the desired properties of the material appeared to be the result of the interaction between the complex defects present in the material resulting from the presence of the Ti and Mg. This was due to the work of Cameron and colleagues [7-8], which at the end of 1963 led to the patentation of TLD-100 by the Harshaw Chemical Company.

Daniels et al. [9] examined a new material which is Al_2O_3. Al_2O_3 is sapphire-shaped, was high-grade optical material, but lost its reliability, due to lack of sensitivity. BeO and CaF_2: Mn are two new materials in 1957, made their appearance. CaF_2: Mn had significant impact in this field due to its brilliant sensitivity and humble glow curve structure [10, 11]. This is the first TLD material in this field and never returned in the seat [12].

In 1960s several new materials like $CaSO_4$: Sm, $Li_2B_4O_7$: Mn, CaF_2: Dy, $CaSO_4$: Tm and $CaSO_4$: Dy entered into the field [13-16]. Natural CaF_2 reappeared along with encouraging material and tissue equivalent, LiF:Mg, Ti [7, 8, 17]. Houstan and Thomas's [18] MgO was another additional authors for this family.

In 1970s, AI_2O_3 reappeared in new form as Al_2O_3: Mg, Y [19] and Al_2O_3: Si,Ti [19, 20]. Another form of CaF_2, namely, CaF_2: Tm was stated in this process. $Li_2B_4O_7$: Cu and MgB_4O_7: Dy or Tm are the two new materials which were reported during 6th International Conference on Luminescence at Toulouse, France, latter MfB_4O_7: Mn was the additional material to this group [21-24].

Another outstanding innovation was LiF:Mg,Cu,P [25], however, the group at the Solid Doimetric and Detector Laboratory in Beijing was not recognized until it reported that it had produced a LiF:Mg, Cu, P TLD material [26], known as GR-200, in 1986. GR-200 has been reported as an ultra-sensitive material with sensitivity as high as 50 times that of TLD-100. More sensitive material followed such as $A1_2O_3$: C [27]. Numerous dielectric materials including rocks, minerals, insulators and inorganic (polycrystalline, amorphous and single-crystal) semiconductors, ceramics and glasses, biological materials, organic compounds and biochemical exhibit TL emission. Many scientists have carried out different thermoluminescence materials to obtain best dosimeter. Dosimeters are used in commercial areas, hospitals, nuclear power plants and research laboratories. In regular dosimetric applications, one can choose an appropriate material with results of cycle of measurement, linear dose response for the type of radiation in question as well as dose-rate independence and longtime stability. However, in retrospective dosimetry this situation is significantly more complicated such as in accident dosimetry where the exposure to radiation is to be determined by using existing materials such as porcelain [28].

A good thermoluminescence dosimeter (TLD) candidate has to need reproducibility, stability, linearity and dose-rate dependence. The reproducibility is an obvious requirement. However, a sensitization effect has been found in some

material e.g. quartz [29]. This is an increase of sensitivity as a result of irradiation followed by an annealing above 500 ^{o}C . The stability is a desirable feature that the sample in hand is irradiated; the potential TL signal should be stable prior to the beginning of the heating. Linearity of the TL signal with dose is very desirable. However, superlinearity has been found in many materials, even in the very well recognized dosimetric material LiF [30].

Ceramics are categorized as inorganic and nonmetallic materials and they are necessary at our daily life cycle such as dental ceramics is an expression of glass-ceramic materials and porcelain that are used in the production of restorative apparatuses of teeth, crowns and prosthetic teeth. Ceramic is powerfully sensitive to radiation and the concentration of both the TL and OSL signals are relative to the radiation dose which was absorbed. Commonly used ceramic materials fix the revelation luminescent features in dental prosthetics. Glass ceramic, feldspathic ceramic and lithium disilicate glass ceramic are commonly used in dentistry and glass ceramic is frequently used in mixture with alumina (Al_2O_3) core or zirconia (ZrO_2), it also show luminescence. Aluminosilicates are known as feldspars and they found in nature, which contain numerous quantities of sodium and potassium. Feldspars used in dentistry to create the glass which are modified in various ways and it is known as feldspathic dental ceramic. Lithium disilicate glass ceramic is formed by crystals of SiO_2-Li_2O.

The ceramic materials used for dose assessment studies with thermoluminescence techniques especially obtained from buildings as a retrospective dosimetry [31-33]. And ceramic has been proven to be a suitable material for determining the exposed dose to the inhabitants in the nuclear accident zones. Appropriate dosimeters in the district of a nuclear accident are tiles, house bricks, crockery porcelains, insulators and plant pots [34-36]. Prior work by Davies [37] showed the possibility of the use of dental restorative ceramic as a dosimetric material with thermally stimulated electronic emission (TSEE) and thermoluminescence (TL) techniques in 1979. Mauricio et al [38] also investigated the dental restorative porcelain as a TL dosimeter to estimate high doses in radiological accidents. Bailiff et al. [39] further underlined the TL and OSL characteristics of dental ceramic for retrospective dosimetry, TL peaks of prosthetic ceramic (~250 µm thickness slices, heated at 2 ^{o}C.s^{-1}) was found to be linear with dose-response in the range 100 mGy to 10 Gy. Though TL and OSL peaks displayed fading more than 50 % over one week, it was possibly appropriate for

retrospective dosimetry applications. As the type of dental ceramics over developed and compositions also changed day by day, with the obtainability of thermally stimulated luminescence (TL) measurement techniques, thermoluminescence properties of dental restorative ceramics which is commonly used in dosimetric applications are reported in this PhD thesis.

For the present study dental ceramics whose ingredients are different have been used in the experiments. Because of its translucency, for aesthetic rehabilitation dental ceramics are measured to be the most biological-looking restorative material. Dental ceramics are potentially exposed to radiation for quick and reliable dose estimations due to nuclear power plants that are close to settlement of people. Dental ceramics can be used for estimation of dose accumulated as a result of an accident or a nuclear attack. Therefore, dental ceramics that used in human teeth as a retrospective dosimetry by thermally stimulated luminescence method has been investigated in this study. Glass ceramic, lithium disilicate and feldspathic dental ceramics which investigated in terms of thermoluminescence properties obtained from Vivadent Ivoclar Company, Sweden and Turkey.

This study consists of 6 chapters. In chapter 1, we give information about scheme of study and a brief description of thermoluminescence. Chapter 2 includes specific literature survey that includes information about luminescence and thermoluminescence. In chapter 3, information about dental ceramics briefly is given. The essential explanations about the experimental equipment, samples and procedures are given in chapter 4. All the experimental results are given in chapter 5. The aim of the study is to investigate the thermoluminescence dose response, the effects of heating rates on the thermoluminescence characteristics, the TL stability of the dental ceramics with respect to the cycle of measurement and also TL fading properties of dental ceramics is given in this chapter. Finally, we have discussed and concluded all experimental results with support of published studies in chapter 6.

CHAPTER 2:

THEORY OF THERMOLUMINESCENCE

2.1 Luminescence

One of the forms of energy is described as light and this form of energy must be provided to produce light. There are two conventional ways to do this which are luminescence and incandescence. The incandescence which is produced from energy of heat is a kind of light. If something is hot to a high temperature sufficient, it initiates to glow. For example, when a metal in a blaze begins to glow then it is named as incandescence. Luminescence is also named as "cold light" as light from another energy bases that may can occur at normal and low temperatures. Some energy sources hit out an electron to out of its "lowest-energy" (ground) state of an atom into a "higher-energy" (excited) state; after that the electron returns the energy in the form of light therefore it can drop back to its " lowest-energy " state in luminescence. There are a lot of types of luminescence and each of them called with respect to source of energy is, or trigger for the luminescence. For instance, photoluminescence (PL) is a less specific term which covers both phosphorescence and fluorescence as the stimulation, is made by photons/electromagnetic radiation; cathodolumineseence, when the stimulation is shaped by cathode rays or energetic electrons; electroluminescence is light production caused by electric effects; radioluminescenee, as the stimulation is formed by γ rays or high-energy X-rays; sonoluminescence, as the stimulation is produced by ultrasonic waves; triboluminescence, as a material is formed mechanical treated, e.g. fractured or polished; chemiluminescence is light produced through the chemical reactions; bioluminescence is chemiluminescence from living organisms; thermally stimulated luminescence (TL), which is also identified as thermoluminescence, is the luminescence that causes thermally subsequently initial irradiation by other means for example γ, α, β, X-rays or UV. On the other hand it is

not same with thermal radiation because thermal excitation triggers lone the discharge of energy from additional source. The process of luminescence can be demonstrated in Figure 2.1. A*, R and NR indicate the excited state, radioactive return and the nonradioactive reappearance to the ground state respectively in the figure.

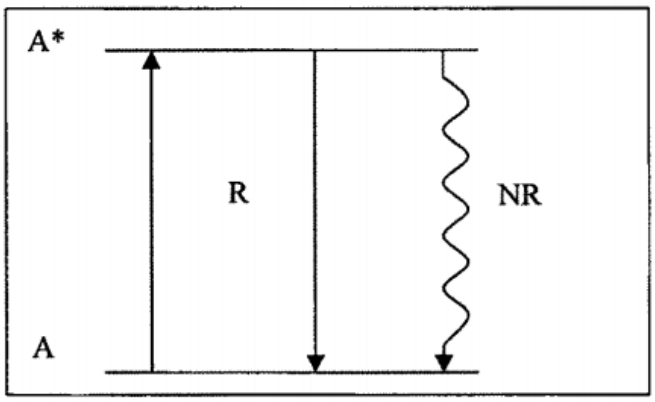

Figure 2.1. Energy level scheme of the luminescent ion A [40].

Two kinds of returns to the ground state as shown above figure and these are radiative and non-radiative returns. The luminescence procedure takes place in the radiative return. Conversely the non-radiative return has no role in luminescence up till now since it takes place with the radiative emission owing to the phonons which are transformed to lattice vibrations that transfer energy in the form of heat. A material in which the radiative transitions govern over the non-transitions is an effective luminescent material. Although the condition is more multifaceted than illustrated in the above figure in the luminescent materials realistically, the activator did not absorb exciting radiation. Luminescence has further sub arrangement as depending on the period of the emission:

(a) Fluorescence: An exponential afterglow is observed on removal of excitation with a period less than 10^{-8} seconds for independent excitation intensity and temperature.

(b) Phosphorescence: Result of afterglow has any other event in which decay is slower with complex kinetics on removal of excitation with period of more than 10^{-8} seconds and depend on the intensity of excitation and temperature. Metastable conditions are produced by the activators, defect centers, impurities, hole or electron traps which existing in the lattice and may be deferred the luminescent emission that reasons this

effect. Meanwhile trap or thermal activation of the metastable activator is the requirement to emission.

Different processes of all these are called as luminescence where non-thermal energy converts into light. An insulated ionic crystal energy band model is not fully understand in terms of its shape and it is the main mechanism of luminescence. Electrons are considered to be at different energy levels which are called as band in this model. The lowest energy band is the valence band, the highest energy band is the conduction band, and the forbidden region is known as the gap between these two bands. In a perfect crystal, there is no electron in this forbidden region [41]. However, some crystals exist in the environment such as feldspar and quartz do not always provide this ideal situation and the crystal structures may have some defects. The point defect is the most common imperfection is observed. These defects are consist of structural intrinsic and non-structural extrinsic defects. The result from the fact that any atom should not be in the place where it should be, or that the result should be somewhere other than where the atom should be is known as structural imperfections defects. The placement of a foreign atom into the crystal structure or the result from the deposition of foreign atoms into the crystal structure is known as non-structural defects as illustrated in Figure 2.2. If the defect is able to capture a charge carrier and emit it back to the band, this type crystal defect is classified as a trap center. A crystal defect is classified as a recombination center if the carriers of opposite sign charge can be captured, resulting in an electron-hole recombination. In the forbidden region, the formation of semi-stable energy levels is due to these defects. The nuclear radiation beam is also carried by the semi-stable energy levels in their memory, thus allowing the luminescence to occur [42]. These defects create only solitary lattice point (not extended) and losing of an atom or also appear due to lack of a vacancy (host atom). Point defect have four different kinds of defects. One of them happens owing to the presence of the similar but an additional atom. The additional atom spaces anyplace among the body of atoms and it is named as atoms of self-interstitial. Another imperfection sort is shaped by the similar atom through host lattice nevertheless the atom is lesser than the bulk atoms. This imperfection is also called as impurity atom of interstitial. Furthermore, in the lattice, dissimilar kinds of atoms also generate the disordered structure in the bulk atoms with replacing. Substitutional contamination atoms are categorized as this sort of point defects. Vacancies are originating from the

lacking atom in the crystal structure and they are also a point defect types. The types of these point defects are shown in Figure 2.2 detailed.

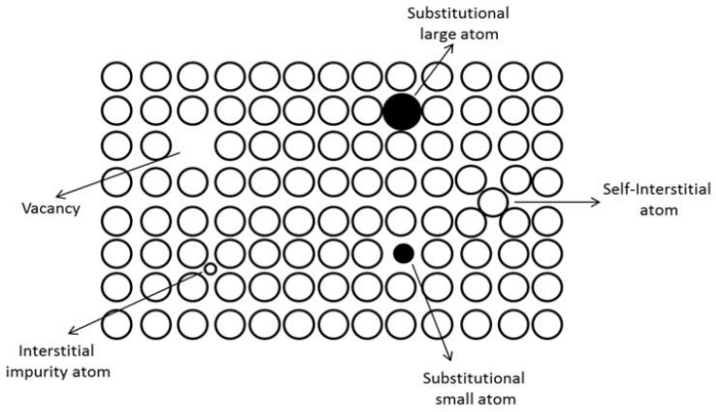

Figure 2.2. Demonstrations of various point defects existing in the crystal [40].

Luminescence has been used to determine the combined radiation dose exposed to geological remains or dating archaeological samples and humans since 1950s either for radiation dosimetry. The combined radiation dose value or the event to be dated, therefore, depend on the setting to zero of the hidden luminescence at a specific time before. This reset happens through heating for some materials such as archaeological pottery, most radiation dosimeters, porcelain and bricks or by exposure to daylight for geological remains. As a result, the hidden luminescence signal is regenerated by exposure to radiation either from the poor natural environmental background radiation or from man-made sources. The luminescence inducing radiation must be notable from other luminescence events that are not dose dependent and therefore not related to dating or dosimeter, e.g. photoluminescence, phosphorescence etc. Therefore luminescence rises from stimulation either thermal or optical of minerals that have been exposed to ionizing radiation before. The time of exposure, radiation energy is composed and deposited in the crystal lattice. This deposited energy is in the form of electrons that have been taken at defects in the lattice. The trapped carrier is released and the signal goes to zero as a result of the luminescence in the period of stimulation. The energy diagrams for luminescence processes are also given in Figure 2.3 (T: Electron trap, L: Luminescence center). These energy diagrams are given below respectively.

(i) Ionization produced by exposure to nuclear radiation with trapping of holes and electrons at defects L and T, respectively.

(ii) Radiation energy storage of over time; if escape is small the duration of the electrons in the traps (lifetime) should be lengthier than the storage time of the sample. This lifetime depends on the energy depth E of the trap below the conduction band.

(iii) The electrons are removed from the electron traps by shining light onto the sample or heating and some of them reach luminescence centers (L); if so, the light (i.e. TL or OSL) is emitted as a result of the recombining process to these centers.

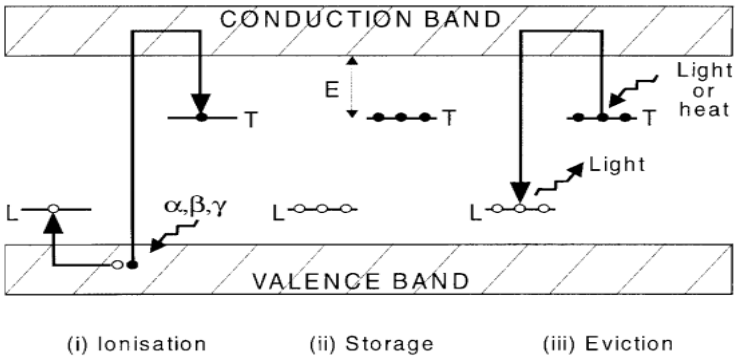

Figure 2.3. Energy-level representation of TL and OSL processes [43, 44].

Nuclear radiation is almost everywhere in nature. It has the ability to ionize this radiation and when it enters into the crystal, electrons move from the valence band to the conduction band. Ionized electrons left behind spaces are called holes and this electron and hole freely move in the crystal. In this way, nuclear radiation energy is absorbed by the electron and hole recombination and can be exported as heat energy. Many charge carriers actually recombine directly in this way although in the other case the electrons and the holes are trapped in any defect center the same as mentioned above. Thus, nuclear energy is temporarily stored in the crystal structure and the system remains semi-stable. In order to stabilize the system, electrons must be removed from these traps. The system must be supplied with external energy to stabilize itself. The amount of energy required is determined by calculating the difference (E) between the energy level at which the electron is trapped and the energy level of the conduction band, in other words by calculating the trap depth.

For trap centers, we assume that only transitions between the center and the conduction band or valence band are possible. For recombination centers, we assume that only recombination of a conduction electron and a valence hole is possible. Finally, an electron-hole pair is assumed initially to consist of a conduction electron and a valence hole. Exchange of charge carriers between the crystal defects is assumed to take place through the conduction and valance band [43]. During the ionizing irradiation of the crystal, electron-hole-pairs are generated by excitation of electrons from the valence band to the conduction band. The excited electrons are freely moving in the crystal until they are captured by an electron trap center T, or by a recombination center R. A hole generated in the valence band is captured into either a hole trap center T or the recombination center R. Recombination are assumed to be accompanied by emission of photons, i.e. luminescence. However, non-radiative recombinations are also possible. Taken electrons and holes can be released thermally into the conduction or valence band with heating the crystal and then make a change to the radiative recombination center R. This treat is called as thermally stimulated luminescence (TL). On the other hand, external light exposure of the crystal can release captured electrons from a trap center to the conduction band from where they can recombine into the recombination center R. This process then is called as optically stimulated luminescence (OSL). That is to say, the luminescence is called according to the energy source which used to stimulate the electrons from the trap [41].

The optically or thermally freed charge carriers can be measured as an electrical current in the conduction/valance band when a voltage source is applied across the crystal. These measurements are termed thermally and optically stimulated conductivity (TSC, OSC) respectively.

2.2 Thermoluminescence (TL)

Thermally stimulated luminescence or thermoluminescence (TL) is a luminescence event of a semiconductor or insulator as the solid is thermally stimulated which can be observed. It has been used widely to degree nuclear radiation doses since the early 1950s [1]. TL was then practical to archaeological dating in the early 1960s [44-46] and geological dating at the beginning of the 1980s [47]. Firstly in [45] authors were proposed some techniques and methods for thermally stimulated luminescence dating. In thermally stimulated luminescence, a luminescence the material exposed to ionizing

radiation is heated at a constant heating rate up to a certain temperature (typically 500 °C) and the intensity of the emitted luminescence is measured with the help of a sensitive photomultiplier tube which is recorded as a function of temperature. A TL signal that is transmitted at different temperatures is evaluated by the glow curve at which significant peaks are observed, which is related to the electron traps existing in the sample. Imperfections in the crystal structure are accountable for these traps [48]. A typical imperfection can be caused by the dislocation of a negative ion, which provides a negative ion vacancy, which acts like an electron trap. When an electron trapped, the trapped electron may eventually escape from the trap by thermal energy causing lattice vibrations. The stronger the vibrations by the higher the temperature, the possibility of discharge of electrons increase from the trap. After that, some electrons recombine with trapped holes as a result of the emission of TL light with radiative recombination. A typical TL glow curve which obtained from LiF is shown in the Figure 2.4. The temperature peaks belong to different electron trap depths in figure.

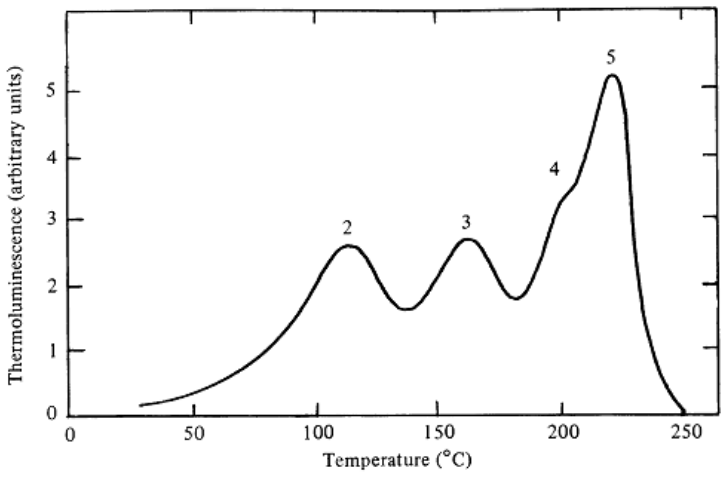

Figure 2.4. Typical thermoluminescence 'glow curve' from LiF, doped with Mg and Ti, following irradiation with 250 rad γ-rays at room temperature, β=3 $^{o}Cs^{-1}$ [40].

Although the TL luminescence curve appears uniform continuity, it is made up of several overlying peaks originated from the thermally released electrons from traps of dissimilar stabilities. In deep traps, electrons have much lifetime later that of electrons in shallow traps. Generally, it is not suitable for dosimetry (dose measurement with any system) as the glow peaks below 200 °C as electrons can be exhausted from these

traps over an elongated time even at room temperatures. Unchanging glow peaks are suitable for dosimetry at 300 ^{o}C temperature or higher. Though, at these high temperature glow peaks, unexpected fading may be observed at room temperature in some feldspar. This is clarified as a quantum mechanical tunneling effect [49]. Another complex situation is thermal quenching for TL measurements.

2.3 Transitions Between Energy States in Thermoluminescence

Potential changes of charge carriers between permitted energy states need to be taken account to clearly understand the thermoluminescence emission mechanism. For a semiconductor material, a basic model is illustrated in Fig. 2.3. The well-known changes in a semiconductor take places between the conduction and valence bands expressed as subsequent transitions:

(i) When the electrons are excited in the valence band with light which energy is greater than band gap ($hv > E_g$) transition in Fig. 2.3 occurs. This excitation is accepted from valance band to conduction band and the technique leads to the formation of free holes in the valence band and free electrons in the conduction band. The creation of free electrons return to the lower energy state and the recombination occurs with the free holes. The direct recombination is identified as this kind of transition. In a crystal, other potential transitions can happen between the lower energy states to higher ones emerging because of impurities and/or the defects.

(ii) This transition exemplifies the trapped holes over the recombination center and electrons over the trap center.

(iii) These transitions are recognized as the trapped electrons and holes are excited from the recombination and trap centers. To stimulate these electrons and holes from the trapping centers, thermal energy (kT) shows an important role in the technique of TL experimental. Exciting electron and hole coming from trapping centers (left to delocalized states) recombination occurs as illustrated in Fig. 2.3. As to the modeling of the modest TL mechanism, electrons in the lower energy state are stimulated by light having greater energy than the activation energy and transition (i) occurs. These stimulated electrons in transmission band are recombined with holes in the valence band or electrons are captured by energy levels

remaining in the forbidden energy gap. The electrons and holes are trapped in the recombination center and are recombined in two ways with trapped electrons. Thermally excited holes (electrons) into the conduction (valence) band are recombined with electrons (holes) at the trap (recombination) center. Thus, light is created. The second way of recombination is clarified by the holes (electrons) recombining with electrons (holes) over a middle localized state instead valence (conduction) band. No luminescence can be produced and this type of transition is known as non-radiative transition.

2.4 Theoretical Approach to Thermoluminescence

Another important parameters for luminescent materials is thermoluminescence intensity (I_{TL}) to have information about the characteristics of trapping centers. The possessions of the defect centers in I_{TL} can define by the theoretical relationships between the trapping parameters and TL intensity to provide the TL density as a function of temperature. In this view, elementary descriptions and theoretical formulas which are about TL intensity for different cases are given in this section of the chapter. The intensity of the trapping levels in luminescent materials is the very important aspect of the physical subject which decides the magnitude of TL concentration. As the number of trapped charge carriers are increases, the freed charge carriers that provide to the TL intensity also increases at a particular temperature. The modest illustration for one electron-one hole model is shown Figure 2.5.

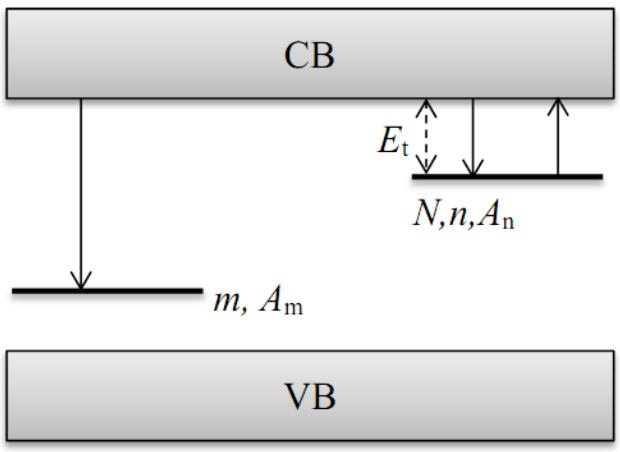

Figure 2.5. A Simple diagram for one electron and one hole traps [55].

Traps and recombination centers can be differentiated by the probabilities of thermal release and recombination. At finite temperature T, a carrier can escape from the trap by the probability:

$$p = s\,exp\left(-\frac{E}{kT}\right) \tag{2.1}$$

In the formula, s, k, T and E represent the frequency factor (sec^{-1}), the absolute temperature (Kelvin), Boltzmann's constant and the trap depth (eV), respectively. The duration of the electrons and holes in the metastable state at temperature T, is given in Eq. (2.2).

$$\tau = p^{-1} \tag{2.2}$$

Charge carrier numbers preventing the traps varies with the transitions along with recombination and trap centers (the localized) and valence and conduction bands (delocalized) states. Pagonis et al. described theoretically these transitions stimulation, recombination and retrapping [50]. Stimulation which is known as the electrons transition by the trap level to higher energy level is an important factor for the intensity of trap levels. Retrapping is determined by the event that occurs for the holes (electrons) freed to valence (conduction) band from trap level. Several of the stimulated holes (electrons) recombine by opposite charge carriers, the additional ones can be retrapped by the defect center. Recombination of holes and electrons is a procedure through that both electrons and holes annihilate with each other: the empty state associated with a hole- electrons occupy - through one or multiple steps. Charge carriers ultimately disappear in the procedure. Therefore, change of electron intensity in the conduction band is accomplished by the event of recombination.

2.5 Models in Thermoluminescence

The purpose of a mathematical analysis with respect to the TL light emission is to reach an acceptable the kinetic parameters' knowledge of the traps occupy in the TL sample. For each site, these kinetic parameters are a frequency factor (s), the activation energy (E) that connected to the transition frequency, and a kinetic order (b) that making the excellence of the occupied event. The kinetic order varieties between 1

and 2 and the explanation of thermally stimulated luminescence by first order, second order and general order equations were presented in some authors' studies [5, 48, 55]. These equations are given below respectively.

$$I(t) = -\frac{dn}{dt} = -nse^{-E/kT} \quad (2.3)$$

$$I(t) = -\frac{dn}{dt} = -\frac{n^2}{N}se^{-E/kT} \quad (2.4)$$

$$I(t) = -\frac{dn}{dt} = -n^b s' se^{-E/kT} \quad (2.5)$$

An experimental case as usual, a linear heating rate (β) is practiced to heat the sample. In the experiment, the change of temperature is expressed as $T = T_o + \beta T$, where β is a linear heating rate and its unit is (Ks^{-1}). Figure 2.6 shows the graphs of temperature, density and TL intensity with respect to the time.

In Equation 2.3,

I : Thermoluminescence intensity,

t : Time (s),

n : The rate of change of the trapped electrons' concentration at any moment t (m^{-3}),

N : The electron traps' concentration (m^{-3}),

s : This expression is known as the frequency aspect or attempt-to-escape aspect. s is measured as a constant (not temperature dependent) in the basic model by a rate in the order of the lattice vibration frequency, namely 10^{12}-10^{14} s^{-1},

s' : Has the dimension of $m^{3(b-1)}$ s^{-1} as the general-order parameter,

T_o : The temperature at time t = 0 (K) [42].

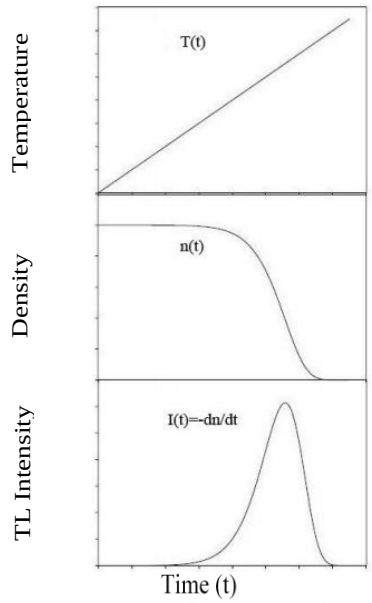

Figure 2.6. Correlation between the number of trapped hole n_h at the recombination centers and thermoluminescence intensity I(t). The linear relation between time and temperature is also shown during heating [112].

2.5.1 First-Order Kinetics (Randall-Wilkins Model)

Chen and McKeever generally used a mathematical statement starting from studies on phosphorescence for each peak in a glow curve [52]. Their mathematical progression was the energy based band model and also gives the well-known statement of first order [52]. In other words, the Randall-Wilkins' theorem takes into account a single trap depth and assumes that the electrons that escape from the trap are not trapped again. According to this theory, the TL intensity I(t) is relative to the number of electrons that are escaped at any temperature. The recombination probability regardless of retrapping controls the TL event. If the trapped electrons' numbers in T is n, and if the fixed temperature is used, after that n reduces with time t rendering to the following statement:

$$\frac{dn}{dt} = -np \tag{2.6}$$

Integrating this equation,

$$\int_{n_o}^{n} \frac{dn}{n} = -\int_{t_o}^{t} pdt \tag{2.7}$$

Eq. (2.8) obtains as below

$$n = n_o . exp\left[-sexp\left(-\frac{E}{kT}\right).t\right] \tag{2.8}$$

At the initial time $t_0 = 0$, in Eq. (2.8) n_o denotes to the quantity of trapped electrons. The fact that, the thermoluminescent material is irradiated at a low temperature sufficiently and the electrons are not released from the trap, the life time of the negative charge carriers in the excited state is short, all the charge carriers released from trap recombine in luminescent center, the luminescence proficiency of the recombination centers are not depends on the temperature, the concentrations of recombination and traps centers are independent of the temperature, negative charge carriers are not released from the trap is retrapped. With respect to the previous assumptions, (I(t)), the intensity of TL is relative to the ratio of recombination of electrons and holes at R in photons at any time t per second throughout heating . If m (m^{-3}) is the intensity of holes trapped at R then the TL intensity can be obtained as in Eq. (2.9).

$$I(t) = -\frac{dm}{dt} \tag{2.9}$$

It is assumed that every recombination generates a photon and which all generated photons are noticed. The ratio of recombination will be relative to the intensity of free electrons in the conduction band n_c and the intensity of holes m as in Eq. (2.10a).

$$I(t) = -\frac{dm}{dt} = n_c mA \tag{2.10a}$$

The recombination probability is shown by A, defined in elements of volume per unit time which is supposed to temperature independent in Eq. (2.10a). Then ratio of variation of the intensity of trapped electrons n is equal to variation of the rate of thermal release and retrapping as shown in Eq. (2.10b).

$$-\frac{dn}{dt} = np - n_c(N - n)A_r \tag{2.10b}$$

N: The electron traps' intensity and

A_r: The retrapping probability (m^3/s)

Similarly, the intensity of ratio of free electrons is equal to variance the ratio of thermal release and retrapping and the rate of recombination as in Eq. (2.10c).

$$-\frac{dn_c}{dt} = np - n_c(N-n)A_r - n_c mA \tag{2.10c}$$

Eq. (2.10 a, b and c) describe the charge carrier transportation in the case of recombination in a single center and release of a trapped electron from a single-electron trap. The ratio equations with the release of holes are similar to Eqs. (2.10 a, b and c) to generate TL. These equations start the foundation of several analyses of TL process. However there is not a commonly analytical solution for TL studies. Some shortening assumptions have to be made to develop an analytical expression. A significant statement can be given as in Eq. (2.11) at any time.

$$\left|\frac{dn_c}{dt}\right| \ll \left|\frac{dn}{dt}\right|, \left|\frac{dn_c}{dt}\right| \ll \left|\frac{dm}{dt}\right| \tag{2.11}$$

Aitken et. al. proposed this statement and called as the quasiequilibrium statement because it needs that the free electron intensity in the conduction band is quasistationary [44]. The trapped holes and electrons are generated in pairs along with the irradiation. Therefore charge neutrality determined as in below Eqs. and n ≈ m for $n_c \approx 0$.

$$n_c + n = m \tag{2.12}$$

$$I(t) = -\frac{dm}{dt} \approx -\frac{dn}{dt} \tag{2.13}$$

Because $dn_c/dt \approx 0$ which are obtained from (2.10a) and (2.10b):

$$I(t) = \frac{mAnsexp(-\frac{E}{kT})}{(N-n)A_r + mA} \tag{2.14}$$

Even if Eq. (2.14) cannot be explained analytically without extra shortening assumptions. Some authors were supposed that insignificant retrapping throughout the heating period, i.e. they supposed that $mA \gg (N-n)A_r$ [42, 43]. Under this assumption Eq. (2.14) can be defined as in Eq. (2.15).

$$I(t) = -\frac{dn}{dt} = n.p = snexp(-\frac{E}{kT}) \tag{2.15}$$

Eq. (2.15) represents an exponential decay of phosphorescence. Eq. (2.16) can be obtained by using Equation (2.8) in Equation (2.15).

$$I(t) = n_o.s.exp(-\frac{E}{kT})exp\left[-s.t.\exp(-\frac{E}{kT})\right] \tag{2.16}$$

Usually the temperature is raised as a linear function of time according to Eq. (2.17).

$$T(t) = T_o + \beta t \tag{2.17}$$

In Eq. β refers to constant heating rate and T_0 refers to temperature at t=0. Heating ratio can be defined as β=dT/dt using Eq.(2.17) and presentation it into equation (2.7). So Eq. (2.18) can be obtained as below.

$$\int_{n_o}^{n} \frac{dn}{n} = -\left(\frac{s}{\beta}\right)\int_{T_o}^{T} exp\left(-\frac{E}{kT^{\iota}}\right)dT' \tag{2.18}$$

And the number of trapped electrons (n) in term of β

$$n = n_o.exp\left[-\left(\frac{s}{\beta}\right)\int_{T_o}^{T} exp\left(-\frac{E}{kT^{\iota}}\right)dT'\right] \tag{2.19}$$

Then, using eq. (2.15), the intensity with respect to the temperature

$$I(T) = -\frac{1}{\beta}\frac{dn}{dt} = n_o\frac{s}{\beta}exp\left(-\frac{E}{kT}\right)exp\left[-\left(\frac{s}{\beta}\right)\int_{T_o}^{T} exp\left(-\frac{E}{kT^{\iota}}\right)dT'\right] \tag{2.20}$$

This statement can be calculated by mean of mathematical integration, and it leads a bell-shaped curve, as illustrated in Fig. 2.7, at a characteristic temperature T_m with a maximum concentration.

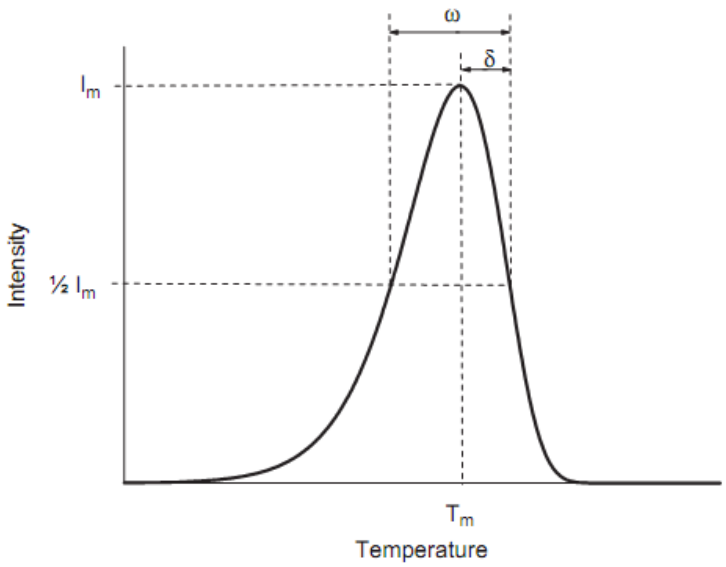

Figure 2.7. Normalized glow peak in [51] first-order TL equation (Eq. (2.20)). The geometry factor μ_g expressed as $\mu_g = \delta/\omega$ has a usual value of 0.42 [55].

Some remarks can be done on Equation (2.20) below:

- ✓ I(T) is dependent of these three parameters E, s and b,
- ✓ E has a value around 20kT in the ratio of incidence of TL peaks,
- ✓ exp(− E/kT) is of the order of 10^{-7},
- ✓ when T is considerably bigger than of T_0, the discussion of the second exponential function is about equal to unity and reduces when temperature increases. Then, I(T) is conquered by the first exponential and increase very fastly with increasing temperature. T_m, at a definite temperature, the treatment of the two exponential functions cancel: at this temperature the maximum temperature happens,
- ✓ the second exponential' decrease is much quicker than the increase of the first exponential for high T_m values and I (T) decreases when the traps are entirely drained.

An important correlation, the so called condition at the maximum, is obtained by equation (2.20) by setting its first derivative equal to zero at T = T_m, i.e.,

$-\frac{dn}{dt} = 0$ at T=T_m (2.21)

Using equation (2.20) it is derived

$$\left[\frac{d(lnI)}{dT}\right]_{T=T_m} = \frac{E}{kT_m{}^2} - \frac{s}{\beta} exp\left(-\frac{E}{kT_m}\right) = 0 \quad (2.22)$$

and the following expression is obtained

$$\frac{\beta E}{kT_m{}^2} = s\ exp\left(-\frac{E}{kT_m}\right) \quad (2.23)$$

From equation (2.23), the frequency aspect is simply decided as

$$s = \frac{\beta E}{kT_m{}^2}\ exp\left(-\frac{E}{kT_m}\right)\ (sec^{-1}) \quad (2.24)$$

Some elementary features and conditions for the first-order kinetic are defined by the Randall-Wilkins Theory from equation (2.23). Furetta and Weng are also pointed out some interesting remarks [54]:

- ✓ The peaks are asymmetric at the first order kinetic. As can be seen in Figure 2.7, the half-width of the low-temperature region is expressed by $\tau = T_m - T_1$ and always 50% larger than the half-width of the high-temperature region expressed by $\delta = T_2 - T_m$.
- ✓ The peak shape and peak temperature depend on the heating rate. T_m moves to higher temperatures when heating ratio increases for a given trap (E and s are constant values) as shown in Fig. 2.8.

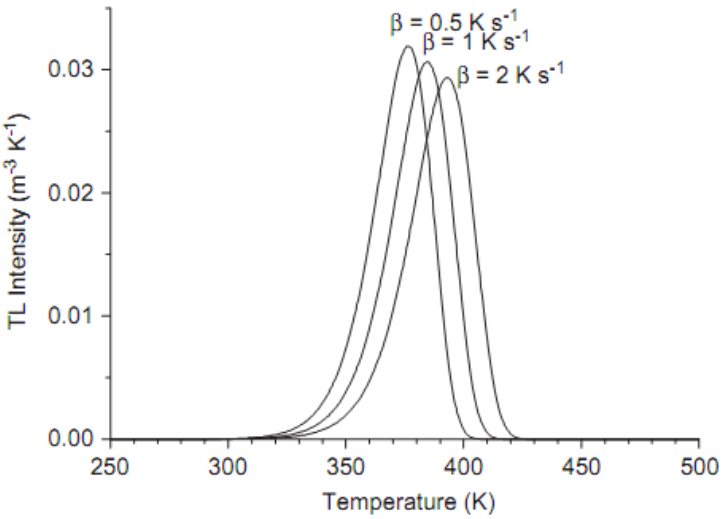

Figure 2.8. Result of the heating rate β on the shape and the location of a first-order Randall–Wilkins glow peak as a function of temperature [55].

Parameter values for Fig. 2.8: $n_0 = 1m^{-3}$; E = 1eV; $s = 1 \times 10^{12}\ s^{-1}$.

- ✓ If E and β are constant, n_o and the peak height changes. But the location of the peak does not change. This is a significant property of TL glow curves from the first order kinetic (Figure 2.9).
- ✓ The value of n_o depends on the pre-measurement dose.
- ✓ According to the Randall–Wilkins first-order TL equation (Eq. (2.20)), the geometry factor μ_g is described as $\mu_g = \delta/\omega$ that has a characteristic value of 0.42.

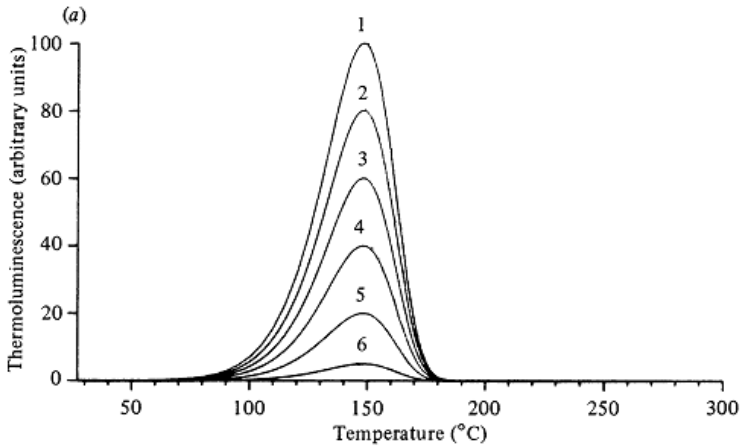

Figure 2.9. First-order-glow curves computed with E=1.0 eV, $s=10^{10}s^{-1}$, $\beta = 10\ ^{o}C\ min^{-1}$ [55].

The curves were calculated with initial trap charge concentrations (n_o) of (1) 1.0, (2) 0.8, (3) 0.6, (4) 0.4, (5) 0.2 and (6) 0.05× 10^{22} m^{-3}. Also the peak maximum location does not change with n_0.

- ✓ For a constant heating rate, with increasing steady-state trap depth (E), the maximum peak temperature T_M shifts towards higher temperatures regions, the peak height decreases and the width increases (Figure 2.10).

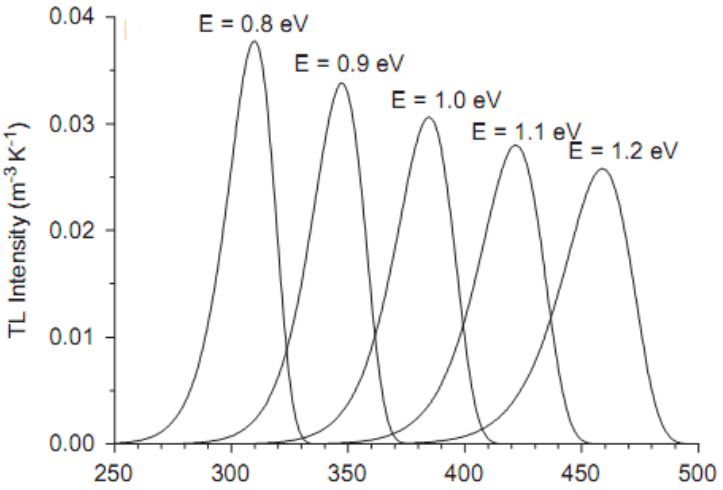

Figure 2.10. Features of first-order TL equation which is obtained the Randall–Wilkins, shows the difference with the activation energy E [55].

Parameter values for Fig. 2.10: n_0=1m^{-3}, s=1×10^{12} s^{-1}. The heating rate β=1Ks^{-1} for all curves.

- ✓ For a constant heating rate, the peak maximum T_M moves to higher temperatures, the peak height decreases and the width increases when the frequency aspect(s) decreases (Figure 2.11).

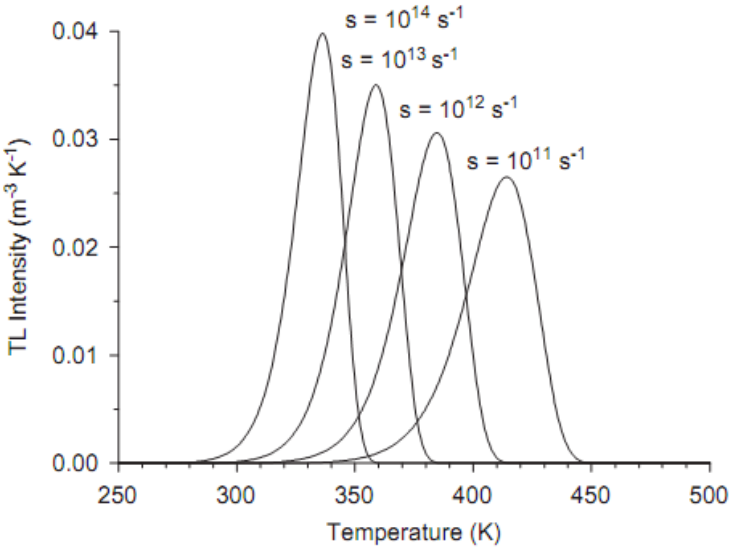

Figure 2.11. Features of first-order TL equation which is obtained the Randall–Wilkins shows the difference with the escape frequency s [55].

Parameter values for Fig. 2.11: n_o=1m^{-3};E=1.0 eV. The heating rate β=1Ks^{-1} for all curves.

- ✓ T_m is independent of n_0.
- ✓ Changes on the peaks: The position of the TL peak concentration does not change out of the temperature for the distinct irradiation dosages on the TL glow peaks from the first-order.
- ✓ Isothermal decay: Isothermal decay effects can supply independent knowledge on the kinetics of TL processes even at different temperatures. First order kinetics relate to exponential isothermal decay curves [51, 55-56].

2.5.2 Second-Order Kinetics (Garlick-Gibson Model)

Retrapping of released electrons controls the recombination of reverse charge carriers in a quick retrapping. Bahar and Göknil [98], at Garlick-Gibson model, much smaller time is necessary for trapped and stimulated electrons to have symmetry thermally as related to the recombination period on fast retrapping. They supposed that the escaping electron from the trap has the same probability of either recombining with hole in a recombination center or being retrapped.

Gibson and Garlick evaluated the probability that retrapping dominates i.e. $mA_m \ll (N-n)A_n$. Moreover they suppose that the trap is very remote from saturation, i.e. $N \ll n$ and n = m. So Eq. (2.14) reformed with these assumptions

$$I(T) = -\frac{dn}{dt} = s\frac{A_m}{NA_n}n^2 exp\left(-\frac{E}{kT}\right) \quad (2.25)$$

It is clearly seen that dn/dt is relative to n^2 which express a second-order effect. Integration of Eq.(2.25) can be explained with the extra statement of equal possibilities of retrapping and recombination, $A_m=A_n$, if a clear temperature profile is accepted. If it is accepted a fix temperature (phosphorescence decay) integration leads to Eq. (2.26) with α=s/N exp(−E/kT)

$$I(t) = \frac{I_o}{(1+n_o\alpha t)^2} \quad (2.26)$$

This variety of decay is called as second-order and noted as a particular case of Bequerel's decay law. It is realized that the decay is not exponential but hyperbolic for this situation of second-order kinetics. Then Eq. (2.27) can be obtained supposing a linear heating profile (according to Eq. (2.17)) integration of Eq. (2.25).

$$I(T) = \frac{n_o s}{N\beta} exp\left(-\frac{E}{kT}\right) exp\left[1 + \left(\frac{n_o s}{N\beta}\right)\int_{T_o}^{T} exp\left(-\frac{E}{kT^{\prime}}\right) dT'\right]^2 \quad (2.27)$$

The second-order kinetics for TL equation is shown above in Eq. (2.27). It is seen from Eq. that it is almost symmetric with the high temperature half of the curve considerably larger than the low temperature half by a distinguishing value of μg=0.52 is the key property of this curve. It is also supposed that significant intensities of released electrons are retrapped in a second-order reaction before recombination occurs, in that way it cause to a delay in the luminescence production and propagate out of the release over a broader temperature range. The first intensity is not seen here not only as a multiplicative constant as in the first-order case therefore its differences at dissimilar dose levels change the shape of the all curve. All these processes are shown in Fig. 2.12. It is seen from the figure that Tm decreases when there are no increases [57]. The change is 25 K with the coefficient values of Fig. 2.12. When E = 1 eV, T1 = 400 K

and the absorbed dose is raised with a factor 1000, which is easy to understand experimentally, a temperature moves of 77 K can be predictable. Coefficient values for Fig. 2.12, E = 1 eV, s/N = 1×10^{12} $s^{-1}m^3$. The heating rate β = 1 Ks^{-1} for all curves. Note that the maximum location of peak changes with n_o.

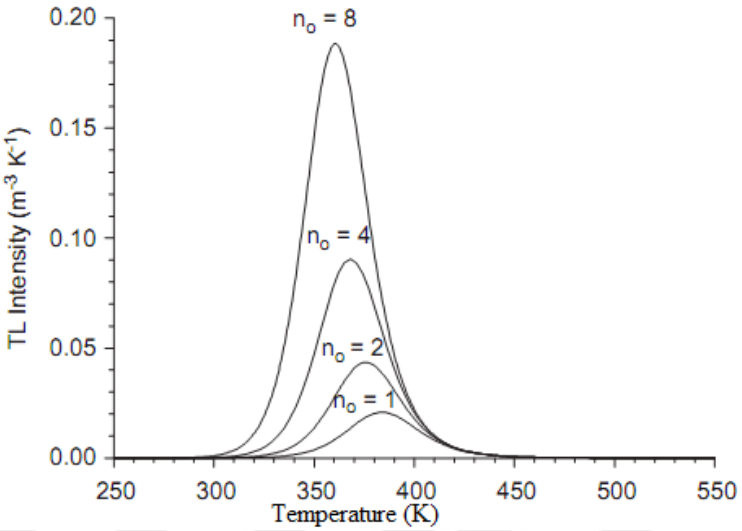

Figure 2.12. Features of first-order TL equation which is obtained the Randall–Wilkins shows the difference with the intensity of trapped charge carriers after irradiation n_o [55].

The similarity in dimension and location of a second-order peak as a function of E is shown in Figure 2.13. The area under the curve is, as in the case of first-order kinetics, relative to the first intensity n_o but the depth of peak is no longer straightly relative to the peak area, although the deflection is small. Coefficient values for Fig. 2.13: n_o = $1m^3$; s/N = 1×10^{12} s^{-1} m^3. The heating rate β = $1Ks^{-1}$ for all curves.

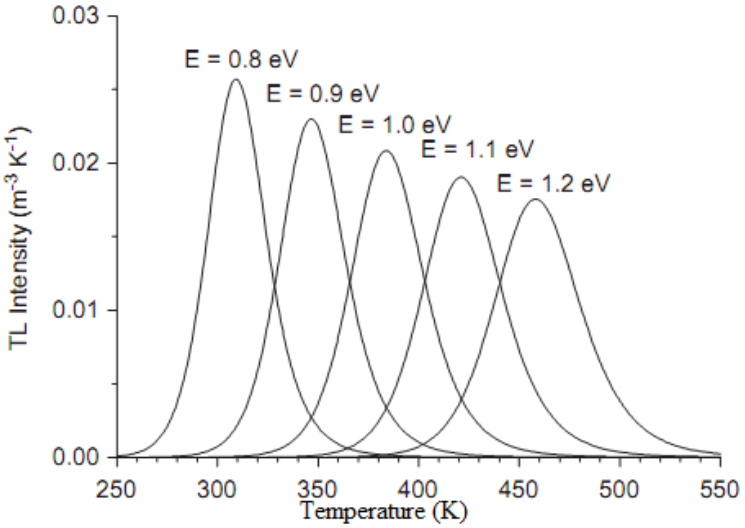

Figure 2.13. Features of first-order TL equation which is obtained the Randall–Wilkins shows the difference with the activation energy E [55].

The expression which is similar to the first-order case dominates the temperature dependency in the initial rise is $exp\left(-\frac{E}{kT}\right)$. So the "initial rise method" for the definition of the trap distance can be performed here too. Fig. 2.14 shows the similarity in dimension and location of a second-order peak as a function of s/N. Coefficient values for Fig. 2.14: n_o = 1 m^3; s/N = 1 × 10^{12} $s^{-1}m^3$. The heating rate β = 1 Ks^{-1} for all curves.

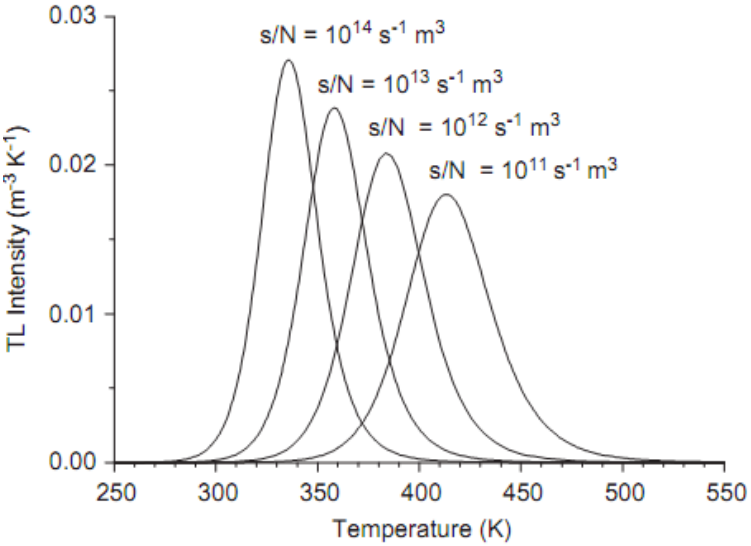

Figure 2.14. Features of first-order TL equation which is obtained the Randall–Wilkins shows the difference with s/N [55].

2.5.3 General-Order Kinetics (May-Partridge Model)

Bohum are proposed a method for the concentration of TL production experimentally to define the TL treatment of the trap levels not to comply with the characteristic of the second and first order kinetics [58]. The definition is shown in the following Eq. (2.28).

$I_{TL} = -\frac{dn}{dt} = -n^b s' \exp(-\frac{E}{kT})$, where $s' = \frac{s}{N^{b-1}}$

(2.28)

In equation (2.28), b refers to kinetic order and s' refers to pre-exponential factor. From the result of the differential equation above, Eq. (2.29) can be obtained.

$$n = n_o \left[1 + (b-1)\frac{s'}{\beta} n_o^{(b-1)} \int_{T_o}^{T} \exp(-\frac{E}{kT}) dT\right]^{-\frac{1}{b-1}} \quad (2.29)$$

Solving the Eq. (2.29) with (2.28), the TL concentration can be defined as in Eq. (2.30) for the traps showing the features of common order kinetic.

$$I_{TL} = n_o s'' \exp(-\frac{E}{kT}) \left[1 + (b-1)\frac{s''}{\beta} \int_{T_o}^{T} \exp(-\frac{E}{kT}) dT\right]^{-\frac{b}{b-1}} \quad (2.30)$$

Where $s'' = s' n_o^{(b-1)}$ and it has a size of s^{-1} same with frequency factor. The Eq. (2.30) agrees to the second order kinetics when the b is equal to two and it decreases to the first order kinetics as the kinetic order b goes to one.

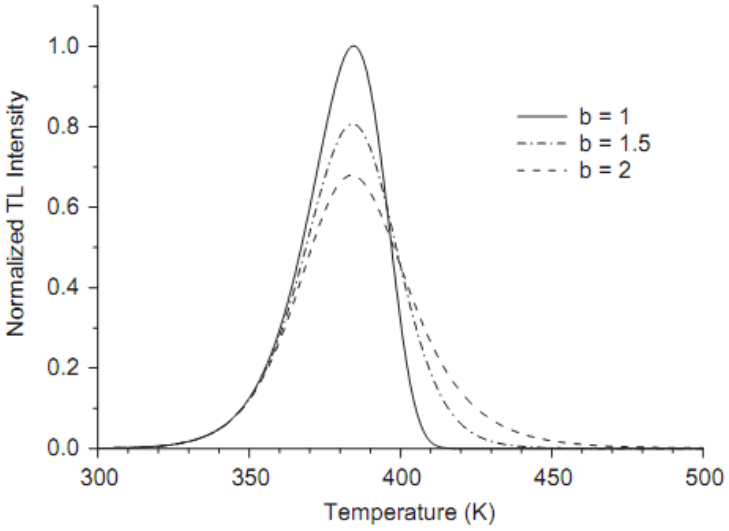

Figure 2.15. Relationship of first-order (b = 1), intermediate-order (b = 1.5) and second-order (b = 2) TL glow peaks, with E = 1eV, s = 1×10^{12} s^{-1} and β=1Ks^{-1} [55].

The glow peaks are regulated to the first-order glow peak. Also all glow peaks encounter in the initial rising part of the curve.

2.6 Theoretical Approach to TL Analysis Methods

A lot of analysis methods in literature can apply TL curves which obtained experimentally. In this part of the thesis, it is taken into account to explain those of the crucial and fruitful analysis techniques which it is used to reach the results of analysis. Applications of curve fitting, peak shape, heating rate and initial rise methods were described in this part particularly.

2.6.1 Curve Fitting Method

Curve fitting (CF) method is utilized to calculate the energies of activation of traps present in the forbidden energy state of insulators and semiconductors. CF method is also useful to explain the kinetics orders. Thus the Eq. (2.20), (2.27) and (2.30) are performed to the experimental TL glow curve by using software [44]. Eq. (2.20) provides the TL concentration for the first order kinetics even though the Eq. (2.27) and (2.30) are dependable for general and second order kinetics, respectively. With

respect to the TL curves' geometry, an equations is used to obtain the best fitting curve convenient with activation energy and the experimental TL curve so the order of kinetics can be found for the traps.

2.6.2 Initial Rise Method

According to this method, the concentration of trapped electrons at the starting of the TL glow curve varies very tiny with temperature and thus it occurs constantly. Initial rise (IR) method is important and widely used methods to describe the trapping levels' activation energy in the TL peaks' analysis due to its unchallenged benefit. IR method is entirely self-governing of the trapping treat and can be used for the entire peaks in any case of the dominant kinetic orders of the traps. For that reason, usage of IR method comprises an opportunity to check the value of activation energy with other techniques dependent on the kinetic orders. Charge carriers which are trapped should be relative to $\exp(-\frac{E}{kT})$ when the excitation of the charge carriers which are trapped to the non-localized states occur, the TL curve's first tail is taken under importance for analysis so the trapped charge carriers associated to the TL glow curve's first tail are supposed to be fixed [53]. In that way, scheming a chart of 1/T versus ln(I) gives a straight line and the gradient of the graph provides the activation energy (–E/k) of the trapping levels as shown in figure 2.16.

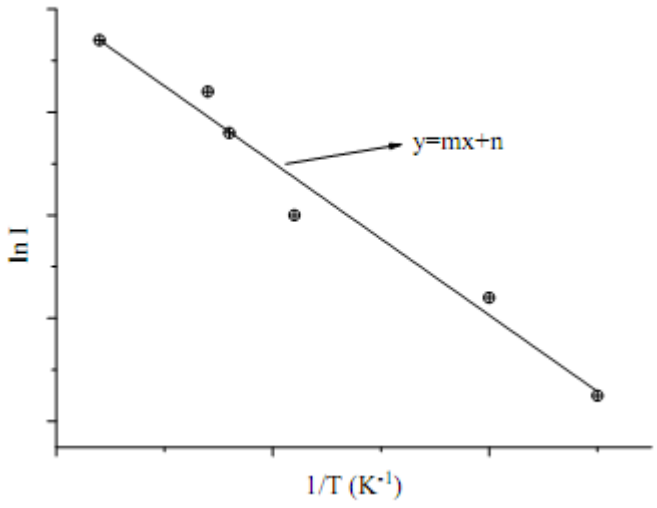

Figure 2.16. Initial rise graph [110].

2.6.3 Heating Rate Method

The heating rate influences the TL glow curve characteristics. The glow peak moves to high temperature regions when the heating ratio increases, all the peaks enlarge and the TL intensity decreases. Due to thermal decrease, TL intensity also decreases. The difference of heating rate (β) is an important marvel which effects the TL process of the trapping levels. The charge carriers' stimulation trapped in the energy levels in the forbidden band of the solid is straightly related to β which plays a key role for location of TL peaks. Even if the factor β is critical for the TL curves of a certain trap, it is not depends the activation energy of the trap levels. In this view, whatsoever the β is used to get the TL curve, the activation energy related to this curve needs to be fixed. There are many computation methods for activation energy for TL theory. For our experiments, it is used the well-known two computation methods. One of them can be implemented to TL glow peak which is obtained experimentally by the next equation using a few heating ratios [53]. A relationship has developed to calculate frequency factor and the activation energy using two different heating rates and first-order maximum emission conditions while operating independently of each other as shown in Eq. (2.31) and (2.32) [59-61].

$$\frac{\beta_1 E}{kT_{M_1}^2} = sexp\left(-\frac{E}{kT_{M_1}}\right) \tag{2.31}$$

$$\frac{\beta_2 E}{kT_{M_2}^2} = sexp\left(-\frac{E}{kT_{M_2}}\right) \tag{2.32}$$

If these two relations are proportional to the each other and one can obtain E as in Eq. (2.33)

$$E = k\left(\frac{T_{M_1}T_{M_2}}{T_{M_1}-T_{M_2}}\right) ln\left[\left(\frac{\beta_1}{\beta_2}\right)\left(\frac{T_{M_2}}{T_{M_1}}\right)^2\right] \tag{2.33}$$

Eq. 2.33 then can be applied to first order kinetic equations. For example, the peak temperatures corresponding to the TL peak intensities selected at $\beta_1 = 1\ ^oC/s$ and $\beta_2 = 2\ ^oC/s$ and obtained at both heating rates can be measured and calculated easily

using Eq. (2.33). This calculated value of E can be specified separately for the two heating rates in equations (2.31) and (2.32) to determine the value of s.

2.6.4 Peak Shape Method

The TL glow peaks' appearance of illustrates geometrical changes is dependent of the trapping method of the stimulated charge carriers from trap levels. Because of trapped charge carriers recombines to reverse ones without retrapping, decreasing portion of the TL curves appears slimmer than the rising part. Moreover, before recombination, if the electrons and holes are captured, rising portion of the TL glow curve begins to be slimmer with increasing amount of retrapped charge carriers. The difference between the TL peaks straightly influences the trapping factors of the energy levels. Peak shape (PS) is the most operational methods to analyze of the TL peaks and offers dependable results. Geometry factor (μ_g) and activation energy can be obtained using the geometric construction of the single glow peak. According to peak shape method, high (T_h) and low (T_l) temperatures edges at half maximum concentration and (T_m), the maximum temperature of peak rate of the TL glow curve support us to calculate the the charge carrier of activation energies emitted from trap using the factors: $\tau = T_m - T_l$, $\delta = T_h - T_m$, $w = T_h - T_I$ and $\mu = \delta/w$ in the following Eqs. (2.34), (2.35) and (2.36) [43].

$$E_\tau = \frac{[1.51+3.0(\mu_g-0.42)]kT_M^2}{\tau} - \left[1.58 + 4.2(\mu_g - 0.42)\right]2kT_m \quad (2.34)$$

$$E_\delta = \frac{[0.976+7.3(\mu_g-0.42)]kT_M^2}{\delta} \quad (2.35)$$

$$E_W = \frac{[2.52+10.2(\mu_g-0.42)]kT_M^2}{W} - 2kT_m \quad (2.36)$$

The frequency factor s, in the general order kinetic which is also defined as pre-exponential factor, can be obtained using the following equations for first order in Eq. (2.24) and general order in Eq. (2.37) kinetics respectively.

$$s = \frac{\beta E}{kT_m{}^2}\left[exp\left(-\frac{E}{kT_m}\right)\left(1 + (b-1)\frac{2kT_m}{E}\right)\right]^{\frac{b}{b-1}} \quad (2.37)$$

2.6.5 Dose Response Method

This method is used to obtain the kinetics order of each glow peak in the glow curve. In the first order kinetics of the TL theory, the maximum temperatures of the glow peaks change only when the heating rate changes. If the heating rate is constant, the maximum temperature does not change with the dose ratio and stays constant within the experimental error limits ($\pm 2\ ^{o}C$) because there is no initially trapped electron number in the maximum emission situation. In the second and general order of kinetics, peak temperatures move in the direction of lower temperatures regions with increasing dose ratio. If the dose ratio increases by a parameter of f, the slope is obtained as in Eq. (2.38) at the maximum peak.

$$\Delta T = T_1 - T_2 = \frac{T_1 T_2 k(i-1)}{E \ln f} \tag{2.38}$$

If $T_1 = T_2$, it is the individual peak location. If $T_1 > T_2$, it is the peak location after dose increases [57].

2.6.6 Computer Glow Curve Deconvolution (CGCD) Method

Computer Glow-Curve Deconvolution (CGCD) is the most mutual programs used to decide trap factors from TL glow curves. This program is actually used to analyze the glow curve. The main CGCD programs can be obtainable free of charge by the programmers are GlowFit [53], MATLAB-based GCAFIT [63], which can decompose only the first- The TL Glow Curve Analyzer (TLanal) programs written by Ki Soo Chung et al. [64] from the Korean Atom Energy Research Institute and which can completely decompose the kinetic parameters [56]. The algorithms of these programs are based on the numerical solutions of the basic thermoluminescence kinetic factors. The program can convolute as many as nine glow peaks from glow curve instantaneously. Two separate models were utilized in the computer program. The TL glow curve is estimated from first order TL kinetic by the Eq. (2.39) in the first program.

$$I(T) = n_o s exp\left(-\frac{E}{kT}\right) exp\left[-\left(\frac{s}{\beta}\right)\frac{kT^2}{E} exp\left(-\frac{E}{kT}\right) * \left(0.9920 - 1.620\frac{kT}{E_a}\right)\right] \quad (2.39)$$

The glow curve is estimated with general order TL kinetics with using the Eq. (2.40) in the second program.

$$I(T) = n_o s exp\left(-\frac{E}{kT}\right) exp\left[1 + \left(-\frac{(b-1)s}{\beta}\right)\frac{kT^2}{E} exp\left(-\frac{E}{kT}\right) * \left(0.992 - 1.620\frac{kT}{E_a}\right)\right]^{\frac{b}{b-1}} \quad (2.40)$$

n_o (m^{-3}): at t=0, intensity of trapped electrons,
s (s^{-1}): the frequency parameter for first-order and the pre-exponential parameter for the general-order,
T (K): the absolute temperature,
E (eV): the activation energy,
β ($^oCs^{-1}$): heating ratio,
k (eVK^{-1}): Boltzmann's constant,
b: the kinetic order.

The summary of all of the peaks and background influence can lead to multiple glow curve equation as illustrated in Eq. (2.41),

$$I(T) = \sum_{i=1}^{n} I_i\,(T) + a + bexp(T) \quad (2.41)$$

In Eq. I(T) refers to suitable whole glow curve and it allows for the electronic noise influence to the planchet and dosimeters infrared influence to the background.
Starting from the Eq. 2.31, the least square minimization procedure and Figure of Merit (FOM) were used to evaluate the appropriate results if they are good enough or not. i.e as shown in Eq. (2.42).

$$FOM = \sum_{i=1}^{n} \frac{|N_i(T) - I(T)|}{A} = \sum_{i=1}^{n} \frac{|\Delta N_i|}{A} \quad (2.42)$$

In this Eq.,
$N_i(T)$: i-th experimental points (total n=200 data points),

I(T): i-th suitable points,

A: integrated area of the suitable glow curve.

The ratio of the FOM decides the fit value by using experiences in [57-58]. If this value are between 0.0% and 2.5% the fit is enough, 2.5 % and 3.5% the fit is fair, and > 3.5% the fit is bad. The computer program also plots the function to have a graphic demonstration of the arrangement between the experimental and fitted glow curves,

$$X(T) = \frac{N_i(T) - I_i(T)}{\sqrt{I_i(T)}} \quad (2.43)$$

which is a standard variable with an expected value=0 and σ=1 where σ^2(T)=I_i(T).

2.7 Reproducibility (Cycle of Measurements)

One of the most important requirements of dosimeter is reproducibility and it is known as cycle of measurement. The same results should be obtained after each repeat of the experiment. We know that this intensity and glow curve can change with the repeat of the experiment. This may be due to the alteration or opening of the traps in the sample at the end of each repetition. Such a change may be harmful to the simple calculation of the measured result; however, a detailed change in sensitivity may increase knowledge about the substance being investigated. During dose measurement with a dosimeter, changing the TL concentration may prevent accurate results [53]. A standard deviation of ± 2% or less is the index for good reproducibility [68].

2.8 Theory of Fading

Fading is the treat in which there is an accidental loss of the hidden knowledge such as its reaction. The TL-signal decreases or fades, with increasing time. The fading has a number of explanations and consist of thermal fading, anomalous fading and fading owing to optical effects. The dominant module is thermal fading, in which the release of trapped charges is thermally induced [69]. In the thermal fading, the traps that present lower entrapment energy will fade quicker than the energetic ones owing to their upper probability of change. This can produce big errors in the dose calculation

[70].The time constant for the thermally induced release of trapped charge from a defect is given in Eq. (2.1).

In principle, the two parameters which dictate the thermal fading rate are the frequency factor s and the trap depth E. As a result of evaluation of these for particular dosimetric peaks has been an important part of TLD material characterization. Nevertheless, the thermally induced loss of the TL signal with time can also be caused by processes other than the simple charge release mechanisms alluded to above. The high temperature pre-irradiation annealing conditions employed with many TLD materials to ensure re-usability place the samples in thermodynamically metastable states. Therefore, the materials should be used as soon as possible after the pre-irradiation annealing treatment [70].

When the TL-signal decays suggestively, even though it is not expected to do so thermally this happen known as anomalous fading is. It is believed that there are two main explanations: quantum mechanical tunneling of the trapped charge carrier to the recombination site and localized transitions which do not occur by the delocalized bands [70]. Localized transition is thermally induced occupation of an energy level from which a transition into the recombination center is allowed [69]. Optical properties contain optical excitation of the charge from the trap and subsequently a decrease in the TL-signal [71].

2.9 Luminescence in Retrospective Dosimetry

The measureable calculation of the radiation dose to the general population needs the accessibility of appropriate methods with amount of nuclear radiation accident and events for reconstruction of doses. Dose reconstruction can be described as the treat of estimating doses to the public from previous releases of radionuclides to the environment and dose reconstruction contributes to society in the following ways: 1) by helping to better understand the significance of past releases of contaminants to the environment, 2) when combined with epidemiology, dose reconstruction provides new information on the implications of risk associated with exposure to environmental radiation and 3) because these studies are leading the way in the designing and testing of measurement methodologies and mathematical models that predict the transport of radionuclides, these studies can thus be helpful in risk analysis and decision making for decontamination of old sites, and evaluation of new sites. [48].

In conditions where no straight radiation observing data are available, luminescence dose reconstruction which gotten using material from the persons in the neighborhood of the incident/accident or from the location of population clearly can be used to confirm values obtained from measurable techniques. TL method has been used in dose calculation in Nagasaki and Hiroshima Atomic bomb explosion sites effectively in Japan [72, 73]. Radioactive effect from the Chernobyl nuclear reactor accident [75] and at Nevada test sites in USA, it also used in the radioactive effect of nuclear tests [74].

CHAPTER 3:

THERMOLUMINESCENCE IN CERAMICS

Ceramics are categorized as inorganic and nonmetallic materials and they are necessary at our daily life cycle such as dental ceramics is an expression of glass-ceramic and porcelain materials that are used restorative apparatuses of teeth, in the production of crowns and prosthetic teeth. It is powerfully sensitive to radiation and the concentration of both the TL and OSL signals are relative to the absorbed radiation dose. Commonly used ceramic materials fix the revelation luminescent features in dental prosthetics. Because of their usage in the body, these materials have an importance in conditions possibly where retrospective dosimetry for persons is necessary but where observing was not planned [40]. The widespread cycle of examination essential for each of the above dosimetry applications underlines the mobility of the features of the luminescent minerals contained by ceramics. The features of such minerals (typically quartz and feldspar) often change with thermal history; as a result building and domestic ceramics do not certainly take the same dose response characteristics. Because of its translucency, dental ceramics are reflected the most biological-looking restorative material for aesthetic rehabilitation. Ceramic dental materials can be produced with different colors that make them identical from the biological dentition. Furthermore, ceramics do not certificate the absorption of dental plaque by products by having an external surface of metal oxides, eliminating therefore, the problem of surface color alterations, unlike composite resin. Because of these reasons, dental ceramics has increasingly become the most used aesthetic restorative material in dentistry [68].

The ceramic materials that used for dose calculation studies with thermoluminescence techniques which especially obtained from buildings as a retrospective dosimetry [69-71]. It is proven that ceramic is a suitable material for defining the exposed dose to the population in nuclear accident regions. Appropriate dosimeters in the region of a nuclear accident are plant pots, insulators, tiles, crockery porcelains and house bricks [39, 72, 73].

Authors showed the possibility of the usage of dental restorative ceramic as a dosimetric material with thermally stimulated electronic emission (TSEE) and thermoluminescence (TL) techniques in 1979 [74]. The dental restorative porcelain was also investigated as a TL dosimeter to estimate high doses in radiological accidents [75]. Authors further underlined the TL and OSL characteristics of dental ceramic for retrospective dosimetry, TL peaks of prosthetic ceramic (~250 µm thickness slices, heated at 2 $^{o}C.s^{-1}$) was found to be linear with dose-response in the range < 100 mGy to 10 Gy. Though TL and OSL peaks displayed fading more than 50 % over one week, its potential was appropriate for retrospective dosimetry applications [40]. As the type of dental ceramics over developed and compositions also changed day by day, with the availability of thermally stimulated luminescence (TL) measurement techniques, thermoluminescence properties of dental restorative ceramics which is commonly used for retrospective dosimetry are reported in this thesis.

3.1 Structure and Properties of Ceramics

Ceramic, which name comes from the Greek word, firstly have been utilized by people for pottery. It is also utilized to define a broad variety of materials that contain brick, glass, pottery, enamel, concrete, porcelain, cement and chinaware. This kind of materials is very broad and it is often simpler to describe ceramics as all solid materials apart from some metals and their alloys which are prepared by the high-temperature treating of inorganic raw materials. The ceramics show either crystalline or glass-like feature. They can be either single-phase materials, pure or combinations of two or more separate materials. Most ceramics are known as polycrystalline materials, with quick variations in crystal direction or components across each grain in the structure. Ceramic materials can have electrical conductivities that look like metals, such as CrO_2 and ReO_3. Tremendous insulators can also be produced by the ceramics such as the glass-ceramics that used in spark plugs. The characteristic features of ceramics is their resistance to being shaped or controlled after they are fired. They cannot be sold by the foot or cut to fit on the job with a clear exclusions such as glass tubing or plate glass. Their dimension and form must be defined on before they are fired and when they break they must be exchanged without repair.

The main distinction between ceramics and other materials is the chemical bonds that hold these materials composed. They are usually considered by ionic bonds between negative and positive ions although they can covalently bond, such as the Si−O−Si linkages in glass. The strong strength of fascination between ions of reverse charge in the planes of ions makes it complicated for one plane to slip past another when they arrange crystals. Therefore ceramics can be easily broken. They attack compression, nevertheless they are prominently fragile to stress applied in the form of bending [76]. The usage of ceramics was discovered at Neolithic times, when clay was used firstly to create bowls that were baked in campfires. Clay is shaped by the weathering of rock to form sand like grains of silica and alumina that retain together when it is wetted to form clay crystals, like as kaolinite, which has the formula $Al_4Si_4O_{10}(OH)_8$.

Nowadays, ceramics show a significant character in the examination of materials that can act as caustic, stand thermal shock or have a well weight-intensity ratio. For example, alumina ceramics are utilized for rocket while silicon carbide (SiC), rocket nose cones and molybdenum disilicide ($MoSi_2$) are utilized in rocket nozzles. Ceramic slates are utilized for thermal isolation to defend the Space Shuttle on return from side to side of the Earth's atmosphere.

Ceramics which are produced from uranium dioxide (UO_2) is utilized for nuclear power plants as the energy elements. For example, ceramic materials are used as laser materials, from the chromium-doped crystals that spread a coherent monochromatic pulse of light to the optics along with the light transition. $BaTiO_3$ is utilized to produce ceramic capacitors that have a big capacitance and it is also utilized to produce piezoelectric materials that produce an electric charge when exposed to a mechanical stress, which are the essentials of phonograph cartridges, ultrasonic devices and sonar. Magnetic ceramics are also utilized in computer memory, permanent magnets and telecommunications and they are shaped by confused FeO, ZnO, NiO, MnO, SrO or BaO with Fe_2O_3. On the other hand, ceramics have an enormous usage in dentistry areas such as synthetic denture teeth, bridges, crowns, abutments, ceramic posts and implants and veneers over metal infrastructure [77-79]. Dental ceramics are generally applied to nonmetallic, inorganic constructions mostly include mixtures of oxygen with one or semi-metallic or more metallic elements such as sodium, aluminum, , lithium, magnesium, potassium, phosphorus, silicon, calcium, titanium and zirconium [77, 80]. Porcelain has a white color and translucent ceramic that is fired to a glazed state [82]. Dental porcelains can be categorized based on their, microstructure, melting

temperature and treating technique [77, 83, 84].The porcelain can also be applied to a particular compositional ratio of ceramic materials which are produced by confusing quartz, kaolin, and feldspar in appropriate amount and fired at high temperature [77, 80, 81].

Ceramics may also be categorized according to their physical combinations, for example, A_mX_n where A metal, X, nonmetal element, n and m refers to integers and the most basic form of this system is the AX structure (m = n = 1), where there are three forms of CsI, CsCl and CsBr as shown in Fig. 3.1. CsCl has a simple cubic shape, as shown in Figure 3.1a. However it should not be mixed with the body-centered cubic (bcc) shape which would have the similar ion or atom occupying the center of the unit cell. For example, CsI and CsBr have the similar CsCl structure. The NaCl has a face-centered cubic (fcc) structure, where negative (Cl^-) and positive (Na^+) ions are enclosed by 6 reverse ions (CN = 6) such as rock salt structure; NiO, CaO, CdO, BaO, SrO, MnO, FeO, CoO, and MgO, which belong to the similar group [85].

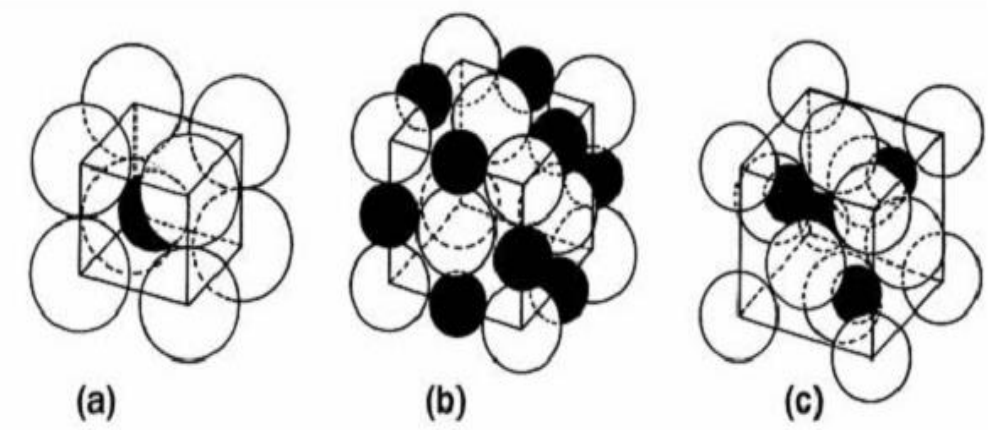

Figure 3.1. AX constructions of ceramics: (a) CsCl; (b) NaCl; (c) ZnS. The dark spheres show the positive ions (A^+) and the circled ones shows the negative ions (X^-) [113].

Crystalline or amorphous solids are one of the ceramic structures [77, 80] and they are also called as glasses. Therefore, ceramic materials can be categorized as crystalline and non-crystalline (amorphous solids or glasses) ceramics generally. The mechanical and optical features of dental ceramics principally hinge on the character and the

quantity of crystalline phase present. More the transparency of ceramics more the glassy phase; conversely, it reduce the power of the structure by decreasing the resistance to crack spreading. Alternatively, more the crystalline phase better will be the mechanical properties which in turn would alter the aesthetics [77, 81]. Feldspathic or conventional porcelains are generally known as non-crystalline ceramics. These conventional porcelains are very powerless and fragile in landscape even under low pressures. The improving of crystalline porcelains have started with developments in the treating technology of dental ceramics by an appropriate fillers such as alumina, zirconia and hydroxy apatite [77, 86, 87].

3.1.1 Non-Crystalline Ceramics

Crystalline minerals consist of alumina, silica and feldspar in an amorphous (non-crystalline matrix of glass) glazed phase. The glass-shaping matrix of dental porcelains utilizes the simple silicone oxygen (Si-O) network with the silicon atom merging with 4 oxygen atoms, shaping a tetrahedral formation as shown in Figure 3.2 in which the bigger oxygen atoms attend as a matrix, with the smaller metal atoms such as silicone put into spaces between the oxygen atoms. Thus each silica unit contains a single silicone atom (Si) enclosed by four oxygen atoms (O).

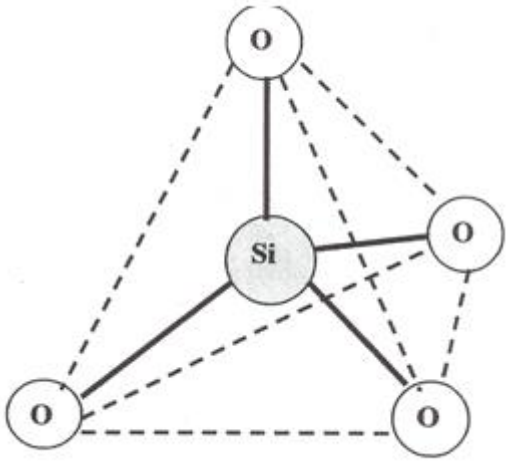

Figure 3.2. Tetrahedral formation of Silica [113].

The atomic bonds in this glass construction have both a covalent and ionic nature so as to make it stable and also silica units to link with each other to shape a chain

formation. Some related silicate component chains shape the continuous SiO_4 (tetrahedral network) in glass as shown in Figure 3.3. This stable construction gives some important features such as excellent thermal and optical insulating characteristics with strong atomic bonds and no free electrons, inertness transparency to the glass matrix. On the other hand, these robust dual bonds may also give fragility to the glass matrix leading to the fracture even under low pressure applications [88-91].

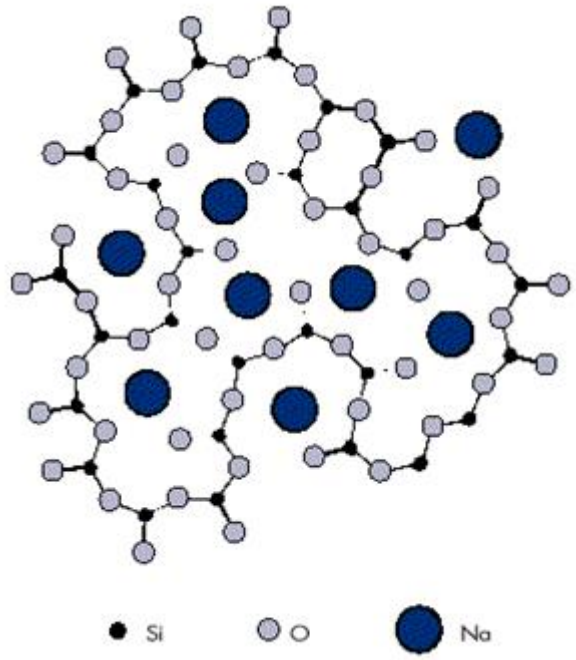

Figure 3.3. Glass construction with the existence of large alkali cations [113].

3.1.2 Crystalline Ceramics

Ceramics are powered with crystalline components such as leucite and alumina into the glass matrix to shape crystal glass combinations as a part of powering the material and recovering its fragile resistance (spreading powering). In [88] the generation of strengthening porcelains for porcelain jacket crowns are introduced first time, which are generally referred to as “aluminous porcelains”. Covalent crystals are very hard and have a big tender point, e.g. silicone carbide.

3.2 Dental Ceramics

In this thesis three types of dental ceramics were used which are glass ceramic (IPS e.max Ceram, Ivoclar Vivadent SW), feldspathic ceramic (IPS Classic, Ivoclar Vivadent TR) and lithium disilicate ceramic (IPS e.max (LS_2), Ivoclar Vivadent TR). All of these ceramics used for dental restorations available on the Swedish and Turkish dental market, Ivoclar Vivadent.

3.2.1 Dental Glass Ceramic

Dental ceramic restoration or prosthesis are frequently used by people. It is known that different types of dental ceramic show a luminescence feature as a result of irradiation and stimulation. Glass ceramic is also frequently utilized in dentistry. New results are added to literature on the dosimetry subject by using this sample in this study [67, 92, 93]. One of the innovative materials utilized in renovations and dental prostheses for the dosimetric application is the fluorapatite veneering glass-ceramic. This material is frequently utilized in mixture of alumina (Al_2O_3) or zirconia (ZrO_2) core and shows luminescence property. Dosimetry features of the ceramic were also examined by using thermoluminescence (TL). We focused on the optimization of the obtained technique and examination of heating rate of TL signals, fading, dose response and features as reproducibility. Dental glass ceramics which available on IPS e.max Ceram, Ivoclar Vivadent SW company were firstly examined by Mauricio et al. [94] and its components was selected as: P_2O_5, F(2-6%), Na_2O(6-9%), Al_2O_3 (8-12%), K_2O(6-8%), ZnO (2-3%), CaO, SiO_2 (60-65%), other oxides (2-8%) and pigments (1%). Fig.3.4 showed the x-ray diffraction spectrum of dental ceramic.

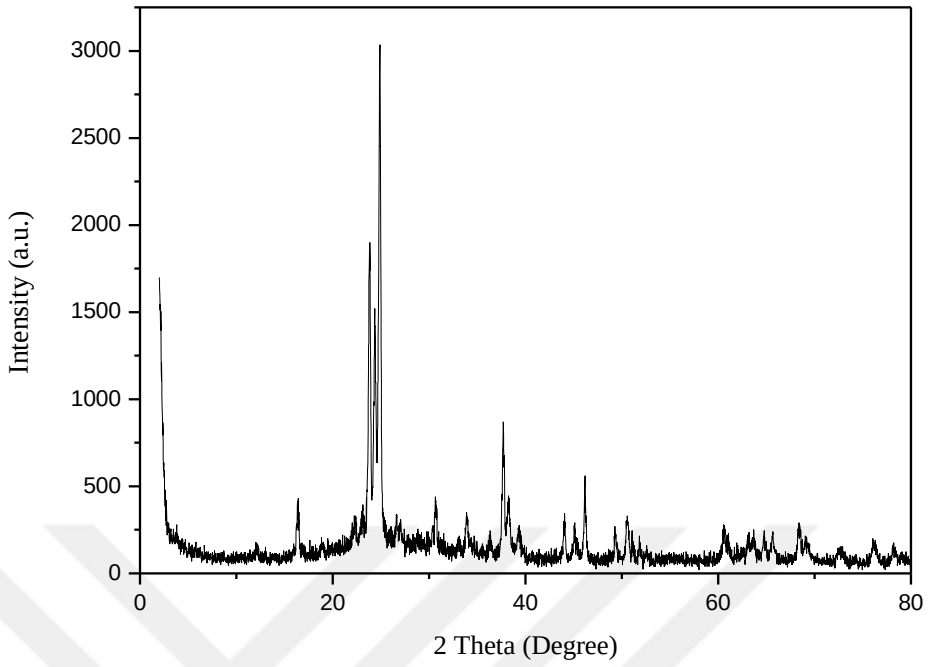

Figure 3.4. X-ray diffraction pattern of dental glass ceramic.

Authors studied numerous dental ceramics of different brands to measure beta dose rates, including zirconia-based ceramics, glass ceramic, feldspathic ceramic and other materials which frequently utilized in dentistry [68]. The radioactivity substance of these materials was sufficiently below the levels that found in the period when adding up to uranium to dental porcelain materials was still allowable [68].

Authors were also examined a possible usage of some kinds of dental ceramics in an accidental dosimetry treatments with TSL and OSL techniques [92]. They concluded from their study that the susceptibility of ionizing radiation was verified and this susceptibility powerfully depends on the kind and brand of ceramic with minimum measurable dose ranging from a small number of mGy up to a few tens of mGy [92].

3.2.2 Feldspathic Ceramic

Although ceramics and glasses show a high compressed force, they can be broken even under very low force (0.1%, 0.2%). Glass-based systems are prepared from some materials and these materials include mostly silicon dioxide (also known as silica or quartz), which includes several quantities of alumina. Aluminosilicates, include numerous quantities of sodium and potassium and known as feldspars. Feldspars are

reformed with many ways to generate the glass that utilized generally in dentistry. For dental ceramics, synthetic structures of alumina silicate glasses are also developed. Dental feldspathic ceramics which available on IPS Classic, Ivoclar Vivadent TR company were examined firstly by McKeever et. al. [68] and its composition is selected as: SiO_2 (59.5-65.5%), Al_2O_3 (13-18%), Na_2O(4-8%), K_2O(10-14%), other oxides (0-3.5%) and pigments (0-2%). Fig.3.5 showed the x-ray diffraction spectrum of dental feldspathic ceramic. Dental feldspathic ceramics were also investigated by Veronese et. al. [92] and authors are concluded from their study that solid and powder form shows same properties. We used solid and powder form of dental feldspathic ceramics in our study and we could not observe any difference between them too.
Luminescence features of several feldspathic ceramics which utilized in the producing of dental crowns were examined with respect to their utility as ubiquitous retrospective dosimeters [95]. Some samples showed weak TL and OSL signals with high natural signals values balanced to the 1.5 Gy related to signals and a linear, as well as, a cubic dose requirement in the deliberated dose ratios (1.5–12 Gy) [95].

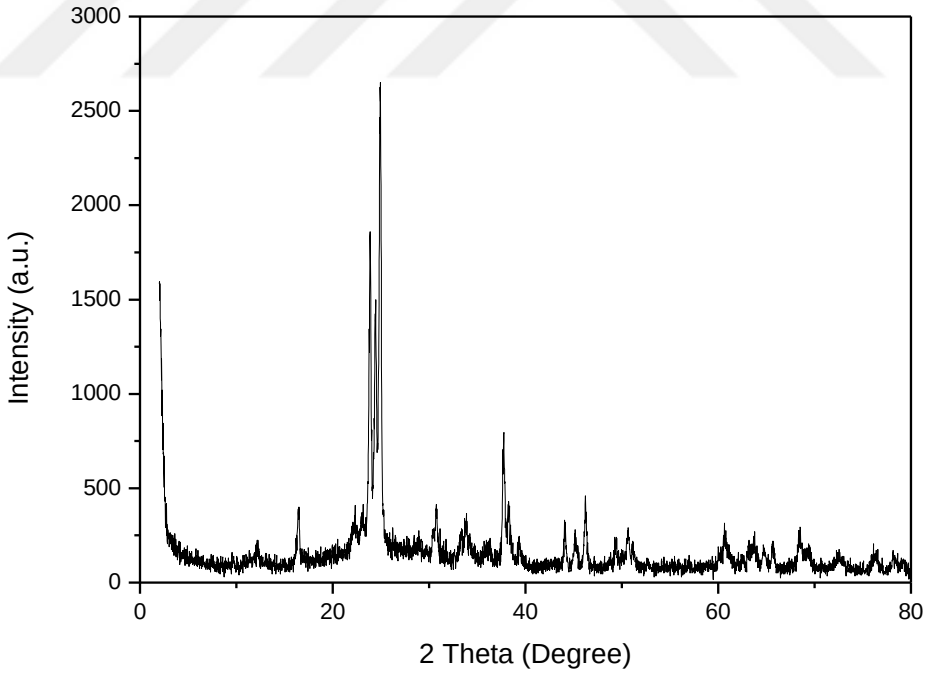

Figure 3.5. X-ray diffraction pattern of feldspathic dental ceramic.

3.2.3 Lithium Disilicate Glass Ceramic

Lithium disilicate glass porcelain was first developed in 1959. However, this material has disadvantages of low chemical resistance, insufficient semi-permeability, uncontrolled micro-crack formation and complicated and time-consuming lab steps and the use of the denture has been also abandoned [96]. Authors have developed a system by forming crystals of SiO_2-Li_2O in glass-phase P_2O_5-added lithium disilicate ($Li_2Si_2O_5$) and lithium orthophosphate (Li_3PO_4) crystals [97, 98]. The chemical structure of lithium disilicate which used today is described by Schweiger et. al. [99]. Dental lithium disilicate glass ceramic which is available on the Turkish dental market (IPS e.max (LS2), Ivoclar Vivadent TR). Its composition is: K_2O(0.0 – 13.0 %) , MgO (0.0 – 5.0 %), Al_2O_3 (0.0 – 5.0 %), P_2O_5 (0.0 – 11.0 %), ZrO_2 (0.0 – 8.0 %), ZnO (0.0 – 8.0 %), Li_2O (11.0 – 19.0 %), SiO_2 (57.0 – 80.0%), colouring oxides (0.0 – 8.0%) and pigments (0-2%). Fig.3.6 showed the x-ray diffraction spectrum of dental ceramic.

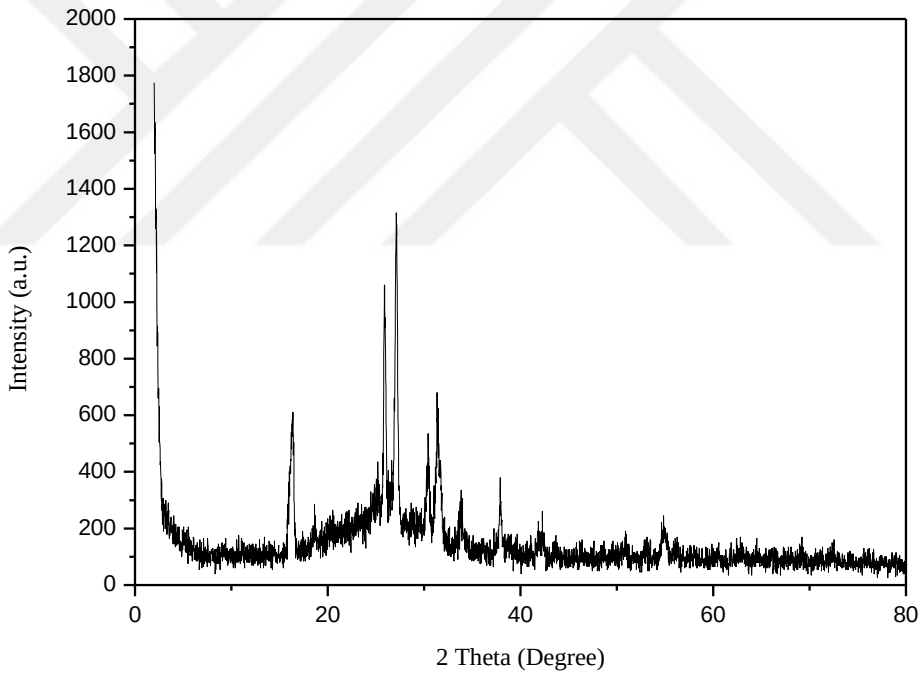

Figure 3.6. X-ray diffraction pattern of lithium disilicate glass ceramic.

3.3 Characterization of Microstructure

The physical feature of ceramics depends on their microstructure, which may be categorized in terms of the comparative quantity of each, the dimension, the amount

and forms of current phase and orientation of each phase. Microstructures is normally tested by thin slice (15–30 μm) on silicon carbide-dressed wafer saw or a diamond and polishing by a rating series of sandpaper. The last polishing includes utilizing diamond paste or alumina on a wheel. Under a plain or polarized light microscope, the thin sections can be detected. If the specimen is attached to a polymer resin and only one side is brightened, a reflected light microscope may be utilized. Because of the large wavelength of light ($\lambda \sim 10^{-6}$ m), optical microscopy can enlarge an object up to 1,500 times, however in theory, transmission and scanning electron microscopy (SEM and TEM) can enlarge an object more than 1,000,000 times ($\lambda \sim 10^{-12}$ m). Furthermore, electron diffraction can be undertaken using TEM, which gives a better understanding of microstructure and fundamental analysis can be organized with an SEM electron microprobe.

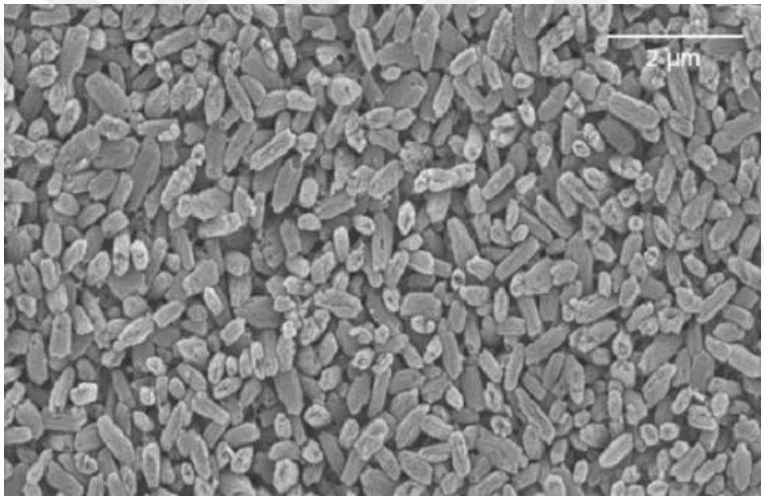

Figure 3.7. Fully crystallized IPS e.max CAD (SEM, carved with HF vapor for 30s). The microstructure contains 70% fine-grain lithium disilicate crystals approximately, $Li_2Si_2O_5$, that are inserted in a glassy matrix. By carving with hydrofluoric acid vapor, the glassy phase is melted and the lithium disilicate crystals become observable [100].

CHAPTER 4:

EXPERIMENTAL EQUIPMENT, SAMPLES AND PROCEDURES

4.1 Introduction

TL studies are generally considered using the TL reader system. An overall description and characterization of the readers are given in this chapter. In addition, detailed characteristics of samples which studied before are listed and the preparation of the sample is defined. The TL laboratory where experiments were done for this thesis consists of two main rooms. The first one has a furnace, a sieve and a digital balance etc. which were used to prepare the samples for the experimental applications. Another room is called as darkroom that has the irradiation and reading devices.

Figure 4.1. TL laboratory.

4.2 Radiation Source and Irradiator

The ceramic samples prepared in dark room that were irradiated at room temperature by a ^{90}Sr-^{90}Y β (beta)-source. The source activity is approximately 100 mCi. It was regulated by the manufacturer on March, 10, 1994. The recommended working life-time is about 15 years. Strontium-90 radiates high energy beta particles from their daughter products (^{90}Sr β-0.546 MeV together with ^{90}Y β-2.27 MeV). Air absorbed beta radiation, beta radiation's intensity decreases with distance much more quickly than inverse square law calculations would indicate. The typical power of a 100 mCi ^{90}Sr-^{90}Y β-source recognized in a 9010 Optical Dating System is 1.42 Gy/sec for fine grains on aluminium, or 0.04 Gy/sec for 100 mg quartz is on stainless still. The irradiation apparatus is an additional part of the 9010 Optical Dating System which is gotten from Little More Scientific Engineering, UK [101]. The irradiation source apparatus is connected to a computer using a serial RS-232 port.

Figure 4.2. ^{90}Sr-^{90}Y β- radiation source and 9010 Optical Dating System (irradiator).

The feature of the 9010 Optical Dating System:

- ✓ Sensitive on paleodose evaluation typically 3-5%, often better (90-125 micrometer quartz).
- ✓ System design changes with the need to handle sample discs after they are first placed in the tray.

- ✓ 64 disc positions make possible large numbers of dose points to be well described.
- ✓ Temperature control of samples during illumination.
- ✓ Reproducible and precise sample positioning.
- ✓ High speed of operation. A short exposure ($\leq$ 1 second) to all 64 samples takes only ten minutes.

4.3 TLD Reader and Analyzer

If a sample which contains luminescence feature is heated at a constant ratio to about 400 ^{o}C then it is called as thermally stimulated luminescence, or thermoluminescence (TL) and registering the luminescence radiated as a function of temperature. The TL signal as a function of temperature is also known as ``glow curve", with a number of peaks occurring at different temperatures, which interest to the electron traps exist in the sample [102]. The glow curve calculations were completed using a Harshaw TLD System 3500 Manual TL Reader for dental ceramics in this thesis which is shown in figure 4.3 [103].

Figure 4.3. Harshaw TLD System 3500 Manual TL Reader.

The mechanical construction of the system includes both a DOS-based IBM and Reader – congruent computer involved through a standard RS-232 serials communication port to control the 3500 Reader. The simple block diagram of this

reader is shown in Figure 4.4. All functions are divided between the specialized TLD and the reader. Shell software runs on the PC. All data storing, tool control, and machinist inputs are made on a PC. Signal gain and training are made in the reader. In this way, each glow curve can be examined by utilizing a best computer program built on a Marquardt algorithm minimization process, related to first order and general order kinetic terms. The program decides the discrete peaks which exist in the curve, giving the best rates for the different peak limits. The tool includes a sample change drawer for removing and inserting the TLD elements. The reader uses contact heating with a closed loop feedback system that generates changeable ramped temperatures linearly from 1 ^{o}C to 50 ^{o}C per second accurately to within ± 1 ^{o}C to 400 ^{o}C in the typical reader [104]. A graphical diagram of a TL reader is shown in Fig. 4.4.

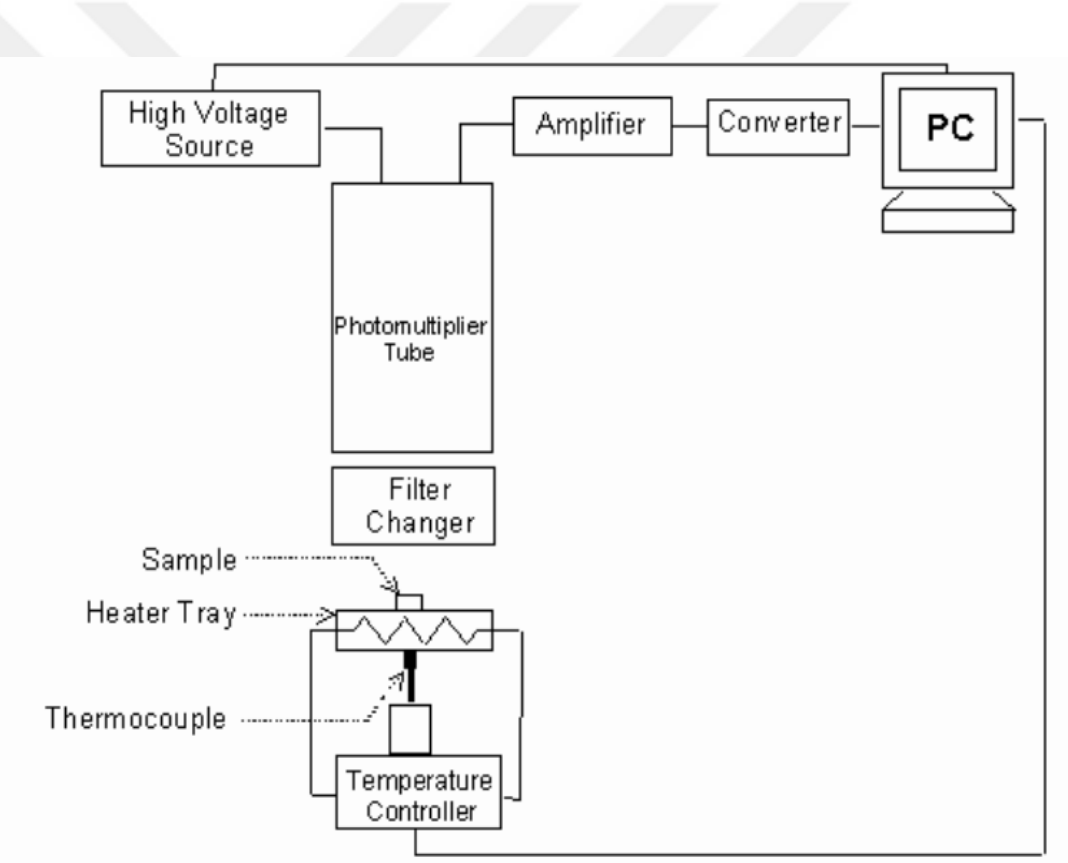

Figure 4.4. Graphical diagram of a TL reader system.

4.4 Equipment Used for Sample Preparation

To prepare ceramic samples before irradiation some equipment used which are a digital balance to weight of the used samples, sieves to sieve crushed samples for

desired dimensions and ring mill to crushed sample. Ring mill was supplied from the central laboratory of Gümüşhane University and the others were obtained from TL lab of Gaziantep University.

Figure 4.5. Used equipment for preparation of sample before irradiation process.

X-ray Fluorescence Spectroscopy (XRF) and X-Ray Powder Diffraction Method (XRD).

The X-ray fluorescence spectroscopy (XRF) method was used to determine elemental content of material. When the atoms of the sample are exposed to a high-energy X-ray photon, the photoelectrons are torn off from the atom. In this case, one or more electron blanks form in the atom's orbit, and the unstable atom will come to a stable state when the electrons in the outer orbits fill the gaps. When each electron cavity is filled, an X-ray photon (characteristic X-ray fluorescence photon) is emitted proportional to the energy difference between the atoms. These characteristic photons are proportional to the atomic concentration of the emitted atom. Therefore, these photons can be used to calculate chemical content.

The most important parts of the XRF spectrometer are; an X-ray source that emits X-rays for excitation on the sample, a sample container in which the samples are placed, a detector that interacts with the incoming characteristic X-ray and converts the generated light into an electrical pulse, a rectifier that processes the signals from the detector, converts the corrected signals into digital and multi-channel analyzer.

The three-dimensional construction of non-amorphous materials such as minerals is described by the repeated regular planes of an atom in the crystal pattern. A number of the light beam is spread when a focused X-ray beam interacts with these planes of atoms. After that some of these light beams are absorbed by the atom, some are

dispersed, and the other is spread. The spread of an x-ray beam by a crystallized solid is related to the splitting of water droplets in the rainbow formation as we know. The X-ray spreads in the different ways, depending on each mineral, the crystal structure of the mineral, and how the atoms are decided. The x-rays used in the examination are produced in a tube under vacuum.

When a hot filament is applied current in the tube, there is a large electron emission from the filament. The production of these electrons is similar to the production of electrons in a television tube. It is usually applied in a high voltage tube of 15-60 kV. This high voltage accelerates the electrons and accelerating electrons multiply in general to a target made of copper, so that x-rays are produced. The resulting wavelength of x-rays shows the characteristic of the target.

The X-rays are collected and sent on to the finely pulverized sample (smaller than 10 microns) and the x-ray signal is detected with the aid of a detector. We can measure the distance between the application of the Bragg Law and the planes of the atoms when an x-ray is broken into an example. The Bragg Law is known as:

$n\lambda = 2d \sin\theta$

- ✓ n: number of diffracted beam (odd number)
- ✓ λ: the wavelength of the incoming x-ray beam
- ✓ d: distance between adjacent planes of atoms
- ✓ θ: the angle of the x-ray beam

Since we know λ and we can measure d so θ can be calculated from the equation. The characteristics of the distances provide a clue as to the minerals or minerals present. When standard references and measurement results are compared and interpreted, these cues lead to the recognition of the material.

Many analytical techniques are used to determine the character of the material. One of these techniques is XRD (X-Ray Diffraction) method. XRD is a useful technique for determining minerals. XRD provides fast and reliable results for the researchers to accurately identify minerals. XRD is mainly suitable for classifying fine-grained minerals and combinations and can supply extra knowledge beyond the basic determinant. If the sample consist of mixture of some minerals, the XRD data may be utilized to control the ratio of the different current minerals. Other information that can be obtained from the XRD method can be listed as the degree of crystallinity of the existing minerals or minerals, and the structural states of the minerals.

All ceramics used in this thesis were crushed and the analyses of XRD measurement of dental ceramics were done in the central laboratory of İnönü University Malatya which is shown in section 3.2. XRD Analysis Laboratories have Rigaku RadB-DMAX II Computer Controlled X-Ray Diffractometer. The voltage generator of this device is between 20kV-60kV and 2mA-80mA. For XRD and XRF analysis, 3 groups of powdered ceramic samples were prepared by crushing in ring mill and their particle size is about 20 μm, each about 1 g in weight.

Table 4.1. The analysis of XRF measurement of the dental ceramics.

Standard composition	Glass ceramic in % by weight	Feldspathic ceramic in % by weight	Lithium disilicate glass ceramic in % by weight
SiO_2	62.45%	58.43%	64.17%
Al_2O_3	9.55%	15.81%	2.04%
Fe_2O_3	0.01%	0.05%	0.01%
CaO	2.65%	1.65%	0.14%
MgO	0.12%	0.17%	0.13%
SO_3	0.01%	0.01%	0.01%
Cr_2O_3	0.035%	10.78%	0.042%
Mn_2O_3	0.02%	4.33%	0.03%
P_2O_5	0.35%	0.028%	3.939%
TiO_2	0.01%	0.023%	0.13%
ZnO	0.025%	0.058%	0.031%
Li_2O	0.001%	0.27%	11.83%
Na_2O	6.78%	0.004%	1.30%
K_2O	7.85%	0.50%	3.79%
other oxides	0-3.5%	0-3.5%	0-3.5%
pigments	0-2%	0-2%	0-2%

4.5 Experimental Procedure

Dental ceramics used in this thesis are obtained from Ivoclar Vivadent dental market. Three different kinds of dental ceramics used in this thesis:

- ✓ Glass ceramic (IPS e.max Ceram, Ivoclar Vivadent, SW)

- ✓ Feldspathic ceramic (IPS Classic, Ivoclar Vivadent, TR)
- ✓ Lithium disilicate glass ceramic (IPS e.max (LS_2), Ivoclar Vivadent TR)

The samples utilized in this thesis were dental ceramics available on the Swedish and Turkish dental market. Dental ceramics were cut by a diamond saw with a thickness of 1mm and also crushed with ring mill with a particle size greater than 20 μm. The samples in solid and powder form were irradiated and heated up to 400 °C to obtain luminescent glow curves. Therefore it is observed that no difference is seen between TL outputs of the powder and the solid form of sample. As a result, the powder form of sample was used for the entire experimental procedure. These experiments consist of four parts which are dose response, heating rate, reproducibility and fading. In each part of this study, one sample was used for each experiment. For dose response experiment, sample was irradiated with $^{90}Sr - ^{90}Y$ β-source (delivering 0.04 Gy/s) up to 6912 Gy and in the other parts of experiments, sample was irradiated with $^{90}Sr - ^{90}Y$ β-source at fix dose value at 36 Gy at room temperature (RT) without subjecting it to any processing. The irradiation apparatus which is connected to a PC by using a serial RS-232 port is an extra part of the 9010 optical dating system to control irradiation period. After the irradiation periods, the glow curves were obtained by using a Harshaw QS 3500 Manual type TLD reader which is connected to a PC where the TL signals were examined. Glow curve readout was carried out on a platinum planchet at a linear heating rate of 1 ^{o}C/s from RT up to 400 ^{o}C for dose response, fading and reproducibility experiment and for heating rate experiment, at linear heating rates of 1, 2, 3, 4, 5, 7 and 9 ^{o}C/s. Each crystal was read out twice after irradiation period and the second read out is measured to be background of reader plus crystal and was subtracted from the first one and all of the analyses have been carried out after subtraction operations.

4.5.1 Dose Response Experiments

During the dose response experiment, all three dental ceramics samples irradiated with $^{90}Sr - ^{90}Y$ β-source up to 6.9 kGy. After each irradiation, TL glow peak was recorded by heating up to 400 °C from room temperature at a heating rate of 1 °C / s. As a result of these measurements, TL glow peaks were determined from the plotted graphs and it was tried to determine the best dosimetric sample among the three samples.

4.5.2 Heating Rate Experiments

TL experiments have been performed by considering the benefit of accessibility in temperature controller to heat the samples at many ratios so as to examine the heating rate dependencies of the dental ceramics. Therefore, the calculated samples were kept at room temperature and the samples were weighted 10 mg. Then, the temperature of the sample was progressively increased step by step at the certain heating ratio. In this thesis, for the crystals each heating application was accomplished for rates between the maximum rate of 9 C/s and the minimum rate of 1 ^{o}C/s. Consequently, final TL glow curves were recorded in a discrete data sheet as a function of temperature difference to examine and understand the behavior of the glow peaks for different heating rates.

4.5.3 Cycle of Measurement Experiments

There should be no change in the glow curve at the end of each usage. A useful dosimetry should give the same TL output at the end of each usage because of this reason cycle of measurement experiment was done for ten samples. In order to use these samples as a dosimetric material there should be no change in the glow curves in more than one use. In this part, it was tried to find the most suitable dosimetric ceramic from these three materials. Each sample was used powder form and each one was exactly weighted 10 mg. They were irradiated with $^{90}Sr - ^{90}Y$ beta irradiator source for 36 Gy at room temperature in the darkroom. The irradiated samples were read out by Harshaw TLD System 3500 Manual TL Reader. This procedure was repeated ten times using the same sample for each experiment.

4.5.4 Fading Experiments

The dental ceramic samples irradiated with β-source at a fixed (36 Gy) dose and a new sample used for each experiment in this study and each experiment repeated three times. After irradiation, samples were waited for different storage times in a dark ambient at room temperature. Each sample were used as powder form and each one was exactly weighted 10 mg. Waiting periods in the dark room were 1 hour, 4 hours, 1 day, 1 week and 6 weeks. After these waiting periods each sample were read out by Harshaw TLD System 3500 Manual TL Reader.

CHAPTER 5:

EXPERIMENTAL RESULTS AND DISCUSSIONS

5.1 Introduction

Thermoluminescence is an efficient experimental method compatible with the known theoretical information to characterize and determine the defects in the semiconductor lattice structure and also learn about dosimetric properties of samples. The analysis of outcomes for the dental ceramics and the TL experimental observations are given in this chapter. The results of cycle of measurement, dose response, heating rate and fading experiments of dental ceramics are presented by using various analysis techniques. The discussions about the analysis results are given clearly by considering the TL theory. Each ceramic was readout twice after irradiation period and the second readout was considered to be a background of reader plus ceramic and subtracted from the first one. All of the analyses were analyzed after subtraction operations.

5.2 Dose Response of Dental Ceramic

TL peaks of glass ceramic, feldspathic ceramic and lithium disilicate glass ceramic were irradiated between 12 Gy and 6.9 kGy dose regions by heating the samples with a rate of $\beta = 1.0\ ^{o}C/s$. The samples were readout between 30 ^{o}C (room temperature) and 400 ^{o}C and TL glow curves were obtained. Variation of shape of TL glow curve, area under the TL glow curve, TL peak temperature and TL peak intensity of three dental ceramics were observed in this part of the study.

5.2.1 Glow Curve Variation of Dental Ceramics

Variation of TL glow curves of three dental ceramics were shown in Fig.5.1. It is well known that when the exposed dose increases, the signal of TL peak increases until it

reaches the saturation point. The TL glow curve of glass ceramic which is illustrated in Fig.5.1 (a) has four major peaks and all of these TL peaks ascended when the exposed dose raised. As seen in Fig.5.1 (a) there is no important change in the shape of TL glow curve of glass ceramic with increasing exposed dose. A characteristic analysis of glow curve of feldspathic dental ceramics is shown in Fig.5.1 (b), although it seems to have two distinctive peaks, it actually consists of four peaks that are overlapping each other. TL glow curve shape of feldspathic ceramic does not change with increasing exposed dose like glass ceramic. In Fig.5.1 (c) no distinct TL peaks were observed when the TL glow curve of the lithium disilicate ceramic is analyzed. It may include five TL peaks overlapping each other and some of these TL peaks are in high temperature regions they are not in the shown temperature interval. A small figure inserted in the TL glow curve to show low dose values clearly. As a result of this part, the TL glow curve shapes of three dental ceramics were not affected by variation of exposed dose.

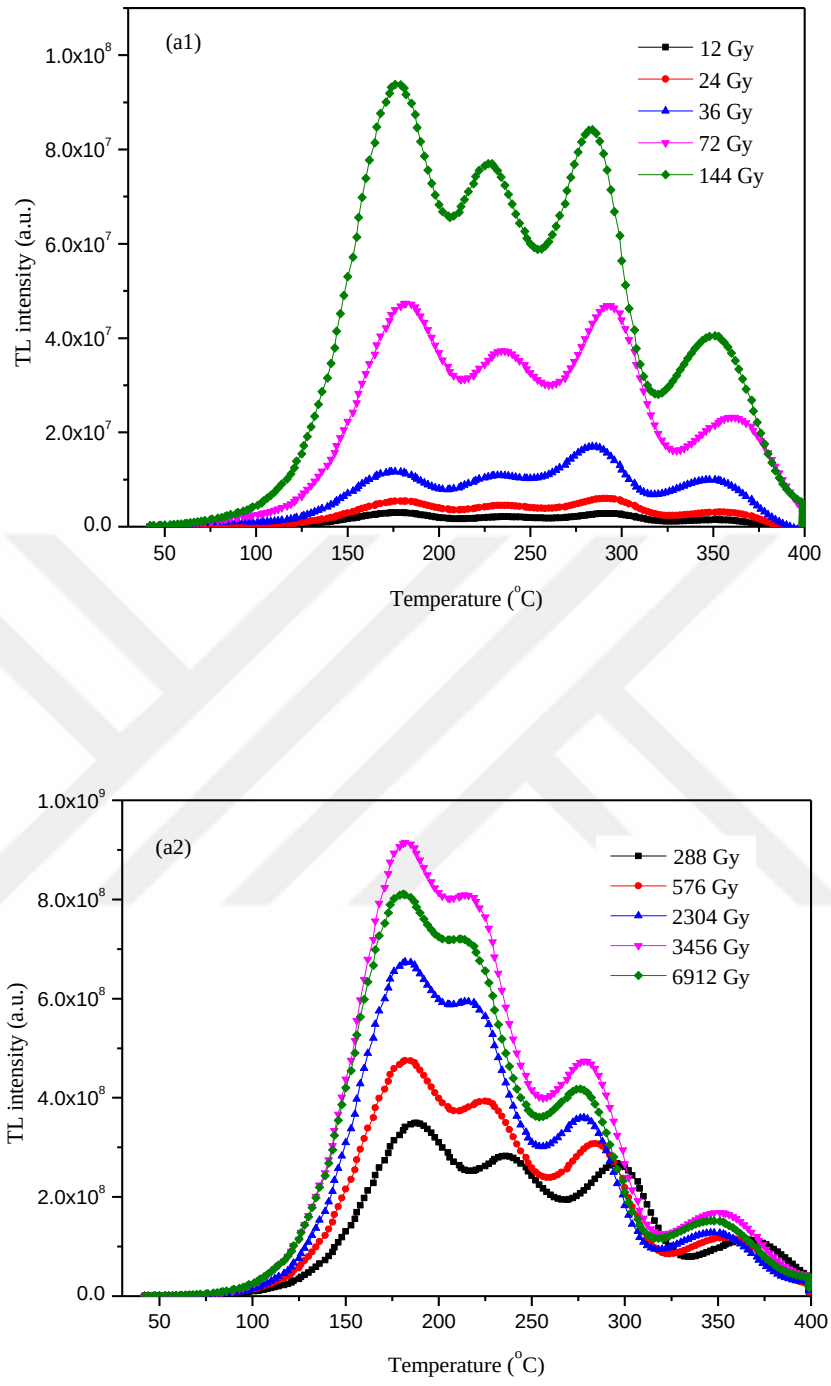

Figure 5.1(a). Typical TL glow curve of dental glass ceramic irradiated with β-source (a1) from 12 to 144 Gy, (a2) from 288 to 6912 Gy at room temperature (RT) with heating rate, 1 $^{o}C.s^{-1}$.

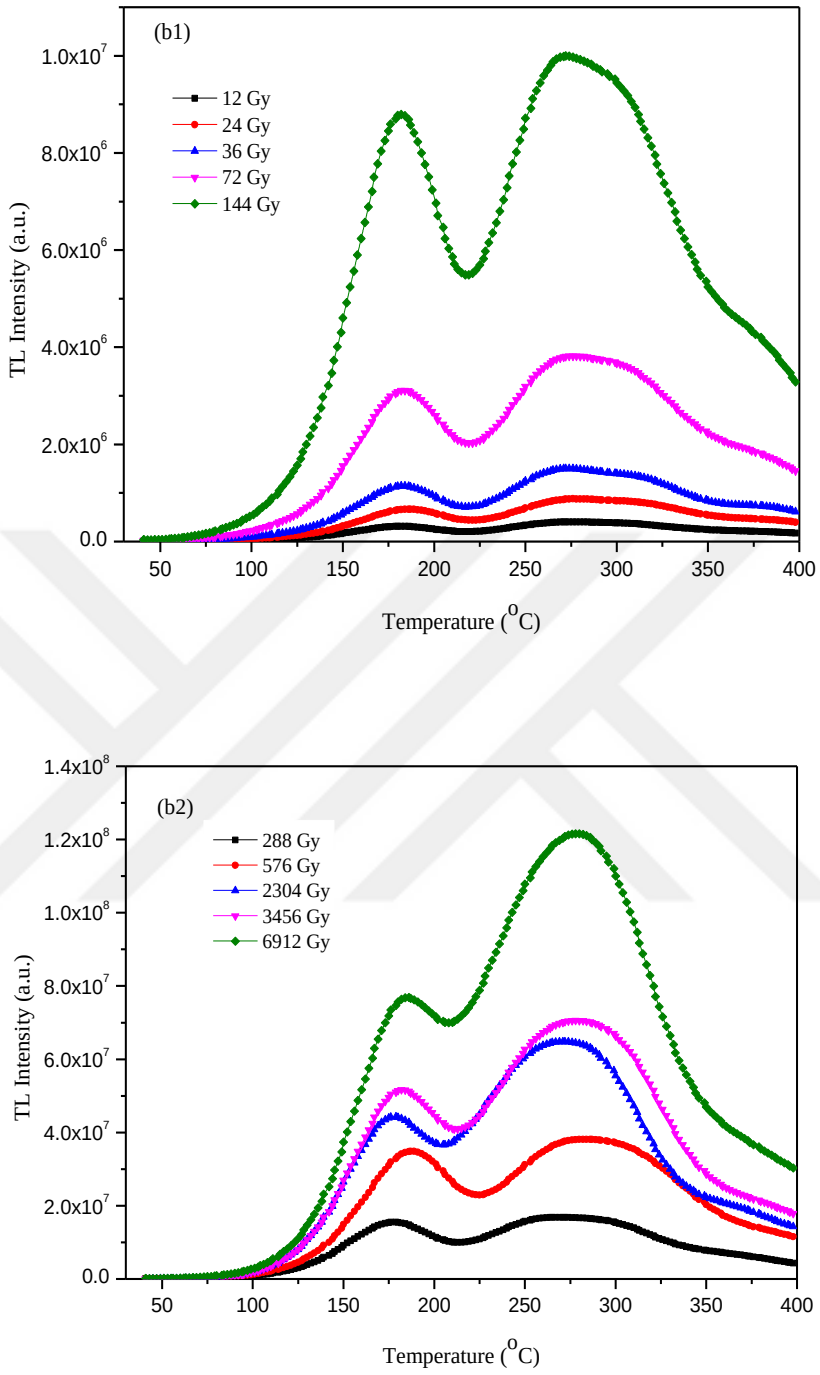

Figure 5.1(b). Typical TL glow curve of feldspathic dental ceramic irradiated with β-source (b1) from 12 to 144 Gy, (b2) from 288 to 6912 Gy at room temperature (RT) with heating rate, 1 $^{o}C.s^{-1}$.

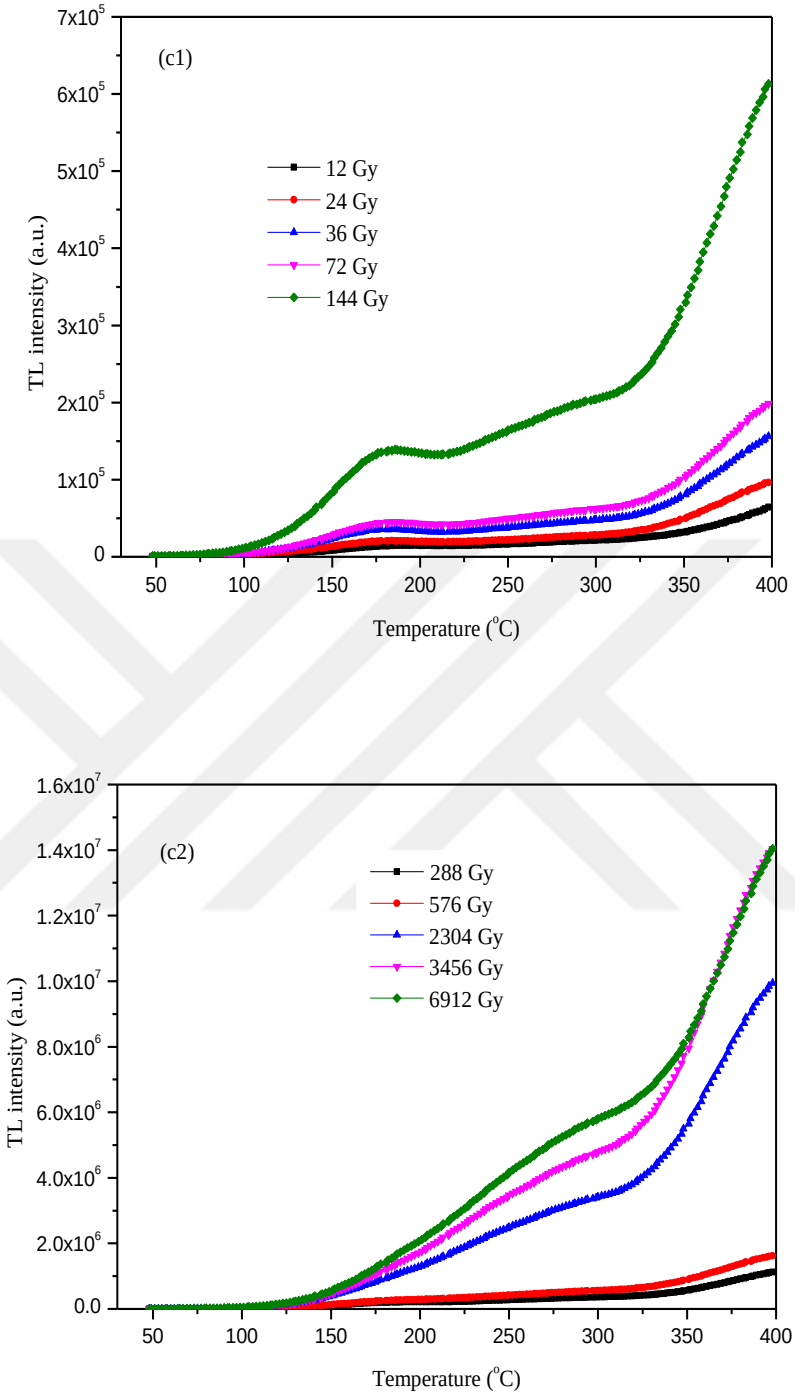

Figure 5.1(c). Typical TL glow curve of lithium disilicate glass ceramic irradiated with β-source (c1) from 12 to 144 Gy, (c2) from 288 to 6912 Gy at room temperature (RT) with heating rate, 1 $^{o}C.s^{-1}$.

5.2.2 Area under the Glow Curve of Dental Ceramics

In determining dose response, the area under the glow curve is a crucial factor. Therefore, in present work, area under the glow curves of all of three dental ceramics were calculated and their changes with applied dose illustrated in Fig. 5.2 (a), (b) and (c). Fig.5.2 (a) shows the effects of different applied dose on the area under the glow curve which is divided into two parts depends on their temperature hence the peak temperature of peak1 and peak2 were lower than 250 ^{o}C and the peak temperatures of peak 3 and peak 4 were greater than 250 ^{o}C. When the dose is increased, area under the glow curve of glass ceramic is also increased nearly linearly up to about 300 Gy and after this point, TL peak area raised slowly and reached the saturation point. The area under the TL glow curves of feldspathic ceramic shown in Fig.5.2 (b) reached the saturation point at about 500 Gy and lithium disilicate ceramic shown in Fig.5.2 (c) reached about 2 kGy then begin to show sublinearity up to 6.9 kGy for both ceramic samples.

5.2.3 The Variation of TL Peak Intensity of Dental Ceramics

The TL glow curve of glass ceramic sample consists of four distinct peaks respectively; they located around 180, 235, 290 and 350 ^{o}C (see figure 5.1(a)). The variation of TL intensity of each peak of glow curve of dental ceramics was examined separately as shown in Fig. 5.3 (a). TL peak intensities of all TL peaks increased with increasing exposed dose for all of peaks. When the dose was increased, TL peak intensities of glass, feldspathic and lithium disilicate ceramics increased linearly up to 300 Gy, 500 Gy and 2 kGy, respectively and after these points TL peak intensities increased slowly. After saturation points, TL intensities have no significant change for all of peaks. Lithium disilicate glass ceramic has lowest TL peak intensity and the highest TL peak intensity is seen in glass ceramic despite the all ceramics irradiated equal amount of dose. The highest TL peak intensity is seen in glass ceramic.

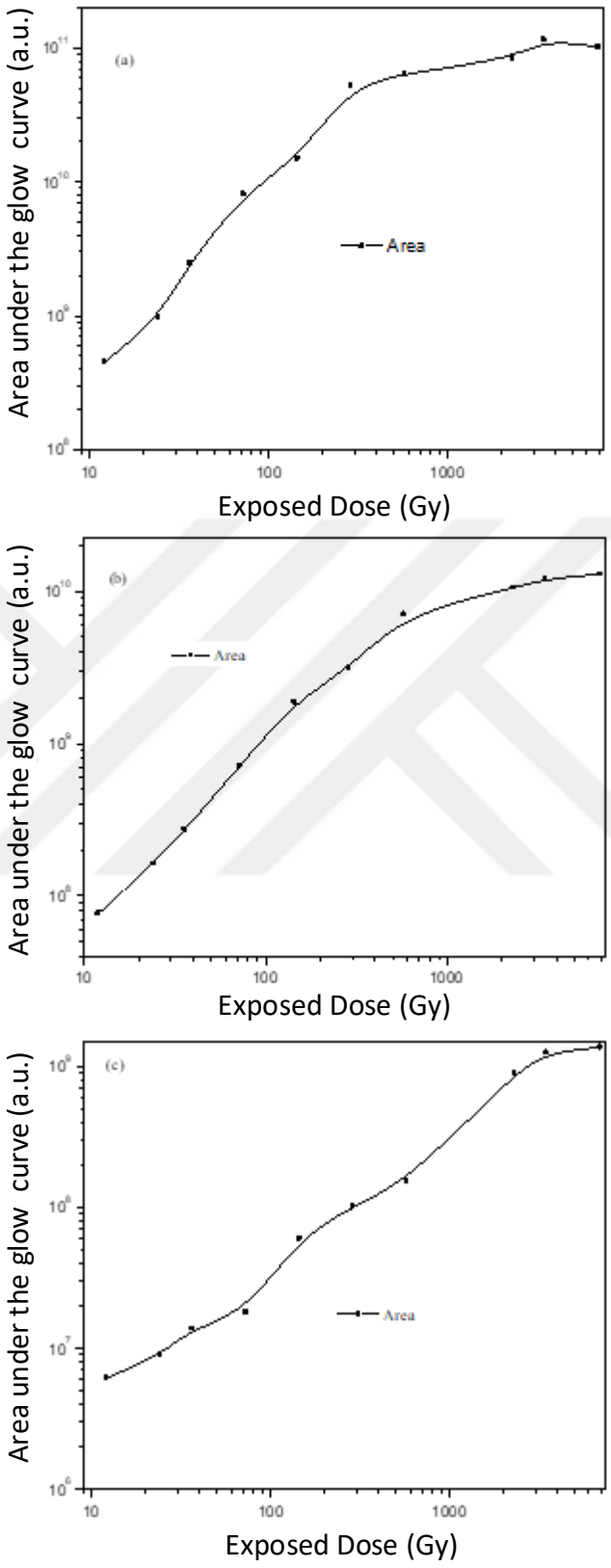

Figure 5.2. (a) Area under the glow curve versus exposed dose of glass ceramic, (b) feldspathic ceramic and (c) lithium disilicate ceramic irradiated with β-source up to 6.9 kGy at room temperature, with heating rate of 1 $^{o}C.s^{-1}$.

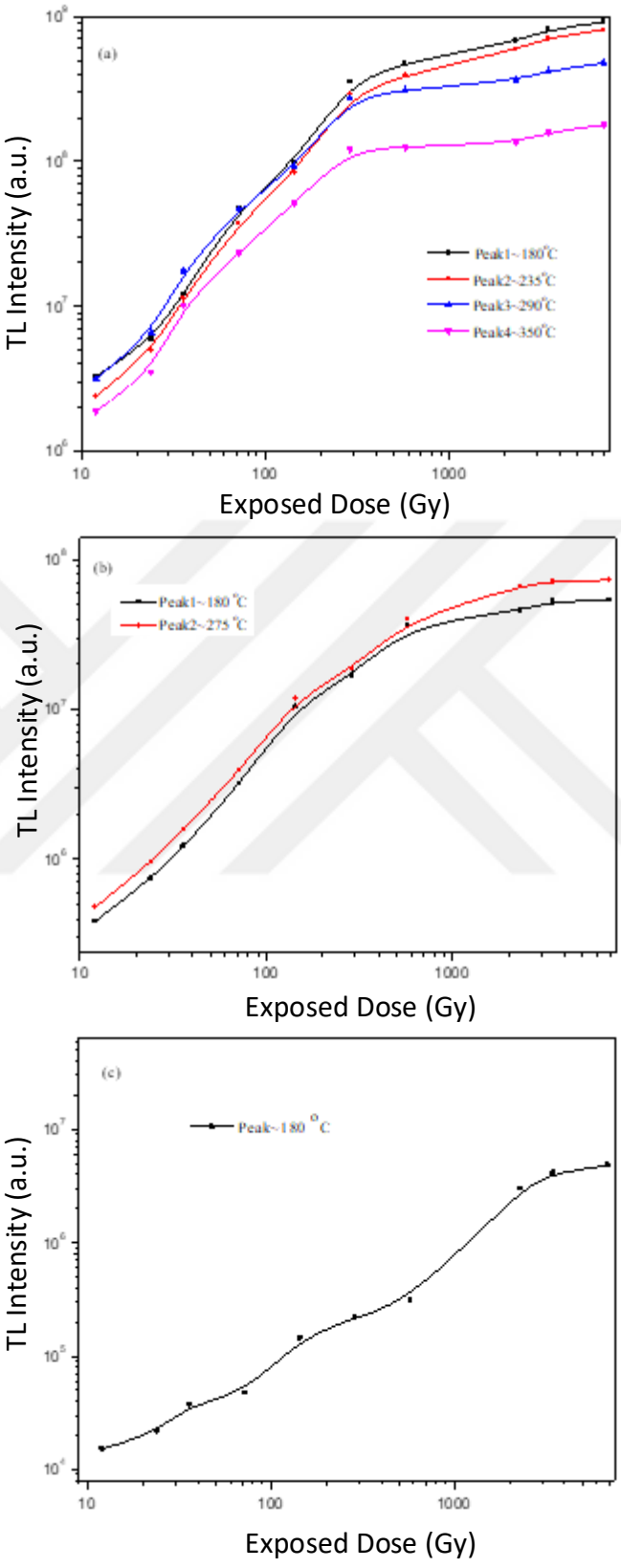

Figure 5.3. The variation of TL peak intensities of (a) glass ceramic, (b) feldspathic ceramic, (c) lithium disilicate glass ceramic irradiated with β-source up to 6.9 kGy at room temperature, with heating rate, 1 $^{o}C.s^{-1}$.

5.2.4 The Variation TL Peak Temperature of Dental Ceramics

All of TL peak temperature characteristics of the dental ceramic sample were depicted in Fig.5.4. Although all of TL peaks of glass ceramic decreased by 10-15 ^{o}C, peak 1 decreased about 5 ^{o}C. For feldspathic dental ceramics of peak temperatures, there is a fluctuation but no significant change as shown in Fig. 5.4 (b). Unlike other dental ceramics, a sudden and significant decrease was observed at low dose values and the TL peak temperature continued to decrease as the applied dose increased in the lithium disilicate dental ceramics. This means that kinetic order of glow peak is equal to 2 (second order-kinetic). The peak temperatures of glow curve of glass and feldspathic ceramic don't change when the dose increases so these ceramics can be a sensitive dosimetric material.

5.3 The Variation of Heating Rate of Dental Ceramics

Heating rate dependencies of TL glow curves which obtained for glass ceramic, feldspathic ceramic and lithium disilicate ceramics were investigated by performing the TL experiments with different heating rates. The effect of heating rate (β) on shape of glow curve, TL peak intensity, TL peak temperature and area under the glow curves of all dental ceramic samples were studied. Seven different heating rates (β =1, 2, 3, 4, 5, 7 and 9 ^{o}C/s) were applied and irradiated with β-source at 36 Gy room temperature. On the strength of TL theory, change of heating rates culminates in alteration of location and structure of TL peak [44].

5.3.1 Glow Curve Variation of Dental Ceramics

TL peak intensity decreases and its maximum value of temperature moves to higher temperatures with increasing heating rate as shown in Fig. 5.5. The TL glow curve is proportional to the initial trap concentration. In the heating rate dependence, it was observed that area under the glow curve decreased with the heating rate increased. This is a demonstration of thermal quenching of luminescence caused by increasing the possibility of non-radioactive transitions as the temperature increases [105-107]. Some explanations for shifting of maximum value of temperature of TL curve to higher temperatures were stated in a TL study on lithium magnesium borate phosphors

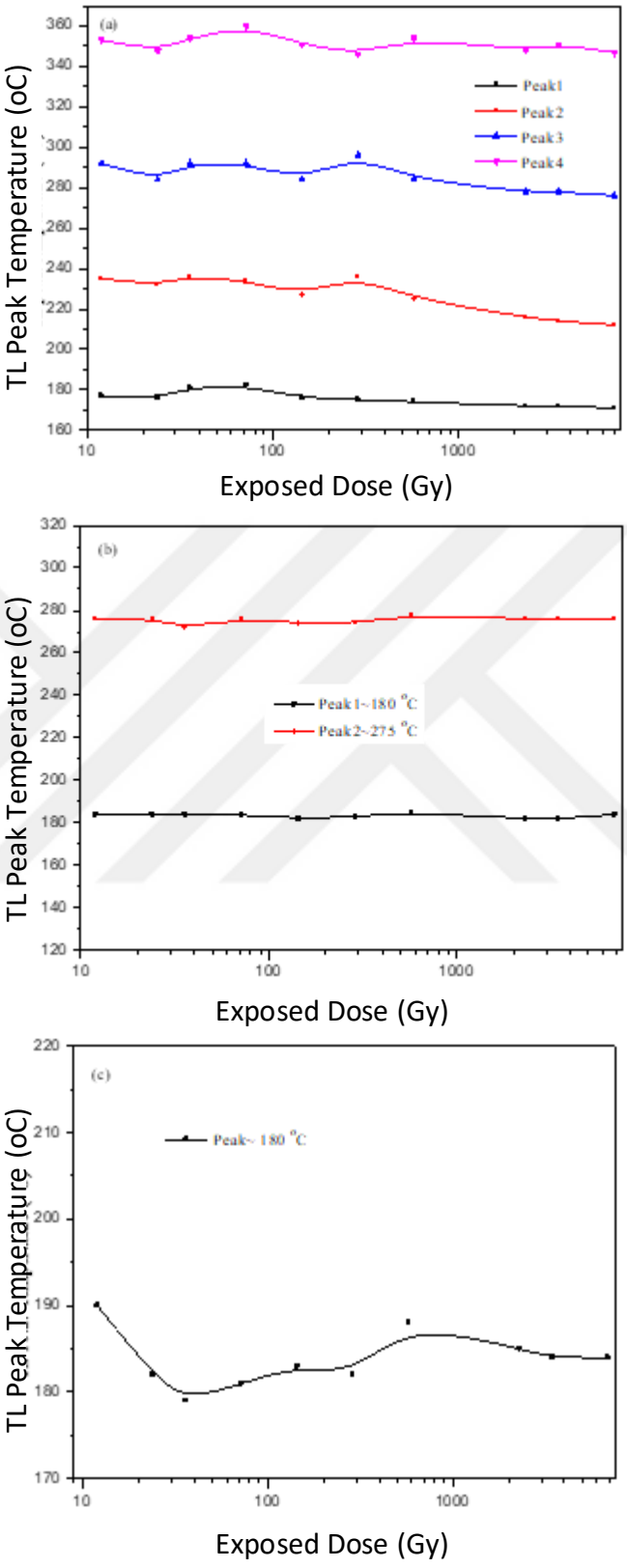

Figure 5.4. The variation of TL peak temperature of (a) glass ceramic, (b) feldspathic ceramic, (c) lithium disilicate glass ceramic irradiated with β-source up to 6.9 kGy at room temperature, with heating rate of 1 $^{o}C.s^{-1}$.

by Anishia et al. [108]. According to the Wintle, TL intensity decreased with increasing heating rate because non-radiative transition probability increased [48]. The glow peak height decreased with the increase of the heating rate for all peaks and when heating rate decreased to 2 ^{o}C/sec TL glow peak height had a major reduction all of three dental ceramics. In brief, the shape of TL glow curve of dental ceramics didn't change when the heating rate increased.

5.3.2 Area under the Glow Curve of Dental Ceramics

The area under the TL glow curve decreased with increasing heating rates at fixed (~ 36 Gy) dose as shown in Fig.5.6. Spooner et. al. [109] proposed that when the heating rate increased the TL peak intensities decreased by using porcelain sample and we also observed the same result with them to use dental ceramic samples. When the heating rate was 9 ^{o}C/sec, the areas under the glow curve of feldspathic and glass ceramics were reduced by about 80 percent of its initial value and 98 percent in the lithium disilicate glass ceramic as illustrated in Fig. 5.6. When the heating rate was 4 ^{o}C/sec, areas of feldspathic and glass ceramics were decreased by about 30-40 percent, but in the lithium disilicate glass ceramic it was reduced by more than 80 percent. Generally, area under the TL glow curve decreased with increasing heating rate for entire dental ceramics.

5.3.3 The Variation of TL Peak Intensity of Dental Ceramics

The variation of TL peak intensities as a function of heating rate is shown in Fig.5.7. Each TL peak examined separately and all of TL peak intensities reduced with increasing heating rate. Peak 1 which had the lowest reduced by about 70 % from the initial value and peak 3 had the highest decrease with 80 % as demonstrated in Fig.5.7 (a). As the heating rate of glass ceramics and feldspathic dental ceramics increased, TL peak intensity of glow curve decreased in a similar way, but TL peak intensity of glow curve of lithium disilicate glass ceramic decreased highly when we compared with the others. At a heating rate of 3^{o}C/sec, TL peak intensity of glow curve of the glass and feldspathic dental ceramics had a reduction of about 60 percent, while TL peak intensity of glow curve of lithium disilicate glass ceramic had a reduction of about 80 percent. For all dental ceramic samples, TL peak intensity was decreased with increasing heating rate.

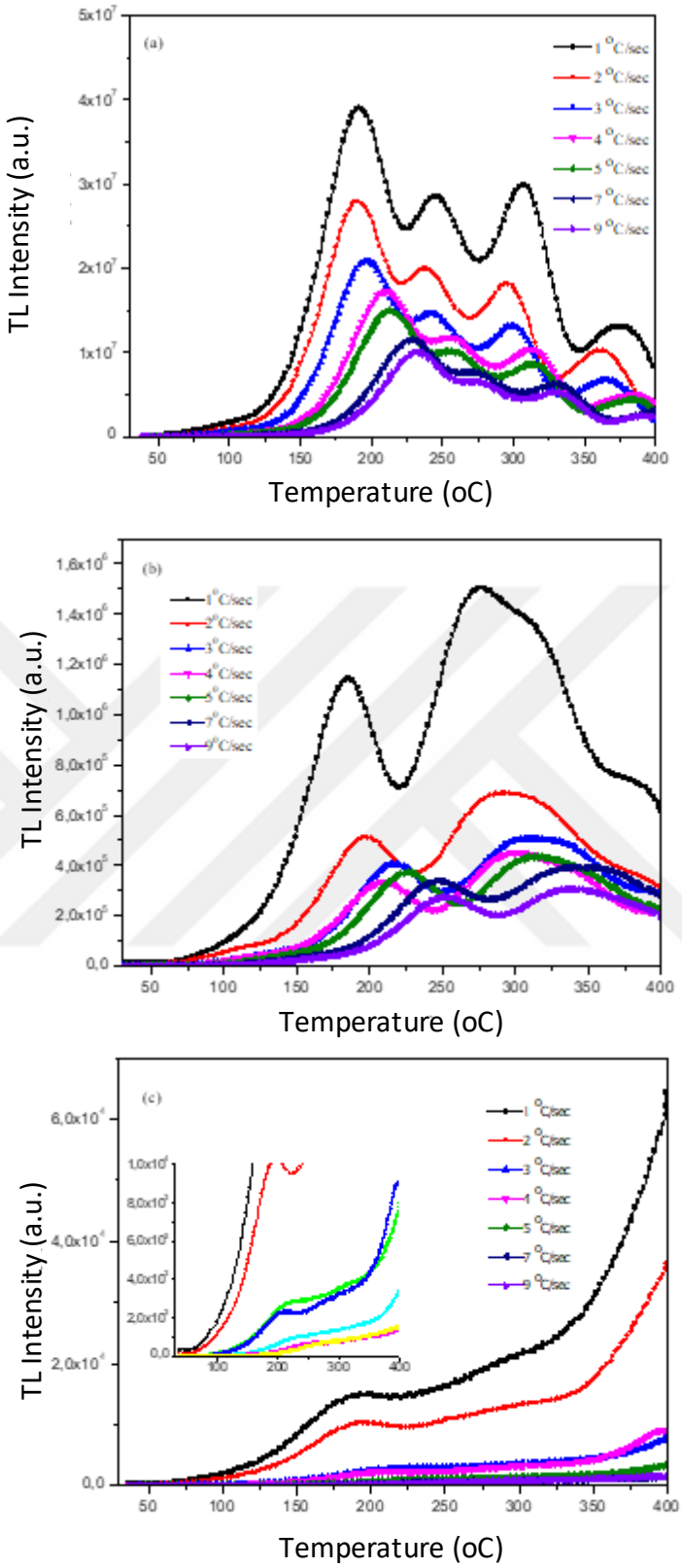

Figure 5.5. The glow curve of (a) glass ceramic, (b) feldspathic ceramic, (c) lithium disilicate glass ceramic as a function of heating rate, irradiated with β-source at 36 Gy room temperature.

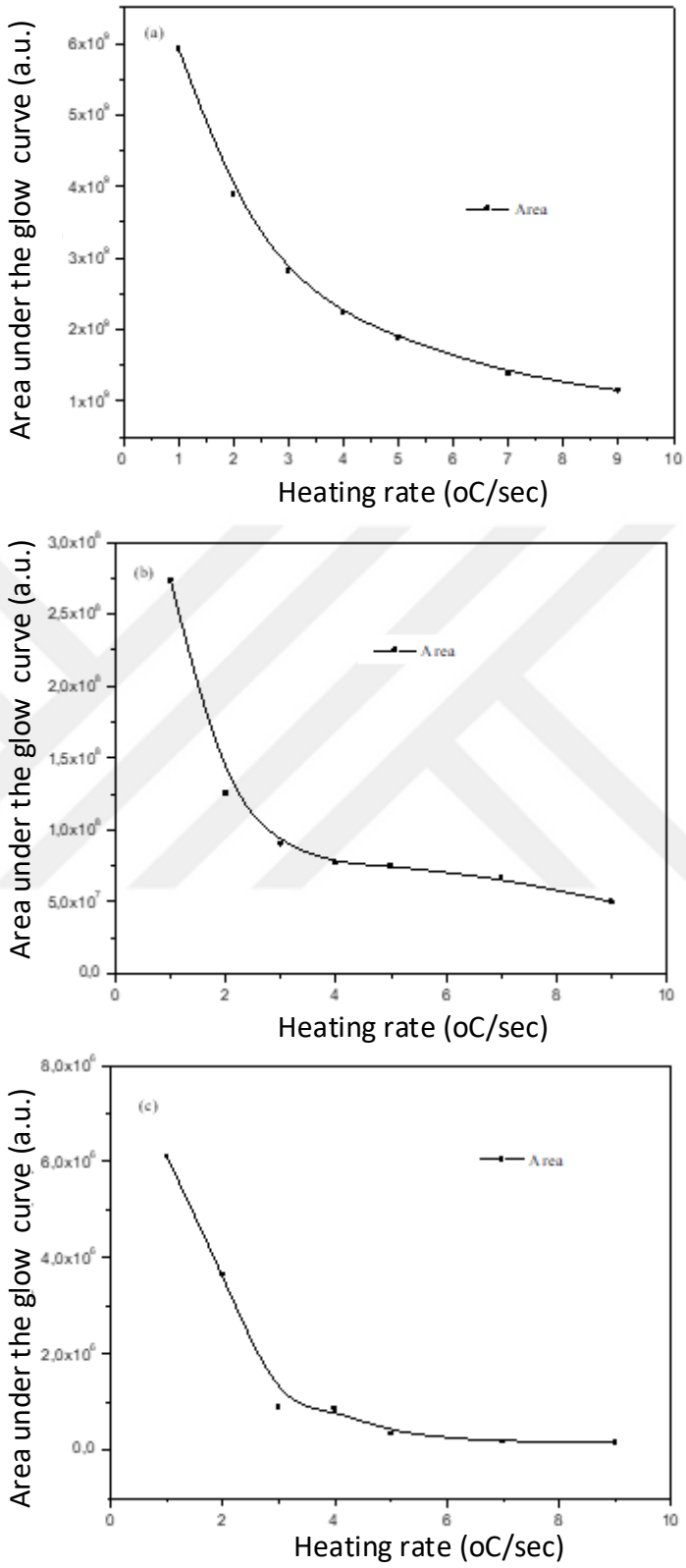

Figure 5.6. The area under the glow curve of (a) glass ceramic, (b) feldspathic ceramic, (c) lithium disilicate glass ceramic as a function of heating rate, irradiated with β-source at 36 Gy room temperature.

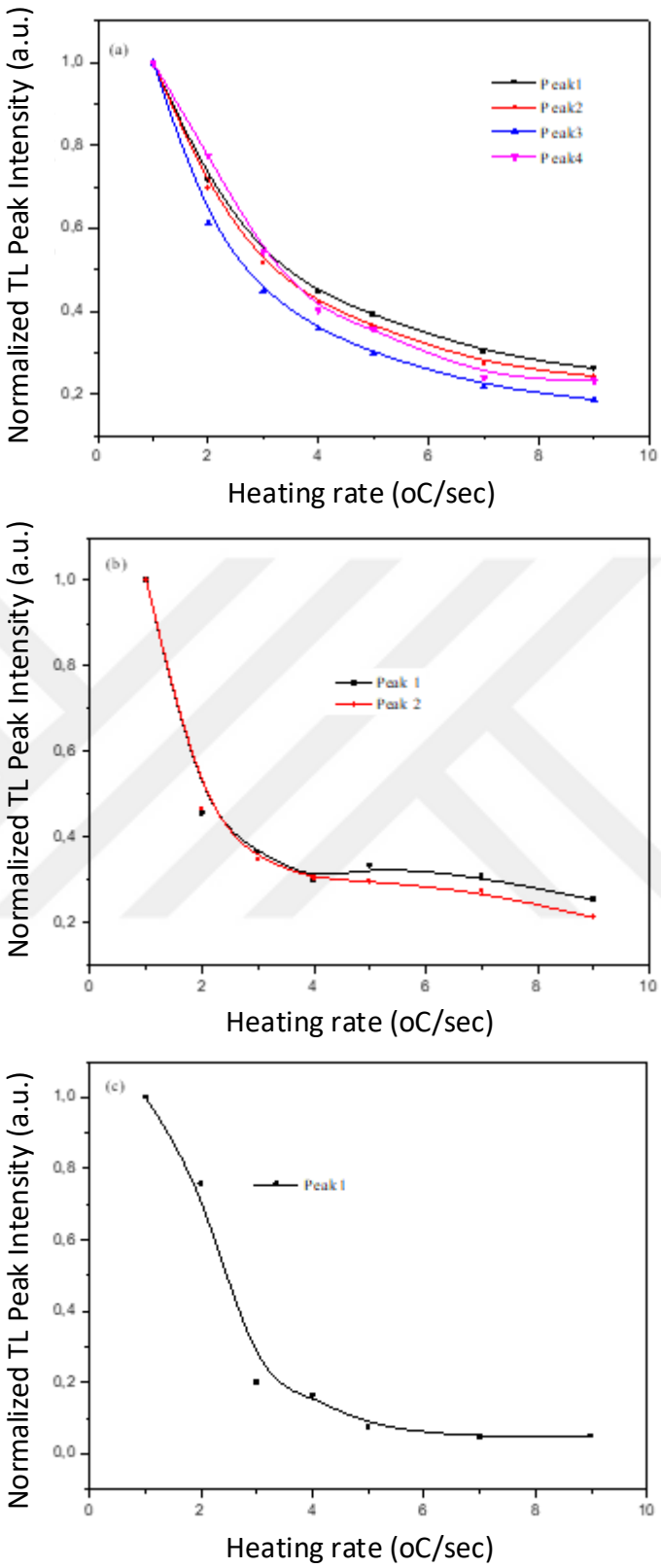

Figure 5.7. The variation of TL peak intensities of the glow curve of (a) glass ceramic, (b) feldspathic ceramic, (c) lithium disilicate glass ceramic as a function of heating rate, irradiated with β-source at 36 Gy room temperature.

5.3.4 The Variation TL Peak Temperature of Dental Ceramics

The variations of each TL peak temperatures of dental ceramics as a function of heating rate as shown in Fig.5.8. The entire TL peak temperatures of all of the dental ceramics raised with increasing heating rate but the heating rate is 2 ^{o}C/sec of glass ceramic and 4 ^{o}C/sec of feldspathic and lithium disilicate ceramics, the TL peak temperatures decreased unlike the other values. For the glass ceramic Peak1 shifted about 40 ^{o}C and peak4 shifted by 17 ^{o}C as shown in figure 5.8 (a). Both TL peaks of feldspathic ceramic shifted about 70 ^{o}C to the high temperature region seen in Figure 5.8 (b). An increase in the TL peak temperature is expected as the heating rate increases, but the TL peak is increased about 100 ^{o}C on the lithium disilicate sample. In summary, all TL peak temperature shifted to high temperature region with increasing heating rate.

5.4 The Variation of Reproducibility of Dental Ceramics

Reproducibility (cycle of measurement) is an important parameter for a useful dosimeter. A good dosimeter should be used over and over again and the same result should be gotten at each usage. So the standard deviation is calculated based on the number of usages and a standard deviation of ± 2% or less is the index for good reproducibility [108]. In this part of the study, each dental sample was exposed to a fixed dose of 36 Gy for the reproducibility measurement and heated to 400 ° C to obtain a TL glow curve. The same sample was used ten times to calculate the standard deviation and the suitability of the samples was determined for the dosimeter.

5.4.1 Glow Curve Variation of Dental Ceramics

Dental ceramic samples irradiated with β-source at a fixed (36 Gy) dose and for these experiments one sample used ten times at room temperature without annealing. Therefore the mean values, standard errors, standard deviations were calculated as shown in Table 5.1. The variations of glow curve with increasing experimental cycle are shown in Fig. 5.9. As seen in Fig. 5.9, when the experimental cycle increased TL intensity of glow curves also increased significantly because sample are not annealed after read out. After the first cycle, TL peak intensity of feldspathic dental ceramic increased more than the other dental ceramics. The peak temperature of each peak had

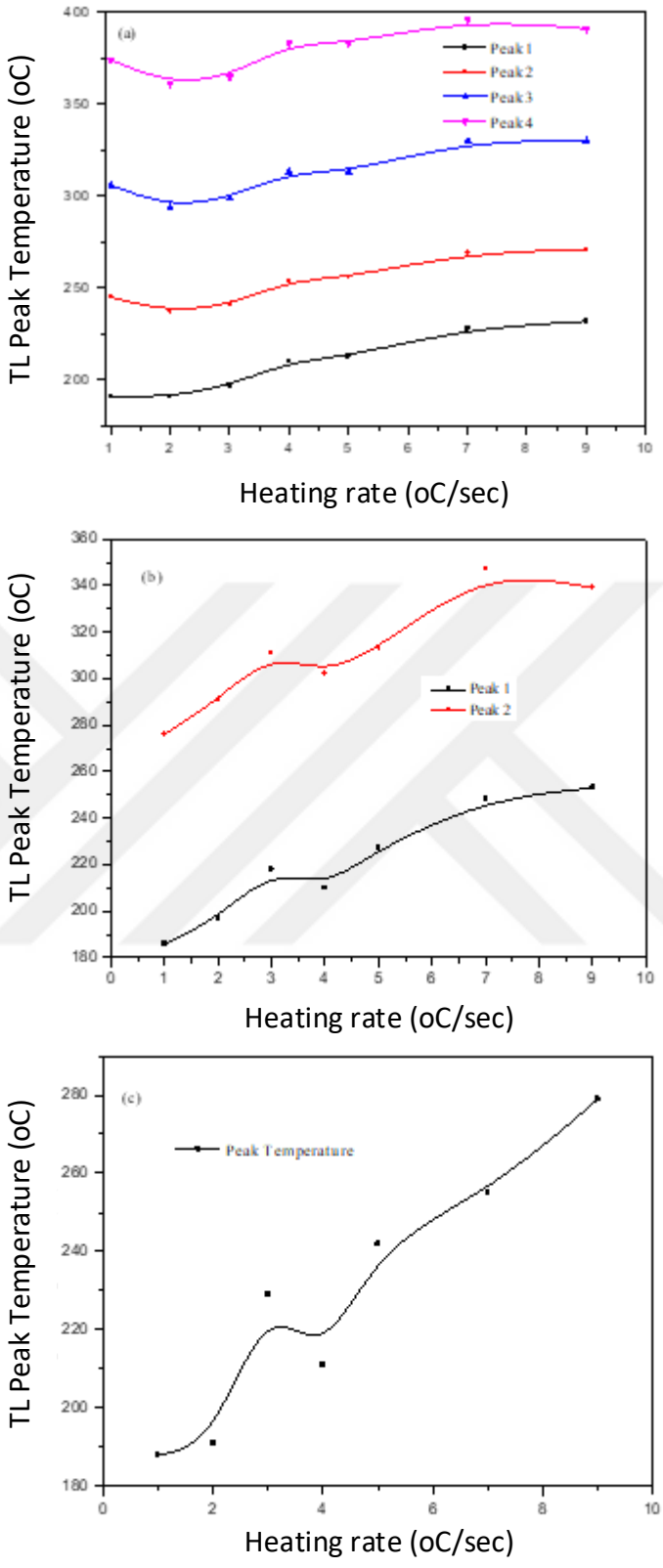

Figure 5.8. The variation of TL peak temperatures of the glow curve of (a) glass ceramic, (b) feldspathic ceramic, (c) lithium disilicate glass ceramic as a function of heating rate, irradiated with β-source at 36 Gy room temperature.

no significant change and the shape of glow curve did not change when the cycle raised. Standard deviations of the peaks in all glow curves calculated and all of them are larger than 2% as shown in Table 5.1. These results show us that shape of TL glow curve of these three samples are not change with increasing experimental cycle. For glass ceramic, standard deviation value of high temperature TL peak was smaller than low temperature TL peaks. Standard deviation value of feldspathic ceramic is greater than the other ones so this sample is not suitable for repeated usage.

Table 5.1. The mean, standard (Std) error, standard deviation of the glow curve variation of dental ceramics as a function of reproducibility, irradiated with β-source at 36 Gy room temperature with heating rate of 1 ^{o}C/sec.

Type of dental ceramic	Mean	Standard Error	Standard Deviation
Glass ceramic	0.895958	0.027728	0.087683
Feldspathic ceramic	0.800376	0.050045	0.158258
Lithium disilicate glass ceramic	0.938056	0.030587	0.096726

5.4.2 The Variation of TL Peak Intensity of Dental Ceramics

The TL peak intensity of each peak of the glow curve increased with increasing experimental cycle at fixed (36 Gy) dose as shown in Fig.5.10. Low temperature TL peaks (less than 200 ^{o}C) increased about 30% and the high temperature TL peaks (higher than 200 ^{o}C) increased about 20% as shown in Fig.5.10 (a). Figure 5.10 (b) also shows us that the TL peak intensity of low temperature TL peak increases more than of high temperature TL peak. The results show that the high temperature TL peaks are more stable than the low temperature peaks. It is well known that as the cycle of measurement increases, the TL intensity also increases, but we observed a fluctuation in the lithium disilicate dental ceramic as demonstrated in Fig.5.10 (c). This is not an expected result for a good dosimeter sample. As a result, dental glass ceramic is more stable than the feldspathic and lithium disilicate dental ceramic.

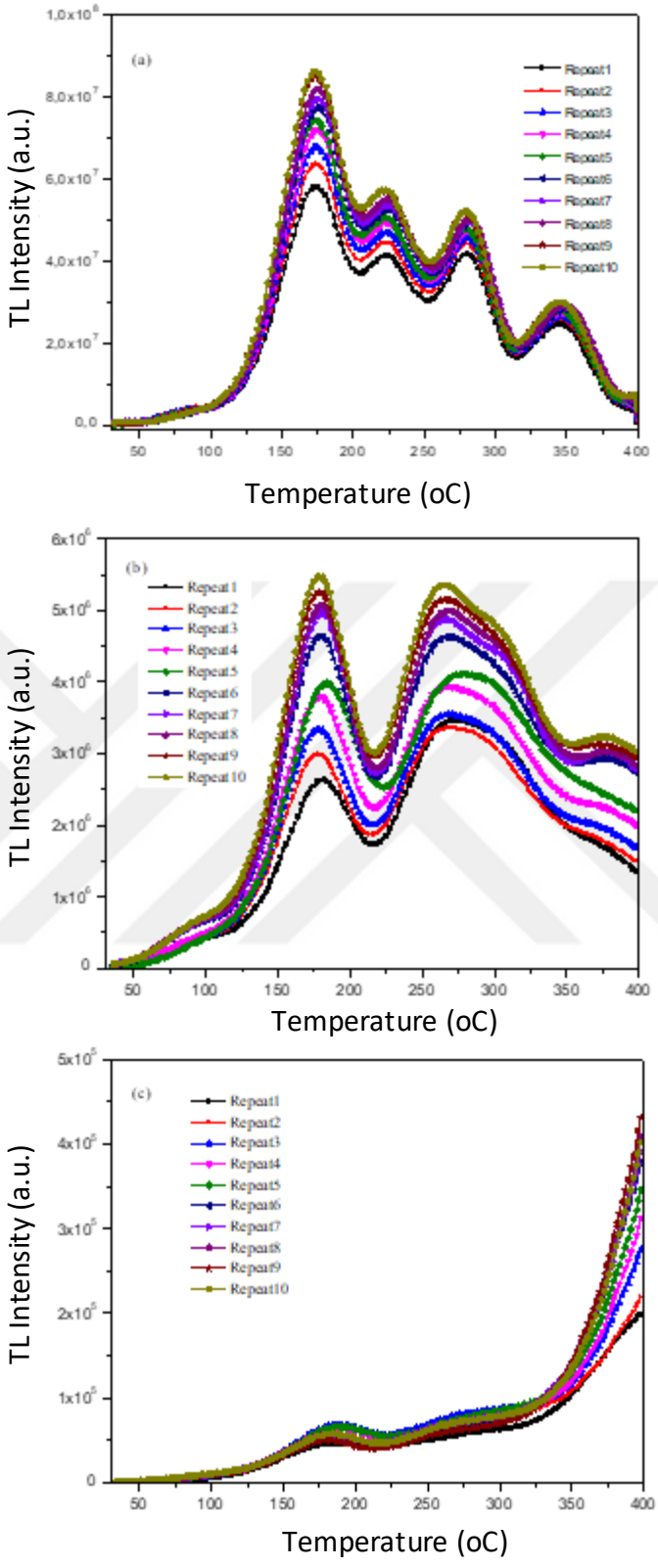

Figure 5.9. The glow curve of (a) glass ceramic, (b) feldspathic ceramic, (c) lithium disilicate glass ceramic as a function of reproducibility, irradiated with β-source at 36 Gy room temperature with heating rate of 1 ºC/sec.

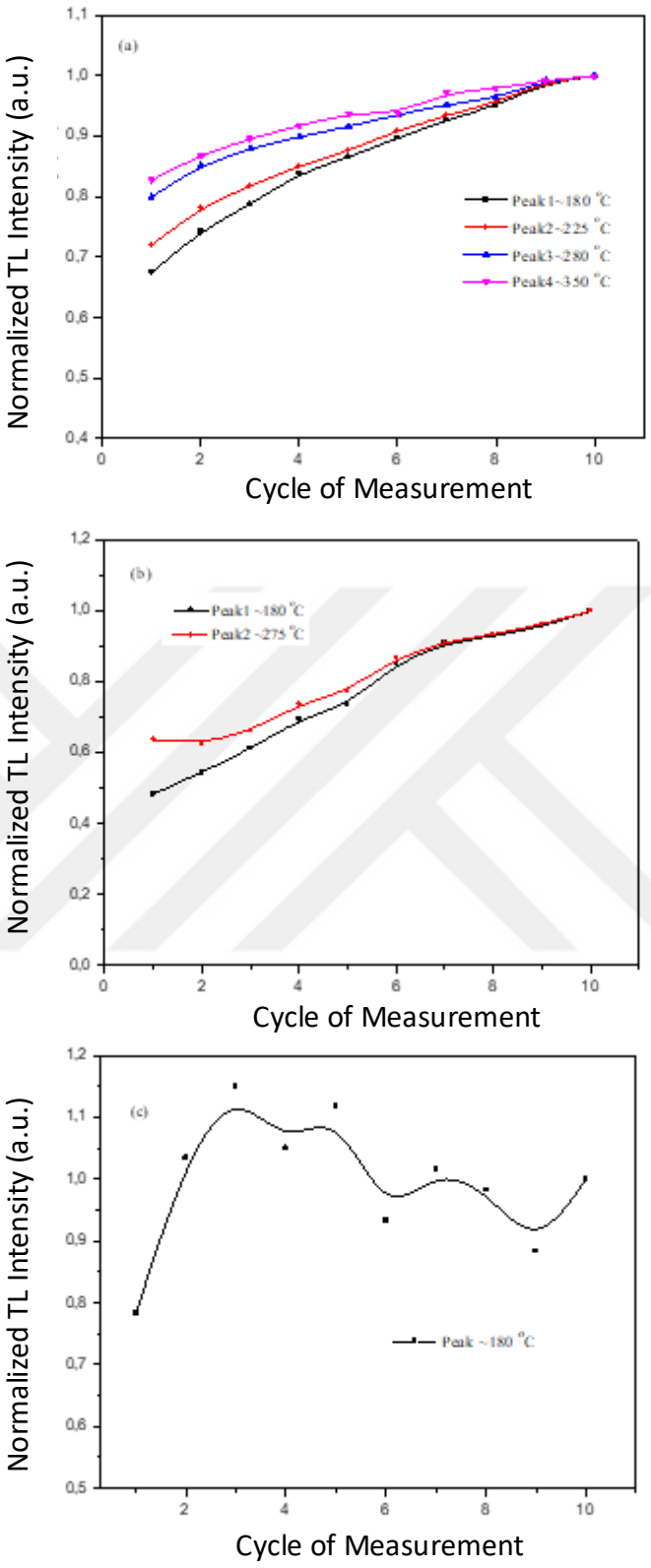

Figure 5.10. The variation of TL peak intensities of the glow curve of (a) glass ceramic, (b) feldspathic ceramic, (c) lithium disilicate glass ceramic as a function of cycle of measurement, irradiated with β-source at 36 Gy room temperature with a heating rate of 1 ^{o}C/sec.

5.4.3 Area under the Glow Curve of Dental Ceramics

The effects of experimental cycles of the area under the glow curves of entire dental ceramics were examined to check the stabilities of TL peaks as shown in Fig.5.11. Studied samples were irradiated by β-source at a fixed dose (36 Gy) and the experimental cycle of measurements was performed with one sample that used ten times at room temperature with a heating rate of 1 ^{o}C/sec for entire dental ceramics. When the experimental cycle increased area under the glow curves also increased but feldspathic dental ceramic increased more than other dental ceramics. As a result, areas under the glow curve of glass ceramic and lithium disilicate ceramic increased by about 25 % but area under the glow curve of feldspathic dental ceramic increased by about 40 % after ten cycles. It is also concluded from the figures that the peak temperature of each glow peak had no significant change.

5.4.4 The Variation of TL Peak Temperature of Dental Ceramics

The variation of TL peak temperature of dental ceramics with respect to the cycle of measurement is shown in Fig. 5.12. TL peak temperatures of glow curves of glass and feldspathic ceramics did not change with increasing cycle of measurement but TL peak temperature of lithium disilicate ceramic had a fluctuation. TL peak temperatures and shape of TL glow curves didn't change with increasing cycle of measurement. These result are very confident for a good dosimetry.

5.5 Fading Properties of Dental Ceramics

When an irradiated sample waits in different ambient, there can be a decrease in its luminescence signal and this is known as fading. It usually becomes necessary to determine if the trapped charge within the material can be lost by heat, light or any other means [110]. The fading of the dental ceramics was worked during a period of 6 weeks in this study. In order to determine the stability of TL signal, the following experiments were measured. The samples were irradiated at 36 Gy by the beta source and readout using heat rate of 1 ^{o}C/s up to 400 ^{o}C and the samples were kept in the dark-room after the irradiation at RT. The readouts were done at different storage times such as 1, 4, 24, 168 and 1000 h.

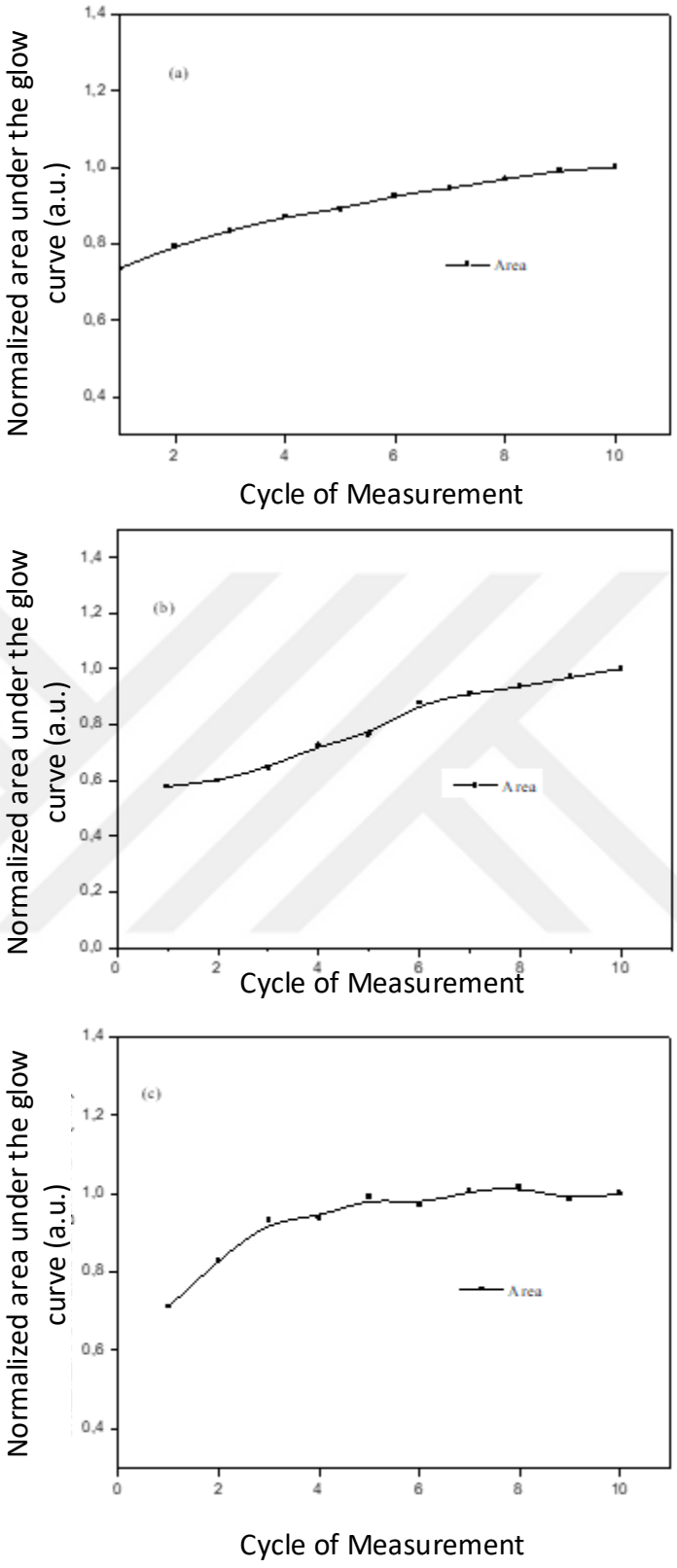

Figure 5.11. Area under the glow curve of (a) glass ceramic, (b) feldspathic ceramic, (c) lithium disilicate glass ceramic as a function of cycle of measurement, irradiated with β-source at 36 Gy room temperature with a heating rate of 1 ºC/sec.

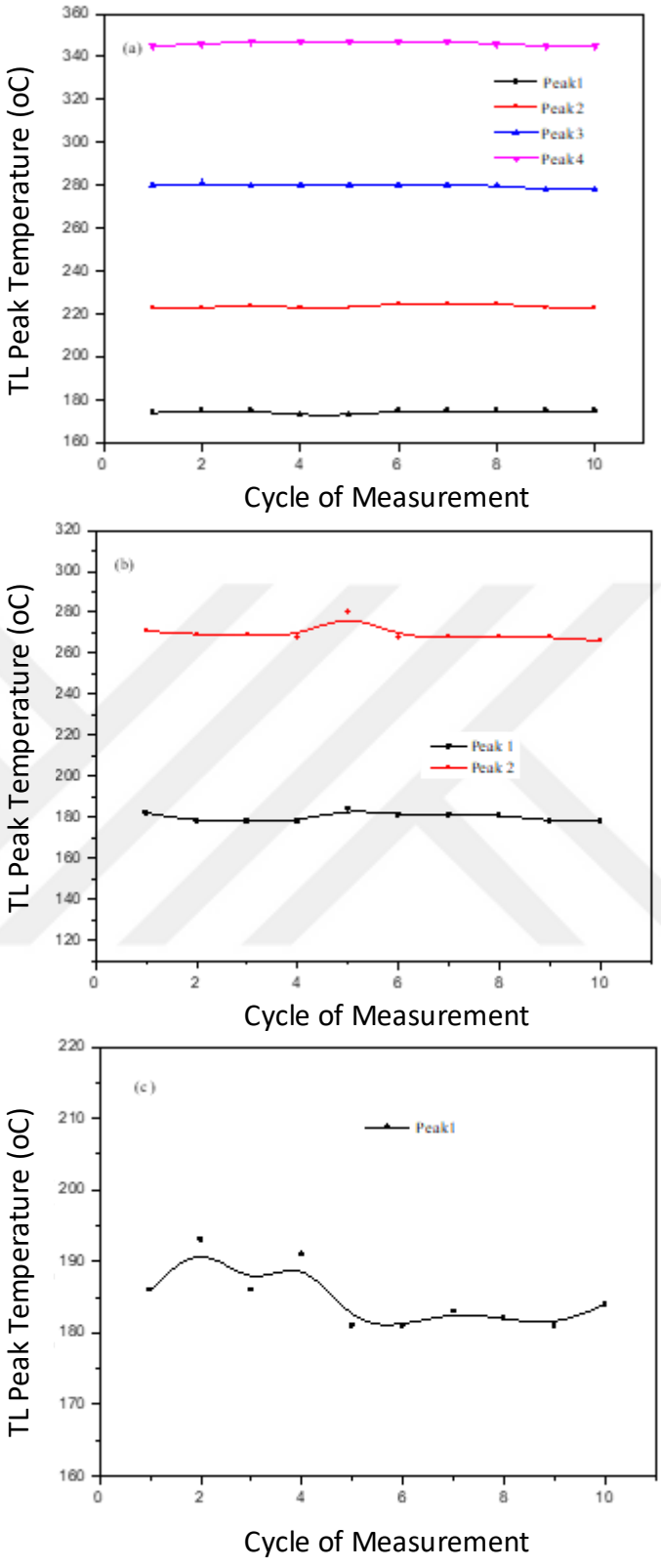

Figure 5.12. The variation of TL peak temperatures of the glow curve of (a) glass ceramic, (b) feldspathic ceramic, (c) lithium disilicate glass ceramic as a function of cycle of measurement, irradiated with β-source at 36 Gy room temperature with a heating rate of 1 ^{o}C/sec.

5.5.1 Glow Curve Variation of Dental Ceramics

The dental ceramic samples irradiated with β-source at a fixed (36 Gy) dose and a new sample was used for each experiment in this study and each experiment repeated three times. Samples were waited in a dark ambient at room temperature up to 6 weeks after irradiated. The fading properties of dental ceramics are shown in Fig.5.13. After one hour waiting, the intensity of glow curves of glass ceramic rapidly decreased. When the waiting time increased the TL intensity decreased but after six weeks the peak at 180 ^{o}C completely disappeared and TL intensities of other peaks increased with respect to one week waiting as shown in Fig.5.13 (a). After one hour waiting the intensity of glow curves of feldspathic ceramic reduced and when the waiting time increased the TL intensity declined but after six weeks the peak at 180 ^{o}C completely disappeared and TL intensities of other peaks increased with respect to 4 hours waiting as shown in Fig.5.13 (b). This is known as anomalous fading. In lithium disilicate ceramic sample, as the storage time ascended TL peak intensity decreased up to six weeks waiting and we did not observe anomalous fading.

5.5.2 Area under the Glow Curve of Dental Ceramics

To clearly examine the fading properties, we calculated the area under the glow curve to observe the effects of fading. As seen in Fig. 5.14 (a), after one hour a sharp decrease was observed which is about 60% of its initial value. When the storage time increased the area under glow curve decreased up to one week. After 6 weeks storage, the area under the glow curve increased, one of the reasons may be anomalous fading [110]. The area under the glow curve of feldspathic and lithium disilicate ceramics decreased about 15 and 45 % of its initial values, respectively. At the end of 6 weeks storage, areas of feldspathic and lithium disilicate ceramics decreased about 45 and 70 % of its initial values, respectively. After six weeks of waiting, the area under the glow curve of feldspathic ceramic decreased the least, making it more useful than the others.

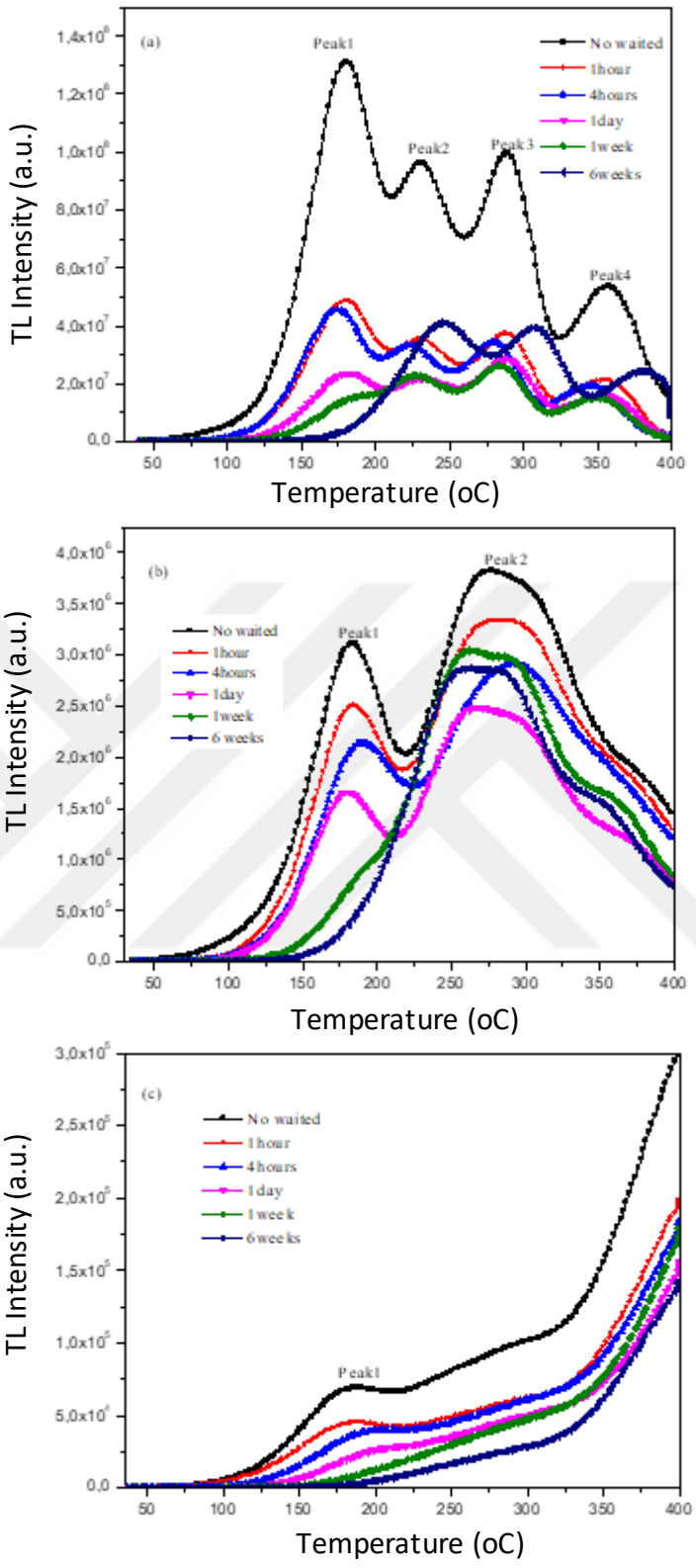

Figure 5.13. The glow curve of (a) glass ceramic, (b) feldspathic ceramic, (c) lithium disilicate glass ceramic as a function of fading, irradiated with β-source at 36 Gy room temperature with a heating rate of 1°C/sec.

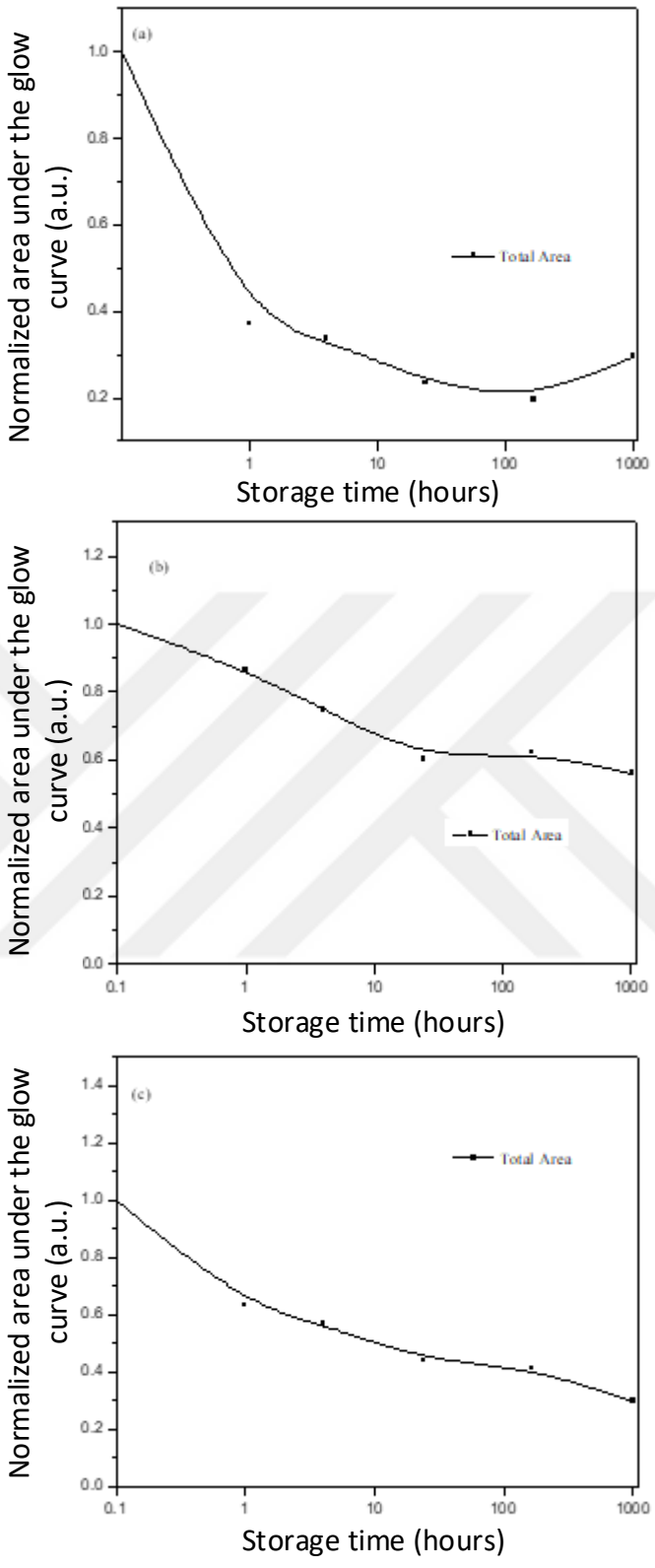

Figure 5.14. The variation of area under the glow curve of (a) glass ceramic, (b) feldspathic ceramic, (c) lithium disilicate glass ceramic as a function of fading, irradiated with β-source at 36 Gy room temperature with heating rate of 1 ^{o}C/sec.

5.5.3 Variation of TL Peak Intensity of Glow Curve of Dental Ceramics

Some of the received TL curves that obtained for entire samples are shown in Fig. 5.15. After one hour waiting, all of the peaks had a major reduction in their luminescence signal for dental glass ceramic so this shows that all of the peaks are unstable. But feldspathic dental ceramic was faded slowly with respect to the dental glass and lithium disilicate ceramics. The low-temperature glow peak of dental glass ceramic faded completely at 175 ^{o}C at the end of one week after irradiation. On the other hand glow peak of feldspathic and lithium disilicate dental ceramic faded completely in 6 weeks at 175 ^{o}C. The high-temperature glow peaks of dental glass ceramic (> 200 ^{o}C) showed a sharp reduction which was about 60% of its initial values after one hour. Low temperature glow peak of lithium disilicate ceramic had also a sharp reduction which is about 40% of its initial values after one hour but there was no sharp decrease for feldspathic dental ceramic which is about 15% of its initial values. As a result, TL signals of dental glass ceramic faded more than feldspathic and lithium disilicate dental ceramic. The TL intensity of the glow curve of dental glass ceramic increased after 6 weeks storage time but there was no significant change on the TL intensity of the glow curve of feldspathic and lithium disilicate dental ceramics. TL intensity of the high-temperature glow peaks and peak temperatures increased during 6 weeks of waiting for glass and feldspathic ceramics. It also shows that the observed fading is anomalous [110].

5.5.4 Variation of TL Peak Temperature of Glow Curves of Dental Ceramics

The variations of each TL peak temperature of dental ceramics as a function of fading are shown in Fig.5.16. The TL peak temperatures of glass ceramic did not change with increasing storage time but at the six weeks waiting the TL peak temperatures increased unlike the other values and also peak 1 completely disappeared. While no important change was observed in the TL peak temperature of glass ceramic of peak1 (just 1 ^{o}C) the other peaks increased by about 20 ^{o}C. The peak 1 of feldspathic ceramic had no significant change but it entirely faded after 24 hours waiting and peak 2 decreased with increasing storage time. At the end of six weeks waiting, the peak temperature of the lithium disilicate ceramic sample increased by about 100 degrees and this increase is not suitable for a good dosimeter sample. As a result, there is no important change of peak temperature for both samples expect lithium disilicate glass ceramic.

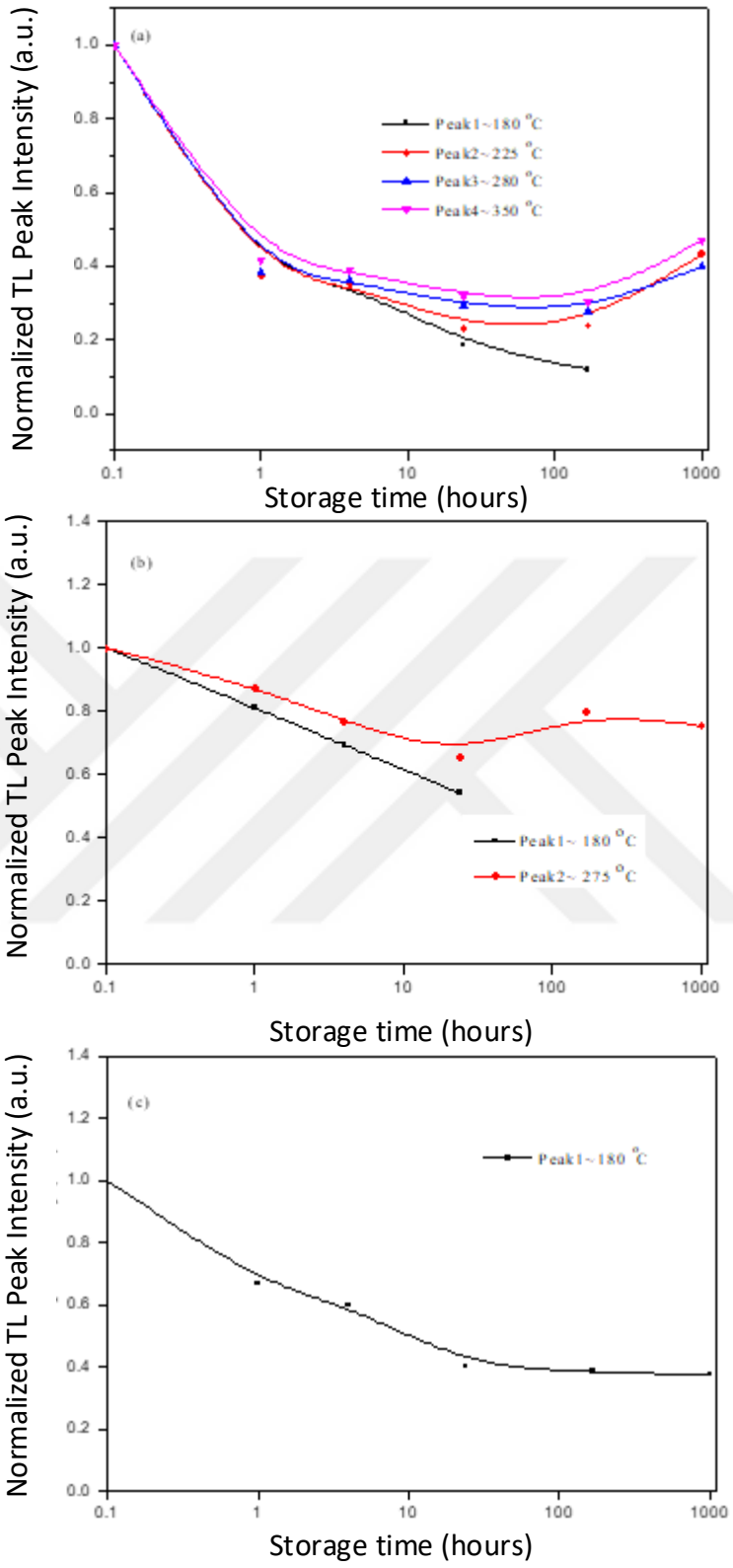

Figure 5.15. The variation of TL peak intensity of the glow curve of (a) glass ceramic, (b) feldspathic ceramic, (c) lithium disilicate glass ceramic as a function of fading, irradiated with β-source at 36 Gy room temperature with heating rate of 1 ^{o}C/sec.

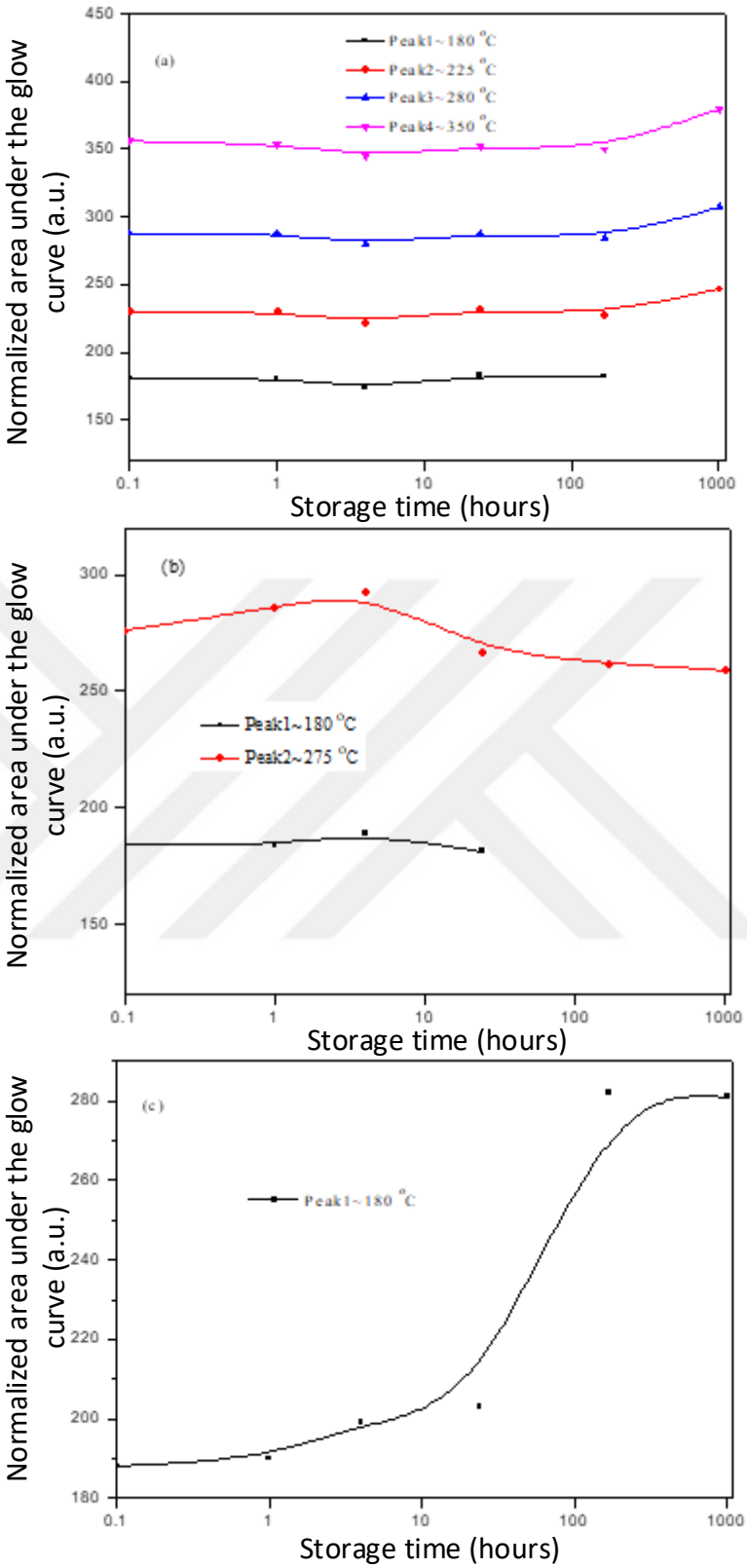

Figure 5.16. The variation of TL peak temperature of the glow curve of (a) glass ceramic, (b) feldspathic ceramic, (c) lithium disilicate glass ceramic as a function of fading, irradiated with β-source at 36 Gy room temperature with heating rate of 1 ^{o}C/sec.

CHAPTER 6:

CONCLUSION

Dental ceramics are used for restorative components of teeth, the construction of crowns and prosthetic teeth. Dental ceramics are of relevance as a luminescence dosimeter material due to their possible to ensure an express of defining cumulative exposure to external gamma radiation arising from large-scale incidents or accidents involving population groups, owing to their intimate contact with the human body [40, 95]. Moreover, the samples occur in the human body that is a substantial advantage of this application and this could provide an individual dose estimate for persons who are not equipped with classical personal dosimeters. Therefore, restorative materials that used in human teeth as a dosimeter by thermally stimulated luminescence method have been investigated in this study.

In this study, the usage of three different types of ceramic that are used in dental restoration as a dosimeter has been examined and which of these three samples has been obtained for a more suitable dosimeter. Glass ceramic, feldspathic ceramic and lithium disilicate ceramic used in this study obtained from Vivadent Ivoclar, Sweden and Turkey, respectively.

Dental ceramic materials are used for dental restoration and could have appropriate characteristics for their possible usage in retrospective and accidental dosimetry. The usage of dental ceramic was proved by preliminary studies which were applied to a few types of dental ceramics by Davies, Mauricio et al. and Bailiff et al [38-40].

The visible peak of glow curve of the glass ceramic was more complex and characterized by four peaks were labeled peak 1 (~175 ^{o}C) and peak 2 (~225 ^{o}C) seen at low temperature (LT) region and labeled peak 3 (~275 ^{o}C) and peak 4 (~350 ^{o}C) seen at high temperature (HT) region (see Fig.5.1a). It should be noted that the shape of the TL glow curve obtained in this study is seen to be very similar to the TL signal measured by Ekendahl et al [94] with samples of fluorapatite veneering glass ceramic. They observed that the curve exhibits three distinguishable peaks at ~100 ^{o}C, ~170 ^{o}C and ~280 ^{o}C. The glow curve of most glass ceramics which used for the veneer and

restoration was characterized by a dominant peak at a temperature of about 100 ^{o}C but dominant peak of glow curve in our glass ceramic at a temperature of about 175 ^{o}C moreover it has a weaker peak at ~350 ^{o}C. These results show us that TL glow curve of glass ceramic used in this study has different shape than in the study of Ekendahl et al. [94].

Aluminosilicates found in nature, which contain various amounts of potassium and sodium, are known as feldspars. The feldspathic material which is used in this study contains 58.43% SiO_2 and 15.81% Al_2O_3. Luminescence studies of feldspathic dental ceramic was previously examined by Pascu et al. [95].

Bailiff et al. [67] and Veronese et al. [92] reported that all the investigated feldspathic ceramics characterized by several peaks gave rather weak TL signals with increasing absorbed doses. And also the glow curve of feldspathic ceramic indicated a wide TL peak in the region 100–200°C, which for most of them was followed by a weaker shoulder elongating up to approximately 300°C. A different shape of the glow curve was obtained for the feldspathic ceramic investigated by Pascu et. al. [95].

Although the dominant TL peak located in the region 100–200 °C was reported by Bailiff, we observed that the weaker TL peak located in the region of 100-200 ^{o}C and dominant peak located in the region of 200-350 °C. Although it seems to have two distinctive peaks, it actually consists of four peaks that were overlapping each other. Feldspathic ceramic displayed a significant increase of the TL signal occurring in the high temperature region, a feature suggesting the presence of deep traps in the sample matrix.

In 1984 Headley and Loehmen developed the system by forming crystals of SiO_2-Li_2O in glass-phase P_2O_5-added lithium disilicate ($Li_2Si_2O_5$) and lithium orthophosphate (Li_3PO_4) crystals [97-98]. The chemical structure of lithium disilicate used today is described by Schweiger et al [99]. The lithium disilicate glass ceramic material used in this thesis contains 64.17 % SiO_2 and 11.83 % LiO_2. Different sorts of dental ceramics were investigated by a lot of authors however lithium disilicate ceramic has not studied before.

The TL glow curve of lithium disilicate sample used in this study shows a narrow TL peak in the region of 250–300°C, which for all of them was followed by a dominant shoulder extending up to approximately 400°C. Dominant peaks may be in the high temperature region which is greater than 400 °C. When the TL glow curve of the lithium disilicate ceramic is analyzed, it is clearly understood that the five peaks

overlapping with each other and some of these peaks are in high temperature regions they are not in the indicated temperature interval.

The dose response experiment is performed to see relation between TL intensity and applied dose. It is well known that if the exposed dose increases, the signal of TL glow peaks also increases until it reaches the saturation point. As a results of dose response experiments performed in this study, entire TL peaks of the glow curve of dental ceramics ascended when the exposed dose raised. The TL glow curve shapes of three dental ceramics used in the study were not affected by variation of exposed dose. TL intensities of glow peak of dental ceramics generally linearly increased up to 300 Gy and then begin to show sublinearity up to 6912 Gy.

To observe the effect of heating rate (β) on the shape of TL glow curve of dental ceramic, TL peak intensity, TL peak temperature and area under the TL glow curves of dental ceramic, seven different heating rates (β =1, 2, 3, 4, 5, 7 and 9 ^{o} C/s) were applied and irradiated with β-source at 36 Gy room temperature. On the strength of TL theory, change of heating rates culminates in alteration of location and structure of TL peak [44]. The area under the glow curve decreases with increasing heating rates at fixed (~ 36 Gy) dose. Spooner et. al. [109] proposed that when the heating rate increased the peak intensities decreased by using dental ceramic sample and we also observed the same results with them for three different dental ceramic samples used in the study. According to outputs of the heating rate experiment, the area under the glow curve of dental ceramics were reduced by about 80 percent of its initial value when the heating rate was 9 ^{o}C/s except lithium disilicate glass ceramic. The area under the glow curve the lithium disilicate glass ceramic was reduced by about 98 percent of its initial value when the heating rate was 9 ^{o}C/s. Generally, an increase in the TL peak temperature is expected as the heating rate increases, but a huge increase is seen in the TL peak temperature of lithium disilicate glass ceramic was observed about 100 degrees.

Reproducibility is an important parameter for a dosimeter. It is desirable that the TL glow curve of the sample should be same at the end of each cycle of experiment. With respect to our experimental results, it was observed that as the experimental cycle increased TL intensity of glow curve also increased. The peak temperature of each peak had no significant change and the shape of TL glow curve did not change when the cycle raised. Standard deviations of the peaks of the glow curve were calculated and all of them were larger than 2%. When the experimental cycle increased, area

under the glow curves also increased, especially higher increase in feldspathic dental ceramic is seen. As a result, areas under the glow curve of glass ceramic and lithium disilicate ceramic increased by about 25 % but area under the glow curve of feldspathic dental ceramic increased by about 40 % after ten cycles. It is also concluded from the figures that the peak temperature of each glow peak had no significant change.

Samples were waited in a dark ambient and at room temperature up to 6 weeks after irradiated so the fading properties of dental ceramics were observed. After one hour waiting the intensity of glow curves of dental ceramic rapidly decreased and when the waiting time increased the TL intensity decreased but after six weeks the TL peaks at low temperature region completely disappeared. The TL peak temperatures of dental ceramics did not change with increasing storage time but the peak temperatures increased at the end of 6 weeks the storage time. After 6 weeks waiting anomalous fading was observed for glass and feldspathic dental ceramic. In lithium disilicate ceramic sample, as the storage time ascended TL peak intensity decreased up to six weeks waiting and anomalous fading was not observed.

Compared with other types of investigated dental ceramics, glass ceramic belongs to those with the widest interval of heating rate value, the best reproducibility and lithium disilicate glass ceramic belongs to the widest interval of dose response linearity. In addition, if the measurement is performed according to the same measuring procedure, the TL signals of glass ceramic fade rather faster than the luminescence signals of other ceramics. For all of experimental procedures, only β-source was used, same samples may be irradiated X-ray and γ-ray for future works.

REFERENCES

[1] Daniels F., Boyd C.A., Saunders D.F. (1953). Thermoluminescence as a research tool. *Science*. **117**, 343-349.

[2] Vij D. R. (1998). Luminescence of Solids. 271-307. Kurukshetra University Kurukshetra, India.

[3] Urbach, F. (1930). Stimulation von ZnS-Phosphoren Mit Temperature, Wiener Berichte 139, 363.

[4] Randall, J. T., Wilkins, M. H. F. (1945). Phosphorescence and electron traps II. The interpretation of long-period phosphorescence. *Proc. Roy. Soc*. **184**, 366-390.

[5] Garlick, G. F. J., and Gibson, A. F. (1948). The Electron Trap Mechanism of Luminescence in Sulphide and Silicate Phosphors. *Proc. Phys. Soc*. **60**, 574.

[6] Townsend, P. D. (1994). Analysis of TL emission spectra. *Radiat. Meas*. **23,** 341.

[7] Cameron, J.R., Suntharalingham, N., Kenney, G.N., (1968). Thermoluminescent Dosimetry. University of Wisconsin Press, Madison. The university of Wisconsin press.

[8] Cameron, J.R., Kenney, G.N., (1963). Radiat. Res. **19**, 199.

[9] Rieke J.R. and Daniels F. (1957). Thermoluminescence Studies of Aluminum Oxide. *Journal of Phys. Chem*. **61**, 629.

[10] Moore L.E. (1957). Thermoluminescence of Sodium Sulfate and Lead Sulfate and Miscellaneous Sulfates, Carbonates and Oxides. *Journal of Phys. Chem.* **61**, 636.

[11] Ginther R.J., Kirk R.D. (1957). The thermoluminescence of CaF_2. *Electrochem. Soc*. **104,** 365-369.

[12] McKeever S.W.S., Moscovitch M., Townsend P.D. (1995). Thermoluminescence Dosimetry Materials: Properties and Uses. Nuclear Technology Publishing. England.

[13] Kraysnaya, A.R., Nosenko, G.M., Rezvin, L.S., Yasolko, V. (1961). At. Energ., **10**, 630.

[14] Schulman, J.H., Kirk, R.D., West, E.J., (1965). 1st Int. Conf. on Luminescence Dosimetry, Stanford. p. 113.

[15] Binder, W., Disterhoft, S., Cameron, J.R., (1968). In: Proc. 2nd Int. Conf. on Luminescence Dosimetry, Gatlinburg. Conf 680920 (NTIS, Springfield, VA) p. 43.

[16] Yamashita, T., Nada, N., Onishi, H., Kitamura, S., (1968). In: Proc. 2nd Int. Conf. on Luminescence Dosimetry, Gatlinburg. p. 4.

[17] Kozlowitz, I., Schayes, R., (1968). Thermoluminescent dosimeter for detecting radiation having a plurality of components, US Patent 3, 399-301.

[18] Thomas, B., Houston, E., (1964). Correlation of optical absorption and thermoluminescence curves for single crystals of magnesium oxide. *Br. J. Appl. Phys*. **15**, 953.

[19] Janas, R., Hübner, K., (1976). Investigations on thermoluminescent dosimetry (TLD) with doped alumina ceramics. *Isotopenpraxis*. **12**, 342.

[20] Metha, S.K., Sengupta, S., (1976). Al2O3 phosphor for Thermoluminescence dosimetry. *Healt Phys*. **31**, 176.

[21] Lucas, A.C., Kaspar, B., (1977). The thermoluminescence of thulium doped calcium fluoride. 5th Int. Conf. on Luminescence Dosimetry, Saõ Paulo. pg. 131.

[22] Takenaga, M., Yamamoto, O., Yamashita, T., (1980). Preparation and characteristics of Li2B4O7: Cu phosphor. *Nucl. Instrum. Methods* **175**, 77.

[23] Prokic, M., (1980). Development of highly sensitive CaSO4: Dy/Tm and MgB4O7 : Dy/Tm sintered thermoluminescent dosimeters. *Nucl. Instrum. Methods* **175**, 83.

[24] Prokic, M., (1993). MgB4O7:Mn as a New TL Dosemeter. *Radiat. Prot. Dosim*. **47**, 191.

[25] Nakajima, T., Murayama, Y., Matsuzawa, T., Koyano, (1978). A development of a new highly sensitive LiF thermoluminescence dosimeter and its applications. *Nucl. Instrum. Methods*. **157**, 155.

[26] Wang, S., Chen,G., Wu, F., Li, Y., Zha, Z. and Zhu, J., (1986). Newly developed highly sensitive LiF (Mg, Cu, P) TL chips with high signal to noise ratio. *Radiat. Prot. Dosim*. **14**, 223.

[27] Akselrod, M., Kortov, V.S., Karavetsky, D.J., Gotlib, V.I., (1990). Highly Sensitive Thermoluminescent Anion-Defective Alpha-Al203:C Single Crystal Detectors. *Radiat. Prot. Dosim*. **32**, 15.

[28] Chen, R. (2001). Advantages and disadvantages in the utilization of TL and OSL for radiation dosimetry. IRPA Regional Congress on Radiation Protection in Central Europe. Dubrovnik, Croatia.

[29] Zimmerman, J. (1971). The radiation-induced increase of the 100°C thermoluminescence sensitivity of fired quartz. *Phys. C: Sol. St. Phys*. **4**, 3277.

[30] Cameron, J. R., Zimmerman, D. W. and Bland, R. W. (1965). TL vs. R in LiF: A Proposed mathematical model. *Rept*. COO-1105-102, USAEC.

[31] Bailiff, I.K. (1995). The use of ceramics for retrospective dosimetry in the Chernobyl exclusion zone. *Radiation Measurements*. **24**, 507-511.

[32] Poolton, N. R. J., Butter-Jensen, L., Jungner, H. (1995). An optically stimulated luminescence study of porcelain related to radiation dosimetry. *Radiation Measurements*. **24**, 543-549.

[33] Stoneham, D. (1995). Accident dosimetry using porcelain: TL analysis of low dose samples. *Radiation Measurements*. **24**, 499-505.

[34] Bailiff, I.K. (1997). Retrospective dosimetry with ceramics. *Radiat. Meas*. **27**, 923-941.

[35] Butter-Jensen, L., Jungner, H. (1999). Application of luminescence techniques in retrospective dosimetry. *Acta Physica Polonica A.* **95 (2),** 275-286.

[36] Bøtter-Jensen, L. (2000). Development of optically stimulated luminescence techniques using natural minerals and ceramics, and their application to retrospective dosimetry. Phd. Thesis. Riso National Laboratory, 185 s., Roskilde, Denmark.

[37] Davies, J. E. (1979). On the use of dental ceramics as a possible second-line approach to accident irradiation dosimetry. *Radioprotection.* **14**, 89-97.

[38] Mauricio, C. L. P., Rosa, L. A. R., Cunha, P. G. (1985). Accident Dosimetry Using the TL from Dental Restoration Porcelains. *Radiat. Prot. Dosim*. **11**, 185–188.

[39] Bailiff, I.K., Correcher, R., Delgado, A., Göksu, Y., Hübner, S., 2002. Luminescence characteristics of dental ceramics for retrospective dosimetry: A preliminary study. Radiat. Prot. Dosim. 101, 519-524.

[40] McKeever, S.W.S. (1985). Thermoluminescence of solids. Cambridge University Press ISBN 9780511564994.

[41] Vandenberghe, D. (2004). Investigation of the optically stimulated luminescence dating method for applicatıon to young geologıcal sediments. Phd. Thesis. Universiteit gent, 298s. Netherlands.

[42] Thomsen, K.J. (2004). Optically Stimulated Luminescence Techniques in Retrospective Dosimetry using Single Grains of Quartz extracted from Unheated Material. Ph.D. Thesis, Risø National Laboratory, 17-41s, Roskilde, Denmark.

[43] Braunlich P. 1979. Braunlich: Thermally stimulated relaxation in solids. Springer-Verlag, Berlin.

[44] Aitken M. J., Tite M. S. and Reid J. (1964). Thermoluminescencent dating of ancient ceramics. *Nature.* **202**, 1032-1033.

[45] Aitken M. J., Zimerman D. W. and FlemingS. J. (1964). Thermoluminescencent dating of ancient pottery. *Nature*. **219**, 442-444.

[46] Mejdahl V. (1969). Thermoluminescence dating of ancient Danish ceramics. *Archaeometry*. **11**, 99-104.

[47] Wintle A. G. and Huntley D. J. (1985). Thermoluminescencent dating of ocean sediments. *Canadian journal of earth sciences*.

[48] Wintle A. G. (1985). Anomalous fading of thermoluminescence in mineral samples. *Nature*. **245**, 143-144.

[49] Chen R., Kirsh Y. 1981. Analysis of Thermally Stimulated Processes, Pergamon Press, Oxford.

[50] Pagonis, V., Kitis, G., Furetta, C. 2006. Numerical and Practical Exercises in Thermoluminescence, Springer Sciencem Business Media, Inc., 232 p.

[51] Randall J.T. and Wilkins M.H.F. (1945). Phosphorescence and Electron Traps. I. The Study of Trap Distributions. *Proc.R.Soc.London Ser. A*. **184**, 366.

[52] Chen R. and McKeever S.W.S. (1997). Theory of Thermoluminescence and Related Phenomena, *World Scientific*, Singapore.

[53] Furetta, C. and Kitis G. (2004). Rewiev of Thermoluminescence. *Journal of Materials Science*. **39**, 2277-2294.

[54] Furetta, C. Weng, P.S., 1998. Operational Thermoluminescence Dosimetry, World Scientific, Singapore.

[55] Bos, A.J.J. (2007). Theory of Thermoluminescence. *Radiation Measurements*. **41**, S45-S56.

[56] Bos, A.J.J., Dielhof, J.B. (1991). The analysis of thermoluminescent glow curves in CaF2:Tm(TLD-300). *Radiat. Prot. Dosim*. **37 (4),** 231–239.

[57] May C.E., Partridge J.A. (1964). Thermoluminescent Kinetics of Alpha-Irradiated Alkali Halides. *J. Chem. Phys*. **40**, 1401.

[58] Bohum, A. (1954). Thermoemission and Photoemission von Natriumchlorid. *Czech. J. Phys*. **4**, 91.

[59] Booth, A.H. (1954). Calculation of electron trap depths from thermoluminescence maxima. *Canad. J. Chem*. **32**, 214.

[60] Parfianovitch, I.H. (1954). The determination of the depth of electron traps in crystal phosphors. *J. Exp. Theor. Phys*. **26**, 696.

[61] Puchalska, M., Bilski, P. (2006). GlowFit—a new tool for thermoluminescence glow-curve deconvolution. *Radiation Measurement*. **41**, 6. pp. 659-664.

[62] Abd El-Hafez, Yasin A.I., Sdek M.N., A.M. (2011). A new tool for glow curve analysis in thermoluminescence nanodosimetry. Nuclear Instruments and Methods in Physics Research Section A: Accelerators, Spectrometers, Detectors and Associated Equipment. **637**, 1, pp. 158-163.

[63] Chung, K.S., Choe, H.S., Lee, J.I., Kim, J.L., and Chang, S.Y. (2005). A Computer Program for the Deconvolution of Thermoluminescence Glow Curves. *Radiation Protection Dosimetry*. **115**, No:1-4, pp. 345-349.

[64] Bos A. J. J., Piters J. M., Gomez Ros J. M. and Delgado A. (1993). Intercomparision of Glow Curve Analysis Computer Programs IRI-CIEMAT Report. **131**-93-005 IRI Delft.

[65] Mahesh K, Weng P. S. and Furetta C. (1989). Thermoluminescence in Solids and its Applications. Nuclear Technology Publishing. Ashford.

[66] Hsu P. C., Wang T. K. (1986). On the Annealing Procedure for CaF2:Dy. *Radiat.Protect.Dosim*. **16**, 253.

[67] Furetta C. (2008). Questions and Answers on Thermoluminescence (TL) and Optically Stimulated Luminescence (OSL). World Scientific. Singapore.

[68] McKeever S. W. S., Moscovitch M., Townsend P. D. 1994. Thermoluminescence dosimetry materials: Properties and use. Nuclear Technology Publishing.

[69] McKeever S. W. S., Chen R. (1997). Luminescence models. *Radiation Measurements*. **27**, 625-61.

[70] Hultquist M. (2005). Analysis of the uncertainties in the IAEA/WHO TLD postal dose audit programme. Stockholm University Karolinska Institute.11.

[71] Ichikawa Y., Higashimura T., Shidei T. (1966). Thermoluminescence dosimetry of gamma rays from atomic bombs in Hiroshima and Nagasaki. *Health Phys*. 12, 395.

[72] Hoshi M., Sawada S., Ichikawa Y., Nagatomo T., Uehara S., Kondo S., Thermoluminescence dosimetry of gamma-rays from the Hiroshima atomic bomb at distances 1.91–2.05 km from the hypocenter. (1989). *Health Phys*. **57**, 1003.

[73] Haskell E.H., Kaipa P.L., Wrenn M.E. (1988). Pre-dose TL characteristics of quartz inclusions removed from bricks exposed to fallout radiation from atmospheric testing at the Nevada Test Site. *Nucl. Tracks Radiat. Meas*. **14**, 114.

[74] Hütt, G., Brodski, L., Bailiff, I.K. (1993). Accident dosimetry using environmental materials collected from regions downwind of Chernobyl: a preliminary evaluation. *Radiat. Prot. Dosim.* **47**, 307.

[75] Veronese, I., Guzzi, G., Giussani, A., Cantone, M.C., Ripamonti, D. (2006). Determination of dose rates from natural radionuclides in dental materials. *Journal of Environmental Radioactivity*. **91,** 15-26.

[76]Ceramics.http://chemed.chem.purdue.edu/genchem/topicreview/bp/materials/ceramic4.html#ceramic. 05.03.2018.

[77] Alla R. K. (2013). Dental Materials Science, Jaypee Brothers Medical Publishers Pvt Limited, New Delhi, India. 1st Edition, 333-354.

[78] Denry I., Holloway J.A. (2010). Ceramics for dental applications: A Review. *Materials, **3***, 351-368.

[79] Babu J., P., Alla R. K., Alluri V. R., Datla S. R., Konakanch A. (2015). Dental Ceramics: Part I – An Overview of Composition, Structure and Properties. *American Journal of Materials Engineering and Technology*. 3, 13-18.

[80] Anusavice K.J. (2010). Phillip's Science of Dental Materials, Elsevier, A division of Reed Elsevier India Pvt Ltd, New Delhi, India, 11th Edition, 655-720.

[81] Sakaguchi R.L., Powers J.M. (2007). Craig's Restorative Dental Materials, Elsevier, Mosby, A division of Reed Elsevier India Pvt Ltd, New Delhi, India, 12th Edition, 443-464.

[82] Lung C.Y.K., Matinlinna J.P. (2012). Aspects of silane coupling agents and surface conditioning in dentistry: An overview. *Dent Mater*. **28(5),** 467-77.

[83] J'Obrien W. (2002). Dental Materials and their selection, 3rd edition, quintessence Publishing Co. Inc, 132-155.

[84] Rashid H. (2014). The effect of surface roughness on ceramics used in dentistry: A review of literature. *Eur J Dent*. **8**, 571-9.

[85] Park, J. (2008). Bioceramics Prooerties, characterications and applications. Springer.

[86] Denry I.L. (1996). Recent advances in ceramics for dentistry. *Crit Rev Oral Biol Med.* **7(2),** 134-143.

[87] Shenoy A., Shenoy N. (2010). Dental Ceramics: An Update, *J Cons Dent*, **13(4),** 195-203.

[88] McLean J.W., Hughes T.H. (1965). The reinforcement of dental porcelain with ceramic oxides. Br Dent J. 119(6):251-267.

[89] McLean J.W. (1979). The science and art of dental ceramics, Volume I: The nature of Dental Ceramics and their clinical use. Quintessence Pub Co., Chicago.

[90] Claus H., Rauter H. (1989). The structure and microstructure of dental porcelain in relationship to the firing conditions. Int Prosthodont 2(4):376-384.

[91] Van Noort R. (1994). Introduction to Dental Materials, Mosby, Spain, 201-214.

[92] Veronese, I., Galli, A., Cantone,M.C., Martini, M., Vernizzi, F., Guzzi, G. (2010). Study of TSL and OSL properties of dental ceramics for accidental dosimetry applications. *Radiat. Meas*. **45**, 35e41.

[93] Mauricio, C.L.P., Rosa, L.A.R., Cunha, P.G. (1985). Accident dosimetry using the TL from dental restoration porcelains. *Radiat. Prot. Dosim*. **11**, 185-188.

[94] Daniela E., Libor J., Lucie S. (2013). OSL and TL retrospective dosimetry with a fluorapatite glass-ceramic used for dental restorations. *Radiation Measurements* **58**, 138-144.

[95] Pascu, A.R., Timar-Gabor, A., Simon, V. (2016). Retrospective Accident Dosimetry Using Dental Ceramics. Romanian Reports in Physics, 68, 658–666.

[96] Yavuz Y. H., Turhan B., Bavbek B., Kurt E. (2005). Tam porselenler *II. GÜ Dişhek Fak Derg*. **22(1),** 49-60.

[97] Höland W., Rheinberger V., Schweiger M. (2003). Control of nucleation in glass ceramics. *Phil Trans R Soc Lond A*. **361(1**), 575-89.

[98] Bahar. E., K., Göknil, E., K. (2012). Lithium Disilicate Ceramics. *Atatürk Üniv. Diş Hek. Fak. Derg*. **5**, 123-131.

[99] Schweiger M., Holland W., Frank M., Drescher H., Rheinberger V. (1999). IPS Empress II : a new pressable high-glass ceramic for esthetic all-ceramic restoration. Quint Dent Technol; (Accession number;99A0746083): 143-151.

[100] Scientific Documentation IPS e.max® CAD.

[101] 9010 Optical Dating System User Manual, Dec. (1993).

[102] Jensen, L. B. (1997). Luminescence Techniques: Instrumentation and Methods. *Radiation Measurements*. **27**, 749-768.

[103] Model 3500 Manual TLD Reader User's Manual, Publication No 3500-0-U-0793-005, July 30 1994.

[104] Gün, E., (2006). Investigation of Thermoluminescence Properties of Calcite (CaCO3). Thesis. Engineering Physics University of Gaziantep.

[105] Kitis G., Furetta C., Prokic M., Prokic V., (2000). J. Phys. D: Appl. Phys., 33, 1252

[106] Kitis G., Spiropulu M., Papadopoulos J., Charalambous S., (1993), Nucl. Instrum. Methods Phys. Res., 73, 367

[107] Ege A., Ekdal E., Karali T., Can N., Prokic M., (2007), Meas. Sci. Technol., 18, 889.

[108] Anishia S.R., Jose M.T., Annalakshmi O., Ramasamy V., (2011), J. Lumin., 131, 2492.

[109] Oks H., Spooner N.A., Smith B.W., Prescott J.R., Creighton D.F., McCulloch I., Adamiec G. (2011). Assessment of thermoluminescence peaks in porcelain for use in retrospective. Radiation Measurements 46, 1873-1877.

[110] Furetta, C. Handbook of thermoluminescence. World scientific ISBN: 978-981-238-240-5 (2003).

[111] Pagonis, V., Kitis, G., Furetta, C., Numerical and Practical Exercises in Thermoluminescence, Springer Science+Business Media, Inc., 232, (2006).

[112] Park J., Bioceramics: Properties, Characterizations, and Applications, Springer (2009).

CURRICULUM VITAE

PERSONEL INFORMATION

Name, Surname: Esme IŞIK

Nationality: Turkish

Birth Date and Place: 1985 / İslahiye

email: esma_boz@hotmail.com

EDUCATION INFORMATION

M.Sc. (2013) University of Gaziantep, Engineering Physics

B.Sc. (2011) University of Gaziantep, Engineering Physics

WORK EXPERIENCE

2012- Research Assistant

PUBLICIATIONS

SCI:

1- **E. Isik**, H. Toktamis, "Influence of Storage in Different Ambiences on The Thermoluminescence Peaks of Quartz", Ciência e Técnica Vitivinícola Journal, Vol. 33, No. 1., Oct. 2018.
2- **E. Isik**, H. Toktamis, "TLD Characteristic of Glass, Feldspathic and Lithium Disilicate Ceramics", Luminescence: The Journal of Biological and Chemical Luminescence, Vol. 34, No. 9, Jan. 2019.

National Conferences:

1- **E.Boz,** H.Toktamış, "Farklı koşullar altında sentetik kuvars kristallerin termolüminesans tepe şiddetlerindeki sönümlerinin araştırılması."6. Ulusal Lüminesans Dozimetri Kongresi, İzmir, 2012.

International Conferences:

1- I. Isik, **E. Isik**, "Analysis of Receptor Models in Molecular Communication Via Diffusion", 2nd International Conference on Advanced Engineering Technologies, ICADET, Bayburt, 2017.
2- **E. Isik**, H. Toktamis, "Comparative Measurements of Dental Ceramics Using in Retrospective Dosimetry with TL Techniques", ICADET 2017, Bayburt, 2017.
3- **E. Isik**, H. Toktamis, "Thermally Stimulated Luminescence Method For Retrospective Dosimetry Of Commenly Used Dental Ceramic", III. International Conference On Engineering and Natural Sciences (Icens), BUDAPEST, 2017.
4- **E. Isik**, H. Toktamis, "The Investigation Of Thermoluminescence And Optically Stimulated Luminescence Properties Of Biomaterials Used In Dental Processes", III. International Conference On Engineering and Natural Sciences (Icens), BUDAPEST, 2017.
5- **E. Isik**, H. Toktamis, "The investigation of thermoluminescence properties of feldspathic ceramic used in dental processes**",** 3rd International Conference on Theoretical and Experimental Studies in Nuclear Applications and Technology, Adana, 2017.
6- **E. Isik**, I. Isik, "Fpga Based Analysis Methods in TL And OSL Studies", 2nd International Energy&Engineering Conference, Gaziantep, 2017.

LANGUAGE INFORMATION

English